POLITECNICO DI TORINO
Repository ISTITUZIONALE

Review of current best-practices in machinability evaluation and understanding for improving machining performance

Original
Review of current best-practices in machinability evaluation and understanding for improving machining performance / Liao, Zhirong; Schoop, Julius M.; Saelzer, Jannis; Bergmann, Benjamin; Priarone, Paolo C.; Splettstößer, Antonia; Bedekar, Vikram M.; Zanger, Frederik; Kaynak, Yusuf. - In: CIRP - JOURNAL OF MANUFACTURING SCIENCE AND TECHNOLOGY. - ISSN 1755-5817. - STAMPA. - 50:(2024), pp. 151-184. [10.1016/j.cirpj.2024.02.008]

Availability:
This version is available at: 11583/2990639 since: 2024-07-11T07:44:26Z

Publisher:
Elsevier Ltd

Published
DOI:10.1016/j.cirpj.2024.02.008

Terms of use:

This article is made available under terms and conditions as specified in the corresponding bibliographic description in the repository

Publisher copyright

(Article begins on next page)

19 March 2025

CIRP Journal of Manufacturing Science and Technology 50 (2024) 151–184

Contents lists available at ScienceDirect

CIRP Journal of Manufacturing Science and Technology

journal homepage: www.elsevier.com/locate/cirpj

Review of current best-practices in machinability evaluation and understanding for improving machining performance

Zhirong Liao [a,*], Julius M. Schoop [b], Jannis Saelzer [c], Benjamin Bergmann [d], Paolo C. Priarone [e], Antonia Splettstößer [f], Vikram M. Bedekar [g], Frederik Zanger [h], Yusuf Kaynak [i]

[a] Faculty of Engineering, University of Nottingham, UK
[b] Institute for Sustainable Manufacturing (ISM), University of Kentucky, Lexington, KY, USA
[c] Institute of Machining Technology, TU Dortmund University, 44227 Dortmund, Germany
[d] Institute of Production Engineering and Machine Tools (IFW), Leibniz Universität Hannover, An der Universität 2, D-30823 Garbsen, Germany
[e] Department of Management and Production Engineering, Politecnico di Torino, 10129 Torino, Italy
[f] Laboratory for Machine Tools and Production Engineering (WZL) of RWTH Aachen University, Campus-Boulevard 30, 52074 Aachen, Germany
[g] Material Development, Research and Development, Timken World Headquarters, North Canton, OH 44720, USA
[h] wbk Institute of Production Science, Karlsruhe Institute of Technology (KIT), 76131 Karlsruhe, Germany
[i] Department of Mechanical Engineering, Marmara University, Goztepe Campus, 34722, Kadikoy, Istanbul, Turkey

ARTICLE INFO

Keywords:
Machinability
Tool wear
Cutting force and temperature
Chip formation
Surface integrity

ABSTRACT

Machinability is a generalized framework that attempts to quantify the response of a workpiece material to mechanical cutting, which has been developed as one of the key factors that drive the final selection of cutting parameters, tools, and coolant applications. Over the years, there are many attempts have been made to develop a standard evaluation method of machinability. However, due to the complexity of the influence factors, i.e., from work material and cutting tool to machine tool, that can affect the materials machinability, currently there is no uniquely defined quantification of machinability. As one of the outcomes from the CIRP's Collaborative Working Group on "Integrated Machining Performance for Assessment of Cutting Tools (IMPACT)", this paper conducts an extensive study to learn interacting machinability parameters to evaluate the overall machining performance. Specifically, attention is focused on recent advances made towards the determination of the machinability through tool wear, cutting force and temperature, chip form and breakability, as well as the surface integrity. Furthermore, the advanced methods that have been developed over the years to enable the improvement of machinability have been reviewed.

1. Introduction

1.1. Background

Machining operations play a pivotal role in the manufacture of final components, whose outcome, depending on the machining conditions and strategies, can significantly influence the material's functional performances [1]. On the other hand, their cost also counts a high proportion of the total manufacturing price. These machining outcomes and their cost, however, are mainly determined by the machinability of the materials. That is, with different materials, their inherent properties can influence the difficulty that the materials can be machined, and eventually yield different machining cost as well as surface integrity [2]. Hence, the materials machinability normally is one of the key factors that drive the final selection of cutting parameters, tools, and coolant applications. Furthermore, as more and more harsh application environments are required, new materials are being developed, which always accompanied with low machinability, namely difficult-to-cut materials. The high surface integrity requirement for these applications, on the other hand, drives the need of developing new machining technologies to address their low machinability [3,4].

Efforts have been made by both the academia and industry to investigate the relationships among the machinability, machining cost, machining outcome and their effect on product's functional performance. The formal evaluation of machinability can be traced back to the earliest efforts of F.W. Taylor in the late 19th century. In his 1906 work 'On the Art of Cutting Metals' Taylor lays out the principles of parameter variation in order to obtain force and wear coefficients for empirical

* Corresponding author.
E-mail address: Zhirong.Liao@Nottingham.ac.uk (Z. Liao).

https://doi.org/10.1016/j.cirpj.2024.02.008
Received 11 April 2023; Received in revised form 14 February 2024; Accepted 22 February 2024
Available online 6 March 2024
1755-5817/© 2024 The Authors. This is an open access article under the CC BY license (http://creativecommons.org/licenses/by/4.0/).

power law relationships [5]. Based on this simple, yet effective semi-empirical approach, subsequent work in the 20th century significantly expanded the approach towards comparing the relative machinability of different metal alloys, most commonly in terms of readily measured variables such as cutting forces, chip form, and tool wear/life. The early well-documented work can be tracked back to 1951 when Woldman and Gibbons published a well-known book on the machinability and machining operations of different metal alloys [6]. Thereby the machinability was surmised as the characteristics of metals such as hardness, strength, ductility, grain size, microstructure, and their chemical composition, upon their influence on the tool wear, chip formation, ease to cut and surface finish [6–9]. In 1960 s Boulger et. al., also studied the machinability of a range of engineering materials such steels alloys [10], nickel and cobalt alloys [11] whereby their machinability has been well documented. The book by Mills and Redford in 1983 [12] provides a range of practical machinability test whereby these machinability tests were subdivided into two basic categories: those which do not require a machining process to take place, and those which do. It implicates that in most cases there is no indication of the magnitude machinability because the measure of machinability does not correlate a predictable scale. An early paper by Fang and Jawahir (1994) also shows the deficiencies of current machinability criteria and emphasizing the need for total machining performance [13].

From Scopus search of the key word “machinability”, it can be seen that there is an increasing number of publications every year (>9000 up to now), as shown in Fig. 1, boosting up from 21-century. It is obvious much of the current practices in machinability are based on some of the major machinability criteria established and practiced for decades. Though many different researches/practices have been conducted to evaluate the machinability, most of them are addressing particular materials with different machining outcomes, and up to now, there is no complete and unanimously accepted definition of machinability concept existing, and so are the evaluation methods [14]. This is because, unlike most material properties, there is no generally accepted parameter used for the measurement of machinability [12].

1.2. CIRP collaborative working group (CWG) on integrated machining performance for assessment of cutting tools (IMPACT)

To revisit the machinability and addresses the actual machining performance by a “machining system” (cutting tool; machine tool; and work material), professor Jawahir proposed a project for Collaborative Working Group (CWG), titled as “Integrated Machining Performance for Assessment of Cutting Tools (IMPACT)”. In this project, we aim to develop active research collaboration among academic researchers, cutting tool manufacturers and manufacturing organizations thus to uncover the machining “DNA” of cutting tools. Therein we developed

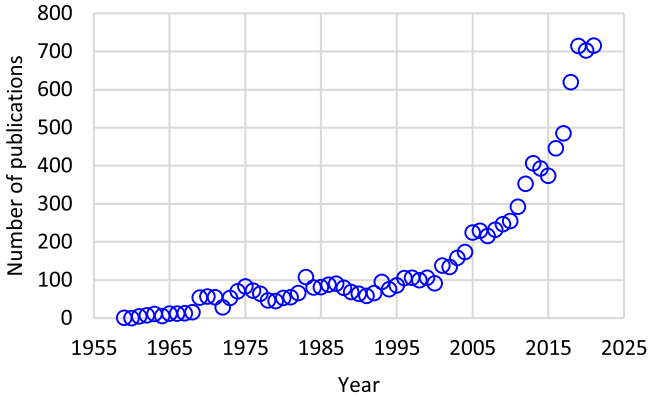

Fig. 1. Evolution of the number of academic publications in reference to “Machinability” [
Source: Scopus].

five different research topics including the machinability evaluation, modelling of cutting tool performance, cutting tool engineered design, smart tooling and AI-based machining optimisation. This paper is one of the outcomes from CIRP CWG IMPACT project on conducting an extensive study to learn interacting machinability parameters to evaluate the overall (total) machining performance, i.e., topic A, contributed by a large number of CIRP and non-CIRP members who actively participated in the collaborative research activities of the CWG.

2. Concept and evaluation methods of machinability

The concept of machinability is a generalized framework that attempts to quantify the response of a workpiece material to mechanical cutting, i.e., chip removal and surface generation. Traditionally, machinability was considered as a unique property of the work material, similar to mechanical properties such as yield strength and toughness. While there are some obvious correlations between a given work material’s yield strength, thermal conductivity, and propensity for strain hardening, any observed machining performance is a complex phenomenon that arises from the combined performance of a total machining system, such as workpiece and tool materials, process parameters, machine tool and fixture, as illustrated in Fig. 2. There are obvious limitations to improvements in machinability that can be obtained for a given workpiece material through optimization of cutting conditions. In practice, this means that even with careful optimization, the machinability of an easy-to-cut material, such as aluminium alloys, will be greater than that of a difficult-to-cut material, such as nickel-based superalloys. Nevertheless, machinability for a given material can be greatly influenced by factors such as the rigidity of the machining setup, tool coatings and cutting speed. Therefore, in addition to basic material properties, machinability necessarily includes the influence of factors related to the process parameters, including cooling/lubricating strategies, as well as the properties of the machine tool, fixture, and cutting tool.

Fundamentally, the study of machinability attempts to quantify factors that influence machining performance, such as cutting mechanisms, and temperatures, in terms of process outputs, such as tool wear and life, forces, and quality metrics (e.g., surface finish and accuracy). For example, a machinability study may compare the relative performance of a number of different cutting tools or process parameters (feeds and speeds) to determine the tool-life and surface finish response against some baseline, such as a previously developed machining operation. Based on machinability data, optimization of machining performance can be pursued within the ‘machinability envelope’ of a given workpiece material. As there are many potential optimization objectives (metal removal, surface integrity, tool-life, etc.) and process parameters, such as cutting speed, feed, depth of cut, tool geometry and coating [19], coolants, tool holders, etc., a machinability evaluation effort will often yield a meaningful improvement in process performance. For this reason, the systematic and data-driven machinability approach has been the foundation for improved machining process performance in industry for over 100 years.

A variety of standards have been formulated to allow for relative comparison of the machinability of different workpiece materials. These include the widely used ISO 3865:1993 (single-point turning) [20] and ISO 8688–1/2:1989 (milling) [21] standards, as well as the simpler American Iron and Steel Institute (AISI) machinability rating {Institute, 1960 #4422}, which compares the relative tool-life (i.e., Taylor plot cutting speed) and surface finish in turning of various metals compared against a 100% baseline of AISI/SAE B1112 free machining carbon steel. Using the AISI standard, cast aluminium will exhibit a relative machinability of 450%, while the superalloy Hastelloy X only achieves a 19% machinability rating. Researchers realized early on that in general, a higher yield strength along greater ductility and strain hardening behaviour will reduce the machinability of a given alloy. In other words, Hastelloy X is expected to have much lower relative machinability

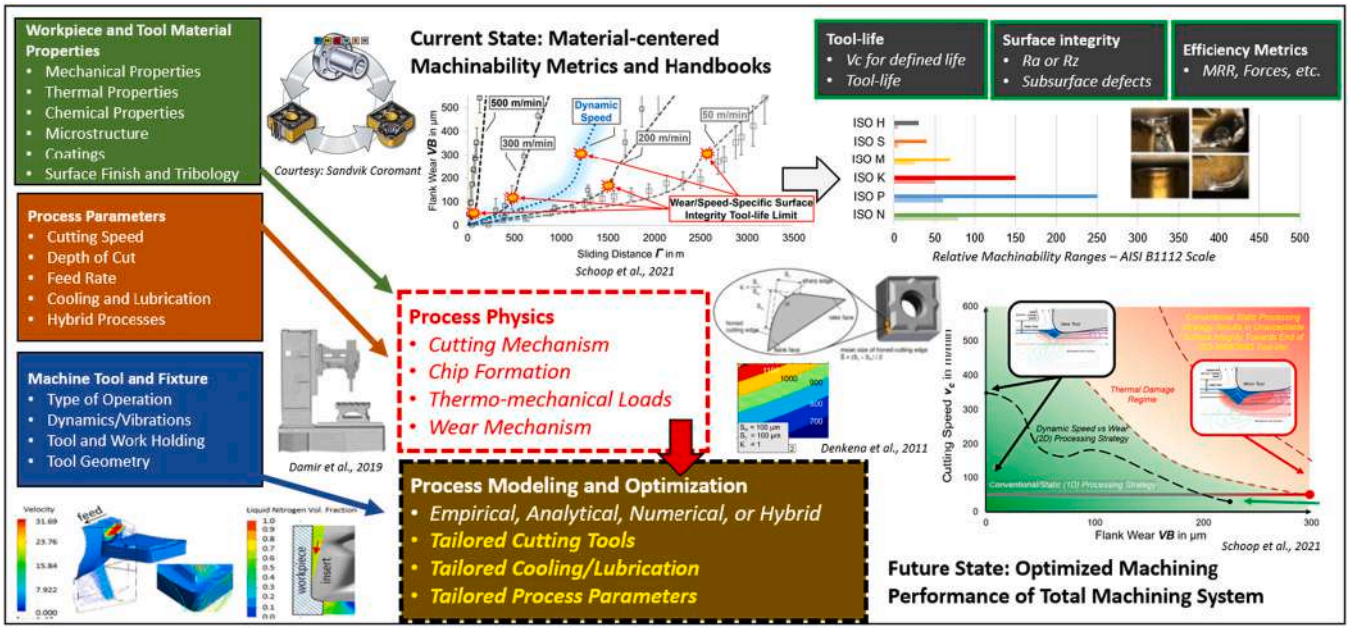

Fig. 2. Overview of Current State and Future Direction in Machinability Research [15–18].

compared to cast aluminium based on material properties alone. This reduced machinability generally exhibits itself in the form of increased cutting forces, less desirable chip form (e.g., continuous chips) and higher cutting temperatures, i.e., increased tool-wear at a given cutting speed. The latter behaviour of reduced tool-life due to increased thermo-mechanical loads on the cutting speed is typically regarded as one of the hallmarks of the concept of machinability, which attempts to generalize the ease with which a given material can be cut. Nevertheless, it should be noted that machinability is not a fundamental material property, but rather a complex assembly of specific behaviours (e.g., forces, temperatures, chip form, surface integrity, etc.) of the total machining system.

When cutting a given material at increasing cutting speeds, there will be increased thermo-mechanical loads on the cutting tool. As increased cutting speeds are often the most efficient method of improve the overall machining performance, there is an ever-increasing need for improved cooling and lubrication. Consequently, studying the influence of coolants/lubricants on machinability has become a well-established means for improving machinability and today's widespread use of cooling lubricants can be explained directly by the powerful impact of such metalworking fluids on improving machinability. Likewise, increasing use of super hard cutting tool materials and coatings, which offer improved 'hot hardness' to cut at ever increasing speeds, is motivated by the incentive to cut at more aggressive speeds and feeds, which offer greater profits and throughput. In some cases, dry or near-dry cutting may become possible with certain cutting tool materials and coatings, albeit with some negative influence on the workpiece material's surface integrity due to the increased thermal loads on the machined surface.

Overall, the key challenge associated with defining machinability primarily in terms of the response of the workpiece material is the fact that the total machining performance for a given cutting operation will always depend on the total machining system, i.e., the workpiece, cutting tool, coolant/lubricant, and machine tool, as shown in Fig. 2. Thus, comparison between machinability data sets is often difficult or impossible, as any change in the total machining system will substantially change the metrics used to define machinability (e.g., forces, chip form, tool-life, etc.). Researchers have long realized this, but even the most careful attempts to maintain consistency between different machinability studies (e.g., using the same machine tool/setup, coolant, etc.) are limited by a constant need to evaluate new tool geometries, coatings, coolants/lubricants, and machine tool and setup configurations. In this manuscript, we will attempt to provide an overview of the various approaches and metrics used to evaluate machinability. Our focus will be to provide a comprehensive overview, while also looking towards a more comprehensive approach to evaluating the total machining performance, particularly of cutting tools and their various design features (micro/edge geometry, chip breaker geometry, macro geometry, tool material, coatings, etc.).

3. Tool performance to evaluate machinability

Tool wear and tool life are the most widely spread used criteria for the evaluation of the machinability, because they deliver measurable, quantitative information regarding the resistance of the material against machining. Even though, as already shown, machinability is a system variable of the machining process and a large number of factors could play a role, the relative comparability of tool wear under identical boundary conditions with a single variable (one factor at a time) is an established method for assessing the material-related machinability of different materials or, for example, the machinability of one material under different cutting values. The machinability of materials with different cutting materials can also be evaluated on the basis of wear and/or tool life. The latter term is often equated with wear, but tool life can also be dependent on other factors than tool wear, so that an explanation of the term follows first.

3.1. Introduction – What is tool life?

Tool wear is defined as a continuous loss of material on the tool leading to a change in micro- and macro-shape. Due to the extensive thermomechanical and tribological load in the chip formation zone tool wear is a result of several superimposed mechanisms like abrasion, adhesion, diffusion and tribochemical reactions. In addition to these four mechanisms, which are commonly addressed in the literature of machining processes, the tribological science defines surface fatigue as a further wear mechanism [22] This results in different forms of wear like flank wear, notch wear, crater wear [23], oxidation [24], crack formation [25], plastic deformation [26] and build up layer/edges [27] occurring on the tool surfaces which are in contact with the workpiece or the chip. The most frequently characterized wear parameters are the

width of flank wear land and the crater wear depth on the rake face [28]. Based on the identified tool wear, an analysis of the tool life can be performed by defining a quantitative limit value for the wear parameters. As soon as the wear parameter is exceeded, the tool life ends. The wear parameter can also be characterized by a quality feature on the workpiece side, such as the diameter or roundness (in turning or drilling) or the surface quality [29], as well as a process parameter like a force or the spindle power [30]. Furthermore, few researchers developed a mathematical model based on machining mechanics and dynamics to predict cutting forces to estimate surface integrity, which is highly dependent on progressive tool wear [31,32]. Similarly Shekhar et al. proposed tool tip dynamics for the machining process [33]. Kumar et al., [34] introducing rolling motion at the tool tip via a rotating roller establishes rolling-sliding contact, reducing chip thickness and plastic strain versus fixed sharp or blunt edges. Generally, the tool wear progression has normally three stages, namely, initial, stable, and severe wear, which eventually leads to the end of tool life. Low machinability of a material normally leads to high tool wear rates and thus low tool life. Therefore, using tool life for machinability evaluation became one of the most common practices in both academia and industry.

3.2. Tool life as an indicator for machinability

Davim identifies tool life as the most important indicator for machinability [35]. This motivates to compare the tool life of diverse studies. However, this is complicated due to several factors. First of all, there are various variables that can be used to characterize tool life: the main time in which the tool was used for cutting [36], the cutting path that could be reached before the tool life criterion was exceeded [37], the number of cuts for interrupted cutting [38], the number of bore holes [39] or the volume of the removed material [24]. Mills and Redford developed a concept to get a comparable measurand for the tool life as an indicator for machinability by introducing the 60-minute tool life cutting speed. They tried to correlate such value to different properties of the machined material like chemical composition, microstructure or physical properties [40]. With this investigation they were not able to find a good definition of wear dependent machinability and concluded that the investigational effort is quite high. Therefore, they changed their basic idea and conducted accelerated wear tests, with which they tried to define the machinability as a property of the workpiece material by rapidly wearing tools through very high cutting speeds and using the resulting wear as a measure of machinability. This concept is very weak because it does not take the cutting conditions into account and uses parameters above the working area of the tools and is therefore not transferable to practical applications [35]. Based on a similar idea, Wang et al. developed a criterion especially for super alloys: the cutting speed at which the tool failure mode changes from uniform tool wear to sudden tool breakage [41,42]. As an alternative concept for machinability characterisation, Liu et al. introduced the tool life reliability, which is a quantity to describe how large the probability of the tool failure is after a certain cutting length. An exemplary course of the tool life reliability can be seen in Fig. 3. This approach might be suitable for making tool life investigations more comparable but requires a great effort in terms of experimental design and evaluation [23].

Moreover, the different types of wear forms and quantities to characterise them which are used throughout the literature make it difficult to compare investigations regarding the tool life-based machinability evaluation. Beside the most frequently used quantities to characterise wear like flank wear land width and the crater wear depth, the length of notch wear [43], the tool diameter of rotationally symmetric tools [44], the cutting edge radius and the weight loss of the tool is used to characterize tool wear [45]. It can be assumed that the tool life assessment is different when looking at flank wear than when analysing crater wear on the rake face. Some studies even use the tool life only as a qualitative factor for machinability by comparing photographs of the tools [46]. Another aspect when using the tool wear and tool life as an indicator for

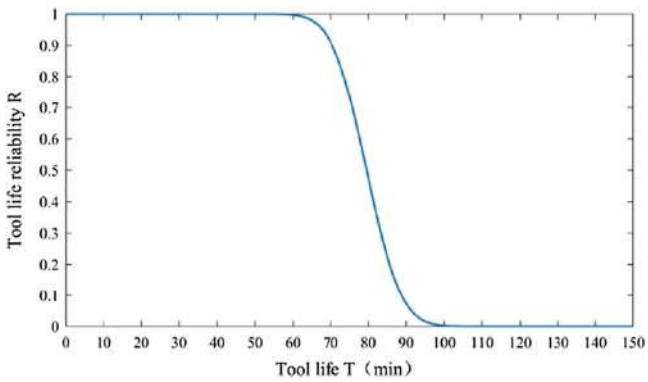

Fig. 3. Exemplary plot of the tool life reliability as a function of the tool life time [2].

machinability that needs to be taken into account is the level of the tool life criterion. For the same material this value can differ significantly. Dadgari et al. defined flank wear land width VB = 37.5 μm as the tool life criterion when micro-milling Ti6Al4V with a tool diameter of d_t = 1 mm and an axial depth of cut a_p = 0.1 mm [45]. Bouzakis et al. used a larger tool and a 20 times higher axial depth of cut a_p = 2 mm and defined VB = 150 μm as the tool life criterion for milling the same material [38]. According to the larger tool, the tool life criterion was increased. However, it does not increase to the same extent as the size of the axial depth of cut is enlarged from one case to the other. While the latter was increased twentyfold, the tool life criterion was only increased fourfold. The choice of a suitable value for the tool life criterion therefore depends not only on the dimensions of the tool and the uncut chip cross-section but also on various factors such as the tolerances of the workpiece quality and is difficult to compare from case to case.

Due to the large number of possibilities for selecting the boundary conditions for tool life investigations to evaluate machinability, comparability of different studies is limited. Within individual test series, however, tool wear or tool life offers a sensitive and validly evaluable criterion for comparing the machinability of different materials. Thus, Abouridouane et al. could demonstrate, that even alloys from one single group of materials can significantly differ in their machinability, like shown in Fig. 4a). For this purpose, the machinability of three different widely used ferritic-pearlitic steels was investigated by comparing the flank wear in twist drilling experiments. Compared to 27MnCr5, drilling of C60 lead to 43% higher flank wear after the same number of bored holes [47]. Based on a similar research hypothesis, Lalbondre et al. used standardized tool-life tests referring to ISO 3685:1993(E), in which they compared the machinability of the bearing steels AISI 51,100 and AISI 52,100 [48]. Even though the two alloys have a quiet similar chemical composition, the tool life for the same cutting speed in case of AISI 52100 only extents to approximately the half of AISI 51100 [49]. Even the content of a single alloying element can lead to relevant and nonlinear impact on the machinability of a material, like Geng et al. descript with the results of a machinability evaluation of 4Cr16Mo depending on the copper content within the alloy. They could show, that the flank wear is in general lower for the same cutting conditions, if copper is added to the alloy. But, this effect is not linear and even reverses when the copper content is increased from 1.4 wt% to 1.9 wt% [50]. Finally, the details of heat treatments can result in significant differences of the machinability. Hoseiny et al. investigated the influence of the martensitic packet size on the machinability of hardened steels, which depends on the heat treatment. The results show a general trend, that finer packet sizes lead to a longer tool life due to reduced mechanical loads on the tool. When the cutting speed is increased, the differences in tool life for the different states of heat treatment decrease, since the temperature in the cutting zone enlarges and consequently the tool properties become the more important

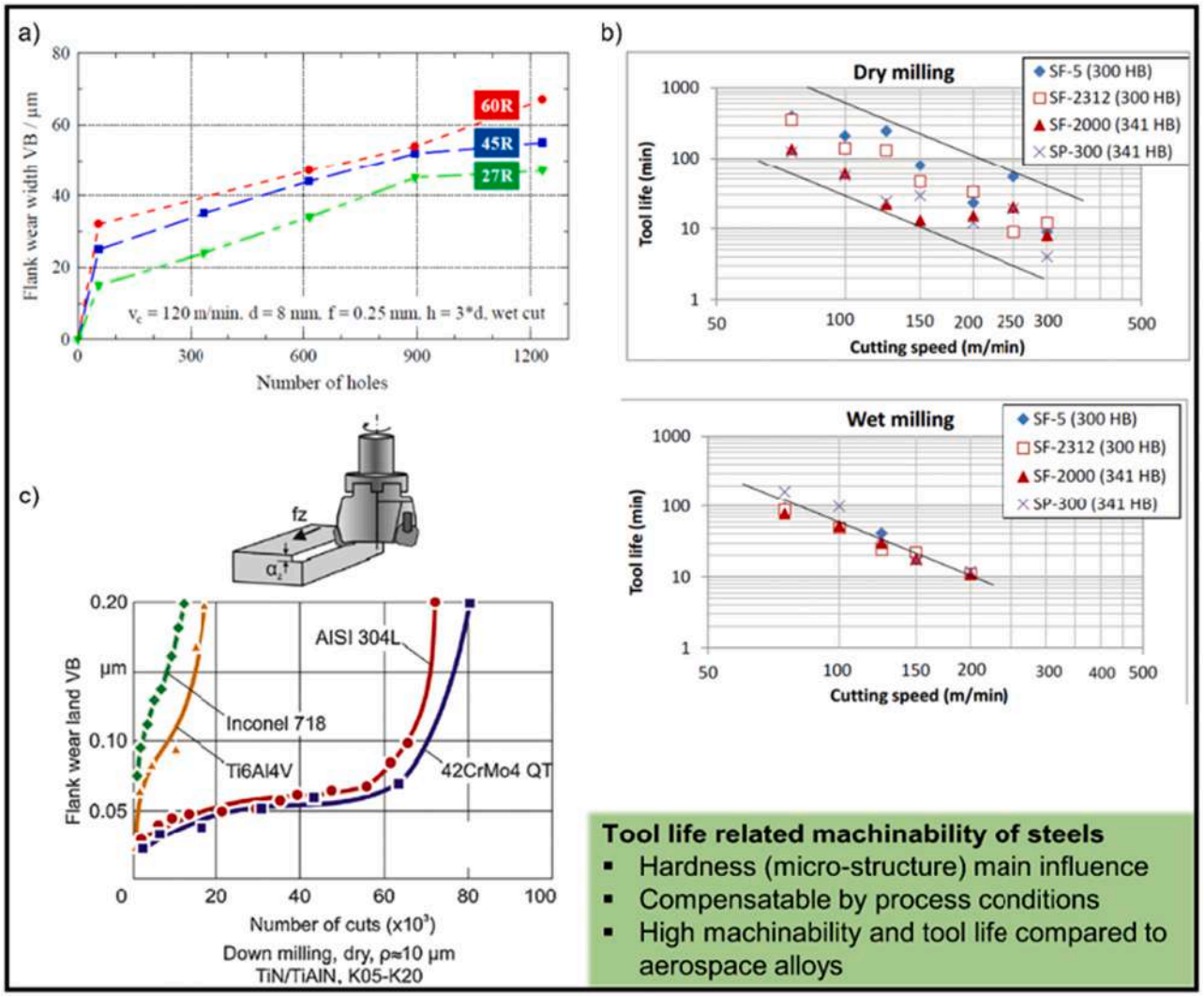

Fig. 4. Tool life related machinability of steels: (a) different machinability in a single group of materials [47], (b) influence of fluid application in machinability [48], (c) comparing machinability of steel with aerospace alloys [38].

influencing factor on the wear induced machinability of the materials [51]. Songmene et al. demonstrated that such significant influence of material properties on the tool life related machinability of steels can be compensated by the process conditions. Like shown in Fig. 4b), the differences in tool life of four tool steels which arise in dry milling, are nearly not measurable when conducting wet milling with the same parameters [48]. In addition, Magalhães et al. [52] investigated on dry turning AISI 1045 steel revealed feed as the governing factor influencing surface roughness, with cutting speed having minimal impact. Flank wear progression above 0.1 mm however accentuated roughness twofold. While micro-hardness reduced slightly, the alloy microstructure showed no detectable defects or cracks even after 35 min of machining at 275 m/min. Hence, dry steel turning with cermet inserts proves viable for tool life and surface quality sustainment.

Corresponding differences within a group of materials also occur in other classes of materials. Nayyar et al. compared the machinability indicated by the tool life for different graphitic cast iron grades for different continuous machining processes. This study showed that while the machining of Compacted Graphite Iron and Spheroidal Graphite Iron materials led to edge chipping on the tools after less than ten minutes of use, the Pearlitic Flake Graphite Iron did not lead to any significant tool wear even after 20 min [53]. Also in case of aerospace alloys the tool wear behaviour of different alloys can significantly differ. In this context, Parida and Maity fundamentally compared the machinability indicated based on different tool life criterions of three different nickel base alloys for room temperature and hot machining. With the help of flame heating, the authors set different initial workpiece temperatures of T = 300 °C and T = 600 °C. For all investigated materials the chip-tool contact length was significantly enlarged by the increasing temperature, which lead to an increase in tool life. This effect differs for the three alloys. While the temperature raise from T = 300 °C to T = 600 °C results in nearly a doubling of the tool life for Inconel 625 und Inconel 718, the effect for Monel 400 is negligible [45]. Olovsjö and Nyborg were able to identify a similar relationship when comparing different nickel-based alloys with varying grain sizes. As shown in Fig. 5a), the resulting tool wear when machining these materials under the same boundary conditions can be more than doubled by changing the microstructure [27]. In case of titanium alloys, also the route of material production shows impact on the tool wear behaviour: Sun et al. compared the machinability of forged and powder metallurgical (PM) Ti6Al4V based on the flank wear and the crater wear behaviour. Independently from the cutting speed, the PM material entails lower tool wear and thus higher tool life. This circumstance is attributed in particular to voids located on the underside of the chip, which reduce adhesive wear and tool temperatures, resulting in longer tool life overall [54].

Especially for machining aerospace alloys, the machinability in form of tool life is very sensitive to the cutting speed and the resulting tool

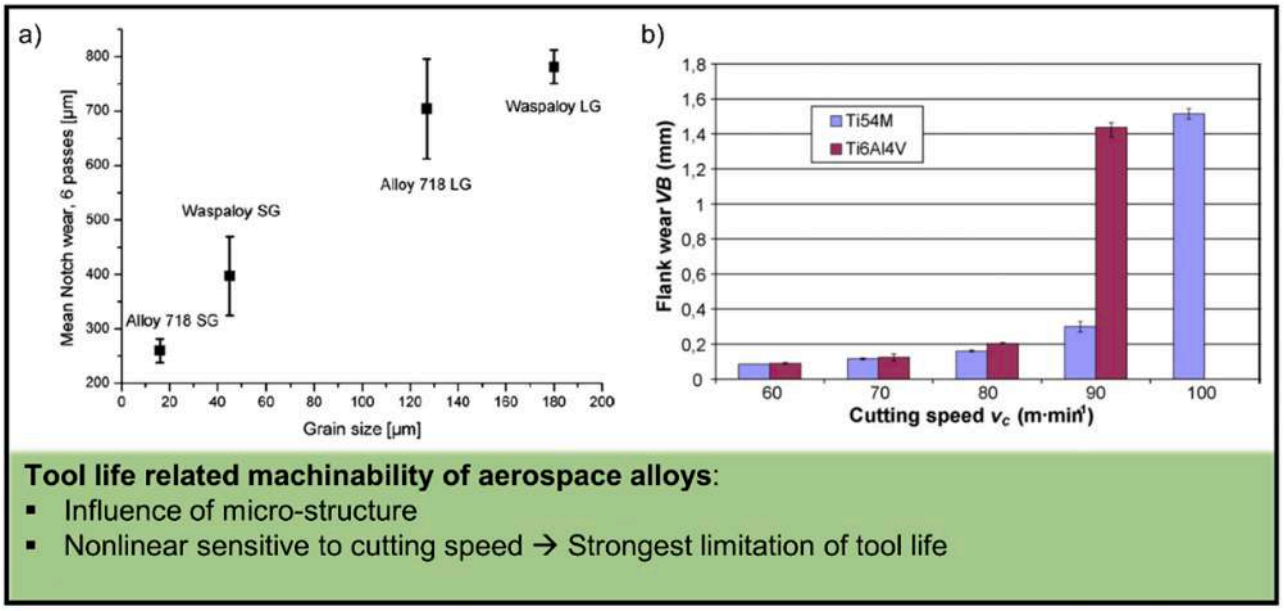

Fig. 5. Tool life related machinability of aerospace alloys: (a) tool wear can be more than doubled by changing the materials microstructure [27], (b) tool wear changes at varying cutting speed [55].

temperatures. Therefore, this factor has often be taken into account in machinability evaluation experiments. So Armendia et al. (see Fig. 5b) referred to the flank wear as an indicator for machinability when comparing the two titanium alloys Ti54M and Ti6Al4V for a varying cutting speed. While the wear of both materials were very similar for cutting speeds of $v_c = 60 \ldots 80$ m/min, it drastically increased for Ti6Al4V and only slightly for Ti54M at a cutting speed of $v_c = 90$ m/min [55]. In course of a production cost calculation, Priarone et al. investigated the tool life as a function of the cutting speed for Ti6Al4V and Ti-48Al-2Cr-2 Nb. The tool life range, which could be realised for Ti6Al4V for cutting speeds in the order of $v_c = 100$ m/min could only be reached for Ti-48Al-2Cr-2 Nb, if the cutting speed lied below $v_c = 40$ m/min [56]. Carvalho did investigations on similar interactions for two engine valve steels in the course of a machinability evaluation, where the tool life in form of removed material before reaching a certain criterion for flank wear was used. The results illustrate, that not only the absolute value of removed material for each single alloy varies depending on the cutting conditions like rake angle, cutting speed and cutting fluid distribution, but also the difference between the two materials does. These studies prove the strong influence of the cutting speed on the machinability of hard-to-machine materials [57].

All above discussed studies illustrate, that machinability evaluations even within one single group of materials is important for the targeted planning of cutting processes. Beside this, researchers have conducted tool life-based machinability evaluations to compare totally different workpiece materials. Klocke et al. conducted experiments on the machinability of 42CrMo4 +QT and Ti6Al4V depending on different positioning strategies of coolant nozzles. They identified significant differences for the two workpiece materials. First, machining of 42CrMo4 +QT resulted in vast notch wear, which did not appear for Ti6Al4V. Moreover, the cooling nozzle orientation, which resulted in the highest notch wear when machining the steel material, lead to the lowest tool wear in case of the titanium alloys. This illustrates the complex interactions of different influencing factors on the machinability analysed by evaluating tool wear behaviour [58]. In a similar approach Nath et al. investigated the tool life as a factor for the machinability for a stainless steel and two nickel-base alloys with the help of milling experiments. Depending on the cutting conditions, cutting the stainless steel leads to 7–10 times higher tool life compared to the superalloys. The authors elaborate that this does not mean, that the cutting values cannot be higher by the same factor, since wear does not increase linearly with uncut chip thickness and cutting speed [59]. Different materials therefore differ not only fundamentally in terms of machinability, but also in the way certain influencing factors change it. In the context of comparing the machinability of different types of materials, fiber composites should also be mentioned, as these can be made from diverse materials. Fig. 6 shows two examples of how much the machinability of composites varies depending on matrix alloy and reinforcement properties under the same boundary conditions with respect to the machining process [60].

While the studies discussed illustrate that tool life is fundamentally a well-suited parameter to characterize the machinability of a material and should always be considered in comparative studies and process planning due to its sensitivity to the material properties, the results of these studies have also shown that the tool life is subject to a large number of influences. The choice of boundary conditions for a study has already been discussed. In the next chapter, it will be discussed in detail that the tool life and thus the machinability are by no means pure material properties and that they are subject to a multitude of technological influences.

3.3. Challenges in tool life based machinability evaluation

The most common description of the machinability evaluated by tool wear is the Taylor equation. It calculates the tool life T_c as a function of the cutting speed v_c scaled by a factor C (1) [5].

$$T_c = Cv_c \tag{1}$$

Although this describes the tool life exclusively as a function of the cutting speed and all other influences are averaged in the scaling factor, it is still frequently used today. In fact, the validity was never proofed for state of the art tool materials like carbide and cutting speeds higher than 25 m/min [35]. In the last decades of research on tool wear behaviour in machining, many factors which significantly influence tool wear and life have been identified and investigated. For example, Basset et al. illustrated how the uncut chip thickness, the cutting speed, a tool coating and a preparation of the cutting edge affect the tool life when machining AISI1045. Within this investigation the tool life varies between less than one minute and more than 20 min [37]. This multitude of influencing factors brings with it the necessity of an extended tool life-machinability

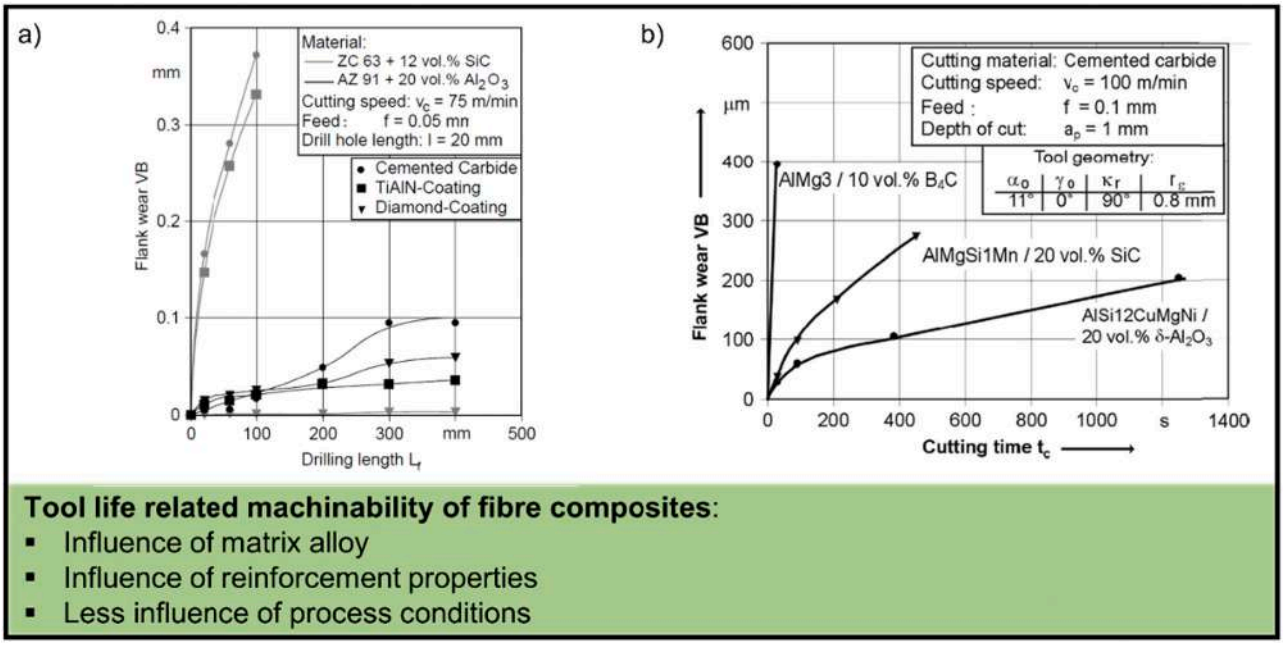

Fig. 6. Tool life related machinability of composite materials [60].

consideration. In order to be able to develop such a consideration, the broad field of influencing factors presented in the literature is briefly discussed below. Due to the large number of publications on this topic, no comprehensive coverage can be claimed. Rather, the aim is to highlight the most important influencing factors on the basis of a selection of high-quality references.

3.3.1. *Influence of workpiece properties on machinability*

As discussed in the previous chapter, in the classical definition of machinability, the workpiece strength is the central quantity which is considered to compare different cases [28]. On side of the workpiece properties there are a plenty of other factors which influence tool wear and tool life and thus the machinability. One important factor is the microstructure of the material. Machinability is for example determined by grain size [27], composition of the inclusions [61] and changes in the microstructure, which are induced by the cutting process [62], like conversion of austenite to martensite when cutting austempered ductile iron [63]. Moreover, the thermal properties of the materials have a significant influence on the machinability [64]. Beside the mechanical and thermal properties of the workpiece material, the chemical behaviour is of central importance for the tool wear. Thus, it is a major obstacle to productivity that tool wear in machining of ferrous materials

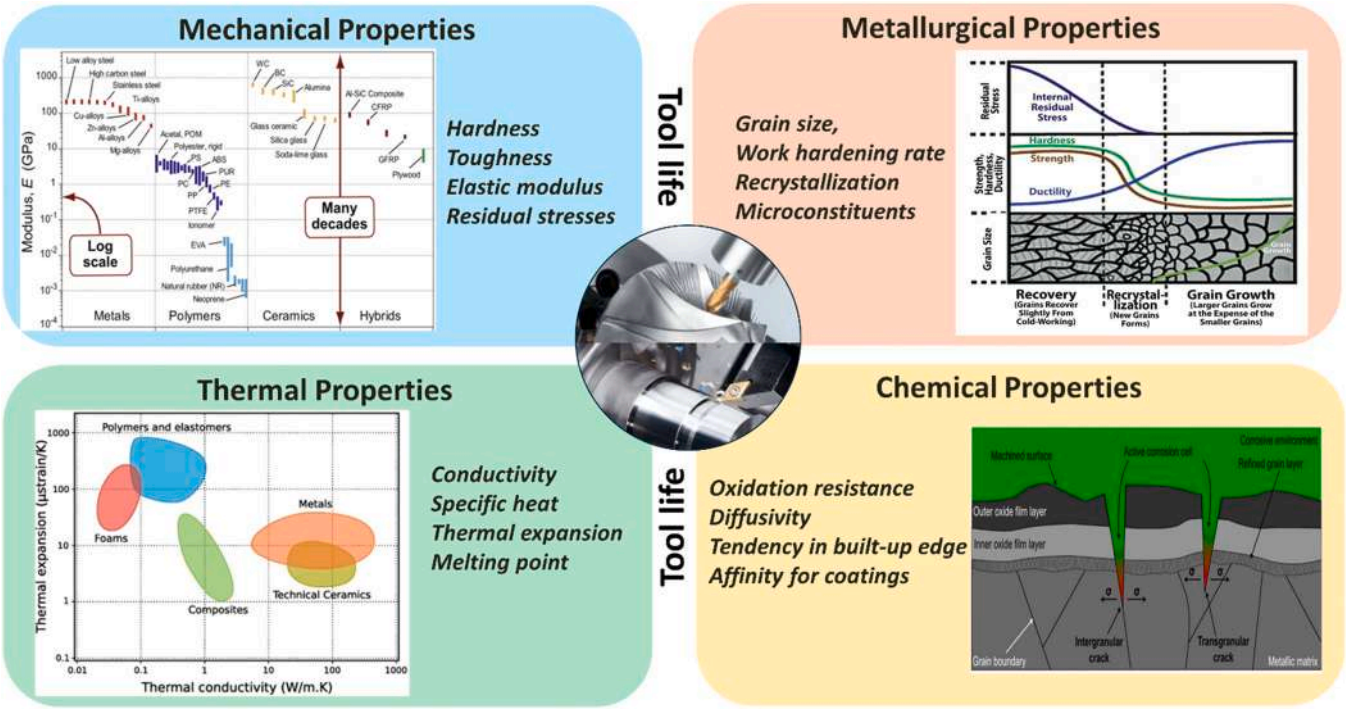

Fig. 7. Properties of the workpiece influencing the tool life as an indicator for machinability [27], [72], [73].

with diamond tools leads to thousands times higher wear rates compared to machining of other material groups with comparable strength [65]. The reason is chemical wear due to the affinity of the diamond to iron [66]. A suitable choice of orientation of the diamond in relation to the direction of loading during machining can enlarge the machinability of ferrous and single crystal SiC materials in precision diamond turning [67,68]. In the tool life-based machinability analysis of advanced materials such as composites, additional influencing factors like matrix alloy [60], type of reinforcing material [69], reinforcement volume fraction [70] and particle size of reinforcement [71] must be taken into account. Fig. 7 summarizes the workpiece-related properties, which influence the tool life-based machinability evaluation.

Contrary to the historical definition of machinability, it is obvious that tool life as a tool-related target value depends essentially on the properties of the tool. First of all, the choice of tool material has a major influence on tool wear. Not only if high speed steel (HSS), which only stands a few millimetres of cutting path when machining titanium [74], and polycrystalline diamond (PCD), which is the hardest known substance, is compared. Even inside a single group of cutting materials like cemented carbide, the tool life can differ up to ten times under completely identical boundary conditions [35].

3.3.2. Influence of cutting-edge treatment on machinability

Moreover, the tool coating has a significant impact on the wear behaviour of the tool. On one hand the type of coating [75] and its wear related properties like the temperature dependent critical impact force [76] fundamentally influence the tool wear and thus the machinability. On the other hand it is remarkable that also the coating application process [76], the detailed structure of multi-layer systems [77] and texturing of coatings [78] as well as the pre- and post-treatment of the tools and layers [79,80] influence the tool life in a considerable manner as well. In addition to the substrate and coating properties, the cutting edge micro shape has a significant influence on the wear behaviour and tool life and therefore on the machinability. As a general correlation it can be claimed that compared to a sharp tool a rounded cutting edge has an enlarged tool life which is justified by the higher mechanical stability and the more uniform temperature distribution [81]. In addition to the size of the rounding, its orientation [82] and a local adjustment of the roundings size [83] also affects the wear behaviour of the tools. Similar to the positive influence of coatings on the machinability, the intensity of the cutting edge shape-effect on tool life depends not only on the final shape, but also on the preparation history [38]. Another method of cutting edge treatment proposed by Cristian et al. [52] utilizes drag finishing, where SiC and Al_2O_3 abrasive mixes demonstrate that factors like plunge depth and drag time critically govern edge rounding levels. Meanwhile, positioning angle and depth impact uniformity across broaching tool teeth. In summary, drag finishing enhances broaching performance through predictable edge tuning superior to traditional blasting processes, with notable surface roughness improvements. To further enhance stability in robot-assisted machining, Guo et al. [84] designed an innovative milling cutter that regulates the contact force between the robot and workpiece to sustain stability during the milling process. The above discussed tool-related properties, which influence the machinability measured by the tool life, are compiled in Fig. 8.

3.3.3. Influence of cutting fluid on machinability

Beside the workpiece and the tool, the properties of the process significantly influence the tool life of cutting tools as an indicator for machinability. These influences are mainly based on the thermo-mechanical load spectrum, which depends on the process parameters. The cutting values like the cutting speed and the uncut chip cross-section [87] are the most important influencing variables and at the same time a measure of the economic efficiency of the process. Moreover, the cooling-lubrication concept fundamentally determines the machinability. While dry machining has become the state of the art for many materials [88], the use of cutting fluids is indispensable to reach an acceptable machinability when machining of difficult-to-cut aerospace alloys [64]. In this case sustainable cooling-lubrication concepts like

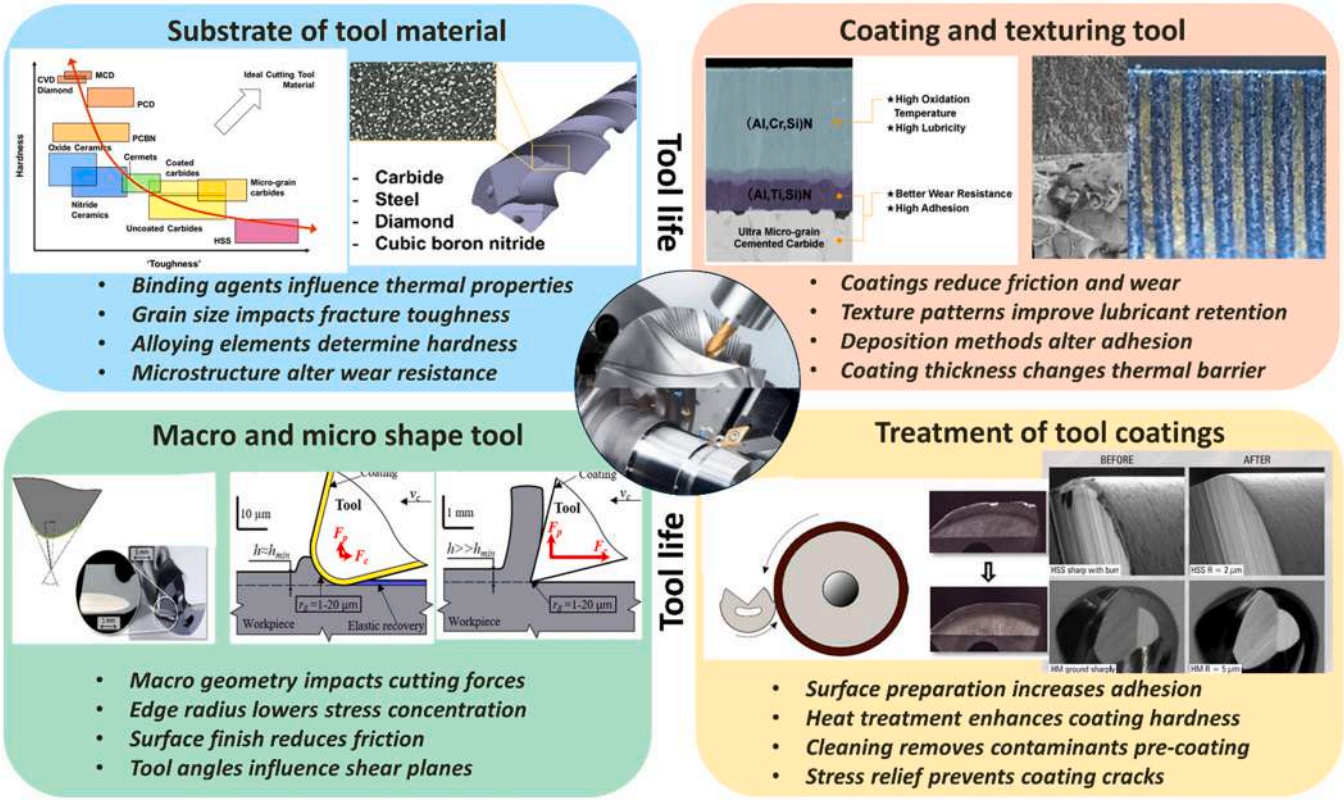

Fig. 8. Properties influencing the tool life as an indicator for machinability [24], [36], [80], [82], [83], [85], [86].

minimum quantity lubrication (MQL) quickly reach their limits and cannot provide sufficient machinability. Accordingly, energy- and cost-intensive cooling concepts such as flood cooling, high-pressure cooling or cryogenic cooling are necessary when machining difficult-to-machine materials in order to keep tool wear controllable and thus enable economical machining [89]. Such cooling concepts can be extended by process control strategies like discontinuous drilling [90] or vibration cutting [91,92], which improve the cooling performance. It is noteworthy that the influence of the cooling lubricant concept depends on the evaluated wear parameter. Machai and Biermann, for example, were able to show that CO_2 cooling compared to an emulsion can significantly reduce the flank wear during the turning of Ti-10 V-2Fe-3Al, but that notch wear is even completely prevented [43]. Pereira et al. [93] paired cryogenic cooling with MQL (CryoMQL) to enhance the machinability of difficult-to-cut alloys like AISI 304. Based on the experiments results of CryoMQL improved cutting tool life and enables higher cutting speeds in comparison to dry machining. CryoMQL also improved surface finish and forces relative to standalone cooling or MQL alternatives. In addition, Pereira et al. [94,95] proposed an innovative nozzle which delivers a hybrid cooling system, which combines CO_2 cryogenic and MQL. The main objective of MQL+CO_2 machining is to minimize or eliminate mineral oil emulsions, creating an eco-friendly and cost-effective process, which achieves machining performance over wet machining. Given the effectiveness and environmental benefits, MQL+CO_2 systems have strong potential for hard-to-machine aerospace titanium alloys and hardened bearing steels [94,95]. Further, cryogenic cooling with MQL lubrication using CO_2 as an internal coolant improved tool life when milling Inconel 718 compared to conventional emulsion coolants, demonstrating technical and environmental benefits [96]. How appropriate cooling strategies are used to increase tool life and thus improve machinability is detailed in section 7.1. Another basic approach to increase tool life and improve machinability by modifying the process is the targeted heating of the workpiece material. However, such an approach requires proper calibration with regard to the workpiece temperatures. If these are set too high, the additional thermal load on the tool can lead to an increase in wear compared to conventional machining without external heating [97]. Fig. 9 illustrates the different influences of the process properties on the tool-life measured machinability.

In summary, the discussion of machinability with regard to the tool clearly shows the complex and superimposed causes of tool wear and how differently sensitive tool life reacts to individual influencing variables, depending on the other boundary conditions. The multitude of correlations discussed in this section reveals that tool life as an indicator of machinability requires a holistic view of the machining process. This approach must include the influences of the workpiece properties, the tool properties as well as the process parameters in order to obtain a reliable assessment of the tool life. In particular, this also means that in comparative studies on tool life within single publications or across the boundaries of several papers, the documentation and presentation of all relevant boundary conditions is of central importance. In the sense of comparability of the investigation results, the parameters for quantifying the tool life as well as the tool life criteria must also be selected on the basis of scientific considerations.

4. Cutting force and temperature to evaluate machinability

Cutting force and temperature, as direct process outcomes in machining, are also widely used as the criteria for the evaluation of the machinability. In general, the more difficult to machine of the material,

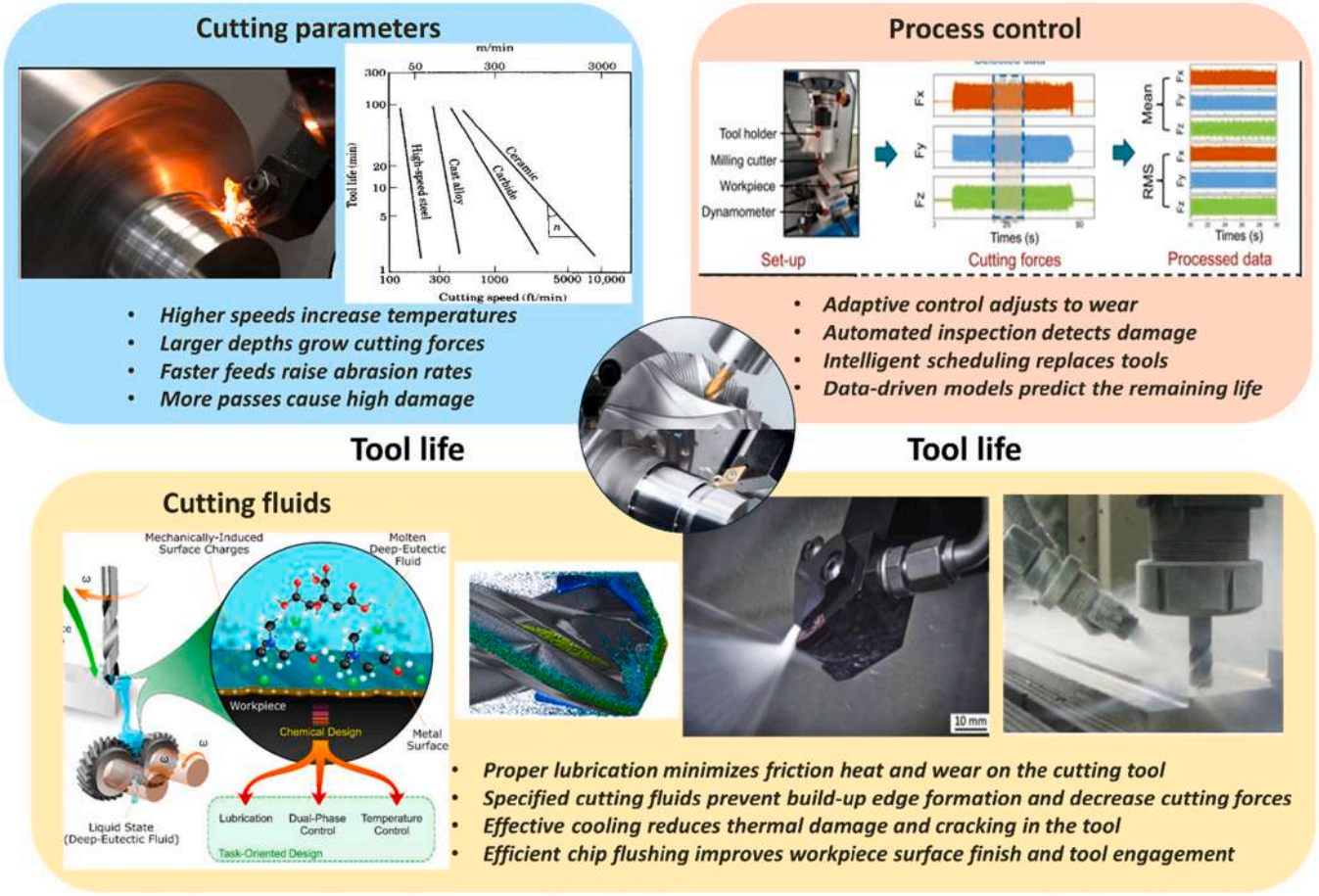

Fig. 9. Conditions of the process influencing the tool life as an indicator for machinability [45,89,90,98–101].

the higher cutting force and temperature will be generated in machining process. However, as they are also significantly influenced by the complex interactions between the tool-workpieces, e.g., cutting parameters and fluid usage, evaluating the materials machinability based on cutting force and temperatures has to be considered under particular circumstance.

4.1. Cutting force and torque for machinability evaluation

Machining processes can lead to high process forces, which can limit the machinability. The origin of process forces can be described based on the shear zones of the cutting process (Figs. 10–12). In the primary shear zone, the actual separation process of the chip takes place. Thus, process forces arise to overcome the shear strength of the material. The chip that slides along the rake face (secondary shear zone), leads to additional friction forces. Moreover, elastic-plastic deformations occur on the tertiary shear zone at the flank face and the cutting edge rounding, which lead to ploughing forces.

When it comes to the evaluation of machinability, the cutting forces are one of the most common mechanical criterions in a qualitative [102] and quantitative [14,103,104] way. The correlation between cutting forces and machinability has been investigated in many cases, for example by comparing the machinability of different steels. Thereby, a higher process force is associated with a reduced machinability. Another mechanical parameter, which is used to evaluate machinability, is the spindle torque [105,106]. In general, a high correlation between spindle torque and process forces exists [105]. The torque is therefore a suitable alternative value for assessing machinability. However, the underlying reasons for limits in machinability due to mechanical loads / cutting forces can be diverse. For example, the machinability can be limited by machine limits [107], high stresses on the cutting tool [108] or unfavourable loads due to the chip formation process [109]. Thus, a more differentiated view on cutting forces to evaluate machinability is necessary. In the following, three aspects of process forces that limit the machinability are discussed in more detail. First, the relation between local loads and machinability is discussed. Thereafter, the influence of the overall process forces is evaluated. Finally, the impact of dynamic cutting forces on machinability is presented.

The overall process force depends on a high number of factors, e.g. process parameters, material, tool geometry, and can be modelled as the result of uncut chip width b, uncut chip thickness h and empirical values (e.g. specific cutting force $K_{c1.1}$ and exponent m_c). One of the most common process force models is the model by Kienzle [110]. The cutting force can be calculated as

$$F_c = k_{c1.1} b h^{1-m_c} \tag{2}$$

The relationship of the cutting force model shows that an increase of feed f and depth of cut a_p leads to an increased cutting force. The specific cutting force $K_{c1.1}$ are, however, known from literature for most materials and therefore can give a good initial estimation to assess the general workability of different materials. The specific cutting force can be used as rough estimation of the local loads. Therefore, specific forces were

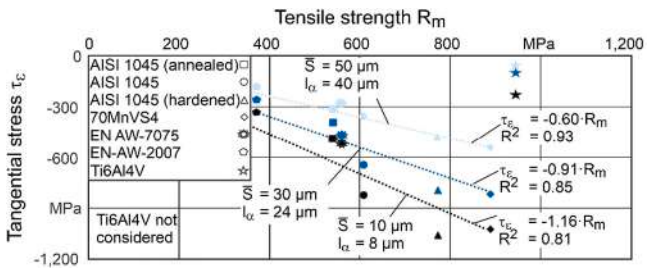

Fig. 10. Correlation of tensile strength Rm of the material and tangential stress τ_e [108].

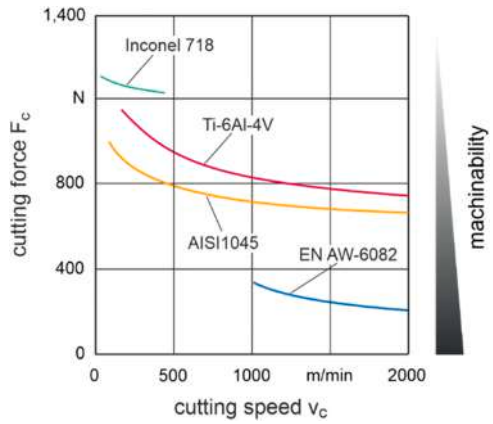

Fig. 11. Correlation between cutting force F_c and cutting speed [119–121].

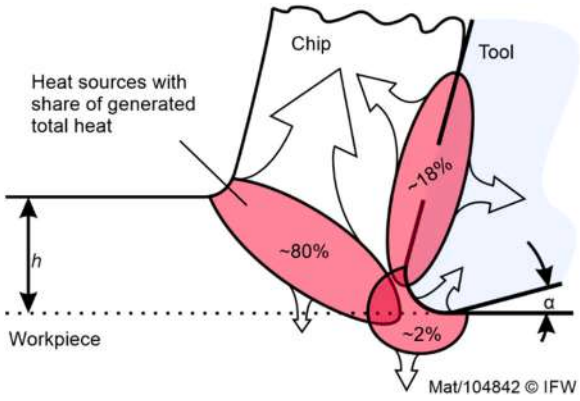

Fig. 12. Heat generation and dissipation adapted after [127,135,136].

already used in several publications to assess the machinability of different materials, e.g. titanium [104], cooper [111] or tungsten carbide [112].

For a more differentiated view on tool wear, the stresses acting on cutting tool can be utilized. Cutting edge failure occurs when the local stresses exceed the strength of the tool material [108]. Consequently, higher stresses reduce the machinability. The stresses on the cutting edge are thereby mainly influenced by the workpiece material and the cutting edge rounding, Fig. 10 [108]. In general, a higher tensile strength of the workpiece material and a lower cutting edge rounding increase the tangential stresses and thus lead to a reduced machinability. The determination of local stresses is thereby associated with a high experimental effort. Early attempts to determine the local stress distribution was to use photoelastic tool material [113,114]. However, the results are not quantitatively transferable to other tool materials. Further experimental methods to identify local stresses are the split tool [115,116] and the reduced contact length [117,118], which both require an extensive tool preparation.

In addition to the relationship between process forces and shape of the uncut chip shown before, the process forces are also dependent on the cutting speed. For increasing cutting speeds, a decrease in cutting force is found [119–121], which is attributed to changing tribological conditions and thermal softening effects. Amor and Suter also indicate changing chip formation with increasing cutting speeds [119–121]. Based on the comparison of the different materials in Fig. 12, it can be said that high process forces are often related with hard-to-cut materials. Nevertheless, the reduction of process forces due to high cutting speeds as indicated in Fig. 11 is unusable in most cases since the thermal loads increase.

Due to machine tool limits, the process forces can limit machining

performance and machinability [122]. In heavy machining operations, the power limit and torque of the spindle, which are the result of the cutting forces, are the main limitation in productivity [107]. Furthermore, high process forces can lead to tool extraction [123]. However, those limitations are based on limits of the machine tool and not the cutting process itself.

Another important aspect when evaluating process forces in terms of machinability is the dynamic behaviour of the cutting forces. When built-up edges occur, the process forces in general decreases. Nevertheless, due to the dynamic load on the cutting wedge and the poor surface finish, the machinability can be classified worse [124]. Negative effects on machinability are also known by segmented chip formation due to the high fluctuation on cutting forces [125] and specific cutting forces [109]. These considerations are currently not taken into account when evaluating machinability based on the process forces.

Finally, it can be said that the overall cutting force is especially associated with machine tool limitations. For a tool wear related evaluation, local parameters, e.g. local stresses or specific cutting forces are more suitable to assess the machinability. However, dynamic chip formation effects, e.g. built-up edges and segmented chip formation, strongly influence machinability and cutting forces and are currently not considered when evaluating the process forces in terms of machinability.

4.2. *Cutting temperature for machinability evaluation*

The heat, generated during cutting operations, affects the chip formation mechanics, the contact friction, the tool wear mechanisms, the tool life, the surface finish and integrity as well as the machined tolerances. Therefore, the knowledge of the heat partition and the temperature distribution in machining is an important issue to evaluate machinability. In geometrically defined machining, the biggest proportion of the introduced mechanical power is converted into thermal energy. According to Schmidt and Shaw, a smaller proportion of the mechanical energy results in structure transformation of the workpiece material [126,127]. Also, Bedekar et al. reported phase transformation and grain refinement next to thermal energy in hard-turning [128].

Temperature measurement in metal cutting has been studied with a wide variety of techniques [129]. However, measuring cutting temperatures accurately during machining operations is challenging due to the small size of deformation zones. Temperatures decrease rapidly within a small distance from the cutting tool edge, hence obtaining reliable data is difficult. In this regard, various empirical, numerical and analytical modelling approaches have been developed to predict the cutting temperatures at different shear zones [130–133]. In general, the same as cutting force, heat sources in the contact zone of tool workpiece and chip are classified in a primary, a secondary and a tertiary shear zone [134]. These average shears of the total induced heat and the heat dissipation according to Kumar and Ajay [135], Shaw [127] Komanduri [136] are summarised in Fig. 12. Although the cutting heat distributions in chip, cutting tool and workpiece have not come to a consensus, a large amount of total cutting heat flowing into chips has been recognized as a main reason leading to a relative low temperature on workpiece surface. Due to the adjacent heat source of the primary shear zone, a large portion of the heat of approx. 70 - 90% is dissipated through the chips, while approximately 10 to 30% go into the workpiece and the tool [126, 127,135].

Vieregge has shown that the exact distribution of the heat quantity depends on the process variables, the manufacturing process as well as the tool-workpiece combination and thus cannot be generalised [137]. The results of Abrao and Aspinwall suggest that the overall temperature increases with the cutting speed, feed rate, depth of cut, and tool wear, and an increase in the thermal conductivity of the tool material causes an elevation in the temperature of the cutting tool and a reduction in the temperature of the chip when cutting hardened bearing steel [138]. For low conductivity materials that means more heat is transferred into the tool and less into the workpiece or chip [136,139,140]. This is also shown in the thermographic measurements from Armendia et al. in an orthogonal process during machining of Ti-6Al-4 V compared to 42CrMoS4 [141]. Comparable results are also given by the calorimetric measurements by Schmidt, in which the heat distribution between chip, tool and workpiece is significantly dependent on the thermal conductivity of the material pairings and the cutting speed [126]. These schematic dependency of the thermal properties of the workpiece material is shown in Fig. 13. First, it can be seen that measured temperatures in the cutting zone significantly vary over the cutting speed. Secondly, it can be seen that materials with low capacity to take up heat e.g. TiAl6V4, lead to high temperatures in the cutting zone, whereas materials like the aluminium alloy AlCu4PbMgMn lead to moderate temperatures even at high cutting speeds and therefore high induced thermal energies into the material. These high portion of heat induced into workpiece and chip enables the dissipation of thermal energy from the direct machining zone and therefore limit wear phenomena and thermal induced material changes like oxidation or thermal induced residual stresses.

For the classification of machinability mostly wear and cutting forces are used. Most studies rely on a supporting role of temperature measurements. The temperature is often used only for materials that result in high thermal wear. For example, Kikuchi used overall temperature directly to assess machinability [145]. The study investigated the machinability of two commercial titanium alloys (Ti–6Al–4 V and Ti–6Al–7 Nb) and free-cutting brass using the cutting temperature. The metals were slotted using carbide square end mills under four cutting conditions. The cutting temperatures of Ti–6Al–4 V and Ti–6Al–7 Nb were significantly higher than that free-cutting brass resulting in lower machinability. This result coincided with the relationship of the magnitude of the cutting forces measured in a previous study as well as with the tool life indicating a better machinability for low temperature conditions [146]. Eric and Nedic introduced a machinability index to evaluate machinability based on investigations on artificial thermocouples when machining steel of various hardness. The machinability index is defined as quotient of the measured temperature of the reference material to the material investigated in percent [147]. This index enables the investigation of the influence of technological parameters like machining regime, tool material, cutting geometry, hard layers etc. on cutting temperature and can be used to determine and compare the machinability of materials [148].

Even though there are only few studies that evaluate the machinability based on cutting temperature, there are a lot of investigations that correlate the cutting temperature with challenging cutting conditions and tool wear. Ueda et al. investigated the temperature on the rake face of a chamfered CBN cutting tool used on hardened steels of various compositions and hardness [143]. There findings indicate that an increase in material hardness leads to significant increase in temperature accompanied by a doubling of the flank wear and cutting forces when turning AISI1045. This is supported by investigations of Mozammel and

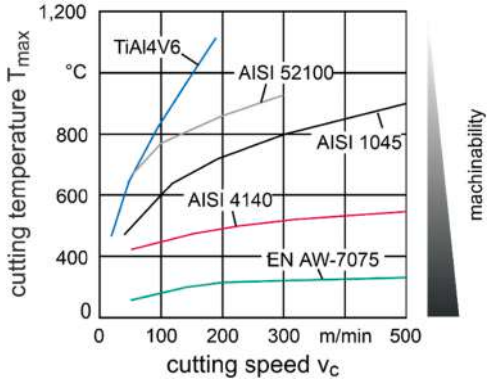

Fig. 13. Schematic temperatures dependency of various materials over cutting speed after [108], [125], [138], [142–144].

Nikhilshowing the material hardness influences cutting temperature for dry and wet cutting conditions, due to an increased restraining force caused by the increased material hardness [149]. This means that the higher hardness leads to higher temperatures and a reduced machinability.

Various studies have shown that in particular an increase of the cutting speed during machining has a great influence on the increase of the deformation rate and the converted power, leading to increased temperatures [150], [151]. In most cases, this changes the material behaviour in the shear zone and leads to an often unfavourable change in chip formation [152–154], e.g. a segmented chip formation. It can be summarized, that temperature is a limiting factor for cutting speed in many materials, leading to increased tool wear and thus tool failure [129]. The main reason for these problems is that the temperature increases asymptotically with cutting speed approaching the workpiece material melting temperature [155]. High temperatures also favour the progress of chemical and diffusive wear on the cutting tool [156].

Temperature increase accompanying with tool wear can also influence the workpiece quality, which is commonly used to evaluate machinability. With increasing tool wear, the friction between the workpiece surface and the tool flank increases and the heat generated in this area becomes more pronounced. As a result, the total cutting energy increases and the temperature of cutting edge rises [157]. Consequently, the influence of the temperature on the surface layer of the workpiece becomes significant. The temperature is closely related to the integrity of workpiece surface such as residual stress, hardness, and surface roughness [158–162]. Umbrello reported white layer formation shaped by thermally induced stresses when machining [163]. This effect is more dominant in case of machining low conductivity materials like Ti6Al4V. For this kind of materials, the temperature distribution is more concentrated in a narrow area near the tool tip [141]. Therefore, the temperature in the cutting zone can limit the part quality for difficult to cut materials. Tanaka el. Al. showed that a low conductivity of the cutting tool as well as high wear leads to increased temperatures on the cutting edge and therefore a reduced surface integrity. This highlights the critical role of temperature regulation during machining operations.

Besides the numerous negative effects of cutting temperatures on machinability, for materials with low heat penetration coefficients, the tendency to thermal softening and therefore a reduction in process forces can be achieved [121]. In this context, the temperature can be used to evaluate the thermal softening and thus the machinability of specific materials to optimise cutting conditions. This effect is used among others in high-speed machining, as well as thermal assisted machining which will be commended in section 7.

4.3. Combination of cutting force and temperature for machinability evaluation

In principle, high temperatures are a factor that have negative influence on machinability and can be used to evaluate machinability. However, because of the complex measurement technology and the positive effects of temperature due to the thermal softening effect, for example in hot machining, it is more common to use cutting forces and wear for the evaluation of machinability [164]. In addition, the temperature itself is not directly of economic relevance, but influences relevant factors like tool wear and surface quality. Therefore, to increase productivity and reduce wear, coolants are excessively used, to be able to machine at higher cutting speeds and consequently higher thermal loads [165].

As temperature and cutting forces are mostly used in combination to evaluate machinability, those dependencies are summarised in Fig. 14. In this way, it is possible to indirect connect the impact of workpiece material properties on machinability by observing cutting force and temperatures.

It can be seen that the resulting temperature at the cutting zone depends on the thermal effusivity of the machined materials.

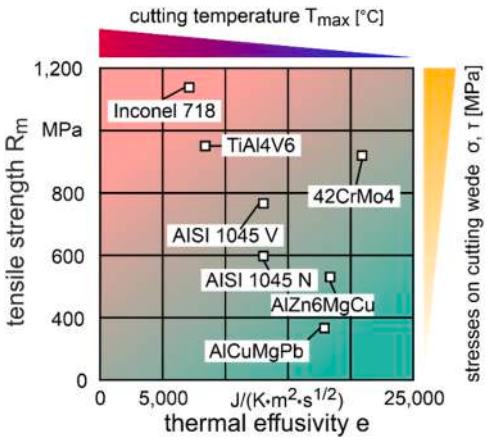

Fig. 14. Material classification according to machinability [108,142,143].

Consequently, titanium alloys and Inconel 718 have a low ability to dissipate heat from the contact zone by the chips in comparison to AISI 1045 or aluminium alloys. Here, the capability of the material to take up heat leads to lower temperatures in the contact zone and reduce thermal induced wear phenomena. For materials with low heat penetration coefficients, thermal induced wear rates result in increasing wear of the cutting edge in form of flank and crater wear. In addition to the thermal properties, most materials with low thermal conductivity also have high tensile strengths. As also shown in in Fig. 13 and summarised in Fig. 14, high tensile strength leads to high stress values on the cutting edge in machining of those materials.

Therefore, the general machinability of materials can be classified by evaluating temperature and cutting forces. On the one hand, good machinability for materials with high thermal conductivity and lower tensile strength, which lead to low cutting forces and lower temperatures in the machining process, are classified by slow wear rates, indicated by the green zone in the Fig. 14. On the other hand, difficult to machine materials like TiAl6V4 with high tensile strength and low thermal conductivity, lead to high thermomechanical loads and therefore increased wear rates, which influence the workpiece surface properties. These materials are in the red zone in the Fig. 14.

5. Influence of chip form and breakability on material machinability

5.1. Influence of chip formation mechanisms on material machinability: principles

Every machining process is based on the separation of chips from the workpiece (Fig. 15a). The cutting edge penetrates the material and shears it over the ‘primary shear zone’. When the maximum shear stress of the material is reached, it begins to flow. The emerging chip is deformed elastically and plastically, and it flows off over the rake face of the cutting edge: this area of deformation is called the ‘secondary zone’. The ‘tertiary zone’ describes the friction area between the flank face of the tool and the new surface [166–169]. The existence of a chip can be divided in chip formation and flow, chip breakage, and chip disposal [170,171]. Overall, chips with different properties result. The type of chip formation strongly depends on the material properties. Nevertheless, it can change while varying process parameters, lubrication/cooling conditions, cutting tool material and geometry[168,172]. The properties of the chip have a significant influence on the machinability criteria, such as tool wear, cutting force and surface quality/integrity [166].

The chips can be classified by their microscopic structure related to the type of chip formation or their appearance, which means the chip shape [166], [168–170,172]. According to Fig. 15*b*, the four types of

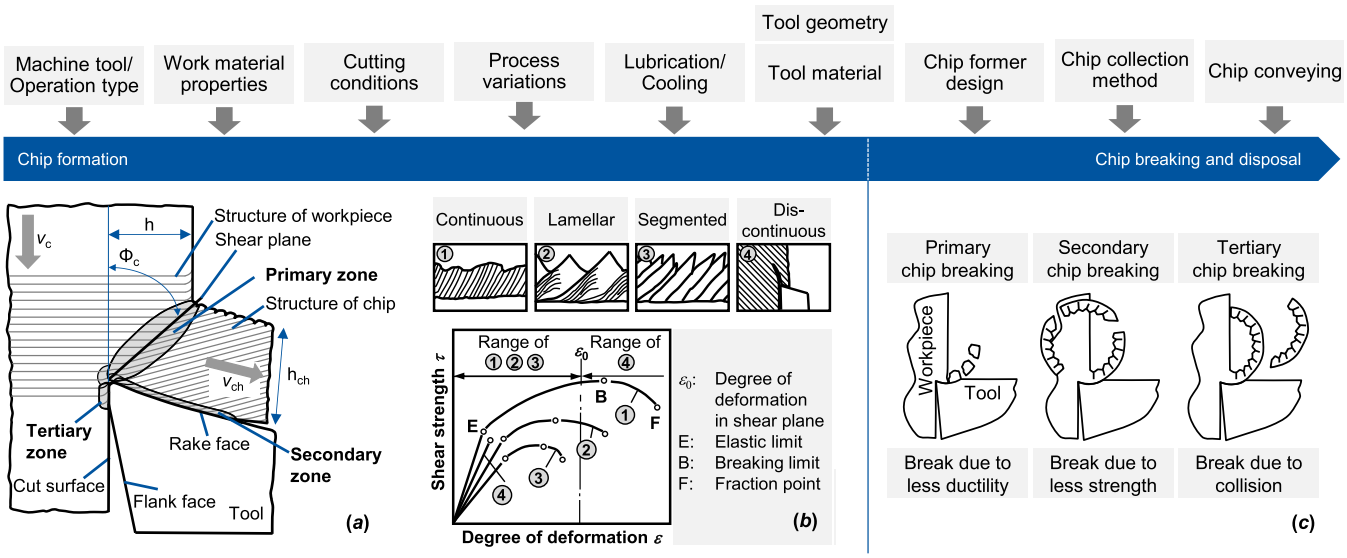

Fig. 15. Influencing factors on chip formation and breakability, according to [170,173]. (pictures are adapted from [167,168,174]).

chip formation are the continuous chip (1), the lamellar chip (2), the segmented chip (3) and the discontinuous chip (4), where the segmented chip can be considered as a special case of the lamellar chip. Continuous chips result under steady conditions when cutting ductile materials like pure copper (i.e., when the degree of deformation in the share plane is $\varepsilon_0 < \varepsilon_B$). The material is evenly deformed under uniform friction conditions. In contrast, lamellar chip formation occurs when $\varepsilon_B < \varepsilon_0 < \varepsilon_F$ or the present friction conditions between the tool and the emerging chip change fast (stick-slip effect). Lamellar chips are characterized by the appearance of areas with locally enhanced structural deformations which are defined as '(adiabatic) shear bands' [168,175,176]. Shear bands are formed as a result of thermo-plastic instability. Under certain conditions, thermal softening dominates over mechanical hardening and the originally uniform deformation is suddenly concentrated in a small area [177–180]. This happens during machining of high-strength materials with good deformability, especially when high cutting speeds are applied [175,176]. Segmented chip formation occurs under comparable conditions when the shear strength of the material is exceeded, following chip segments are detached and fusing again ($\varepsilon_F < \varepsilon_0$). Segmented chip formation further appears as a result of deformation induced embrittlement of the microstructure. Discontinuous chips form when no plastic deformation takes place before fracture which happens mostly when cutting brittle materials like cast iron or titanium aluminides [168,181]. Machinability is strictly correlated to the chip shape and chip formation mechanism, as detailed in Section 5.2 for the most common workpiece materials. Moreover, in the industrial practice, chips are usually classified on the basis of their macroscopic shape [172, 174]. One possible classification of the chip form is shown in Fig. 16. To achieve reliable machining processes with high levels of productivity, chip control is mandatory. It includes efficient breaking and effective removal of the chips. The chip shape determines how effectively the chips can be evacuated from the cutting zone and out of the working area of the machine tool. Unfavorable chip forms lead to unplanned interruptions of machining processes for manual chip removal by the machine operator, which inhibits the automation and subsequent digitalization of processes. Lack of chip control can further lead to degradation of part quality, as well as rapid tool wear and catastrophic tool failure [170]. In addition, estimating the temperature generated during machining in the tool and formed chip is very essential in order to eliminate progressive tool wear and obtain good surface integrity [182].

Three causes of chip breakage can be distinguished based on the stage of chip existence at which breakage occurs, as shown in Fig. 15*c*. A

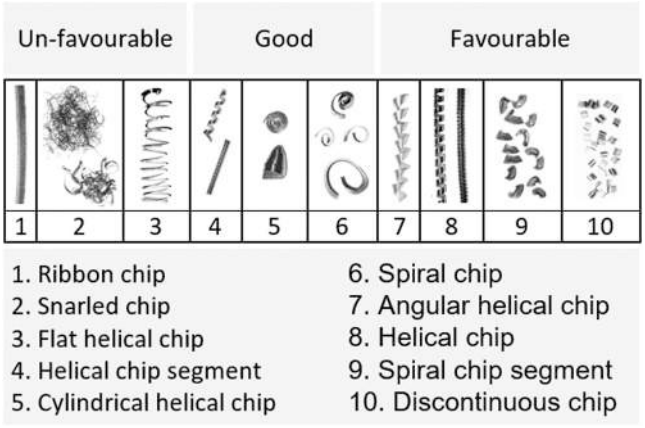

Fig. 16. Chip shapes according to [168].

primary chip breakage happens in the stage of chip formation due to low ductility of the machined material. Chip breakage in the chip flow stage is specified as secondary chip breakage when it is caused by low fracture resistance of the chip. Tertiary chip breakage is induced by collisions of the chip with the tool, workpiece or other external objects [174]. The handling of the chips during disposal can be evaluated by means of the chip volume ratio RZ. This value represents the ratio of the bulk chip volume to the removed material volume. Long ribbon chips lead to high ratios of RZ > 100, small chip segments show ratios of RZ < 10 [183]. How the chip curls when is no longer in contact with the rake face depends on multiple conditions of the cutting process [171].

5.1.1. *Qualitative Metrics*

Chip morphology has long served as a valuable qualitative indicator for machinists to gauge the performance of cutting processes, especially for steels. Decades before quantitative sensors, experienced operators intuitively inferred the machining state from visual and tactile chip characteristics. In addition to chip morphology, monitoring chip color provides valuable real-time assessment of cutting temperatures, as color directly indicates heat generation during shear and friction, influenced by parameters like speed, feed, depth of cut, and workpiece thermal properties [184]Color gradients from blue/purple to yellow/brown signify rising temperatures from oxidative reactions. By comparing chip

colors to established thermal ranges, operators can prevent defects like tool wear or metallurgical changes. Strategically selecting conditions to control temperature, aided by the visual feedback of chip color patterns, is thus critical for maintaining surface integrity. Taylor's tool life model relates cutting variables to wear rates (see equation 3) [185]. Taylor's pioneering tool-life tests linked incipient tool failure to a transition from continuous to discontinuous steel chips. Integrating such quantitative prediction models with expanded chip colour databases can enable adaptive control of speeds for optimal tool life. Beyond temperature, colour also signals issues like built up edge from adhered work material.

$$VT^n f_z^a a_p^b = C \tag{3}$$

Where n is the exponent related to the tool and work pieces; f_z is the feed per tooth; a and b are the exponents depends on what materials for the tool and work pieces; a_p is the depth of cutting, and C is the constant.

The color spectrum follows principles of metal oxidation - blue and purple chips indicate temperatures up to 500 °C from high speeds and loads. Balancing heat input by adjusting conditions based on colour is thus key for machining quality surfaces. The chip colours blue and purple shades warn of undesirable effects like work hardening or crack initiation on the cutting tool. Colour gradients hence serve as early indicators of unsuitable conditions before visible tool damage. Prompt parametric corrections can thus improve process performance. Korkut et al. [186] demonstrate how feed rate, cutting speed, and depth of cut influence cutting temperatures. Slower thick blue chips imply higher forces and poor evacuation. Optimised machining hence produces efficient thin chips. Other studies by Cook, Wright, and Armarego established that steel chips turn bluish or straw-colored at low speeds due to strain hardening and improper heat dissipation. Bright yellow chips indicate suitable 25–100 m/min speeds for medium carbon steels. Higher speeds produce darker yellow to brown chips associated with excessive temperatures softening the material. The inclusion of interactive colour-feed matrices into existing tool life models would facilitate automated adaptive control for optimal parameters. Overall, chip colour provides a visual metric to gauge temperature, identify improper conditions, adapt speeds, prevent tool damage, and maintain surface finish and accuracy [187].

Problems like inadequate coolant or lubrication also manifest as color changes in steel chips. Flood cooling is critical for regulating interface temperature and flushing away hot debris. Insufficient coolant flow rates directly contribute to thermally dominant machining where chips and workpiece surface turn blue due to temper colors. Similarly, low lubrication deprives the cutting zone of critical boundary layer protection, accelerating tool wear, and temperature rise. This manifests again as blued chips with oxidized segmented edges, signaling dysfunctional lubrication. Overall, qualitative analysis via physical chip examination forewarns operators about suboptimal speeds, cooling, or lubrication well before quantitative sensor detection or product inspection. However, qualitative reliability depends heavily on consistent operator background and experiences for accurate inference. Enabling automated quantitative monitoring of chip traits like color, shape, and surface textures can potentially boost the value of morphological analysis.

An overview concerning the correlation between chip morphology, breakability and machinability of the main material groups of engineering interest is given in Table 1, and further detailed in the following. The order of the sub-sections is based on the typically-occurring types of chip formation, from continuous to discontinuous, according to Fig. 15*b*.

5.2. Influence of chip formation mechanisms on material machinability: case studies

5.2.1. Copper alloys

Copper and its alloys are frequently used for applications in electronic, automotive and sanitary industry. In these cost-sensitive

Table 1
Effects of chip formation on machinability criteria.

Material	Frequent Type of Chip Formation and Chip Shape	Mechanisms/ Observation	Possibilities to Improve Machining Performance
Copper alloys	Continuous chip formation (binary brass materials) [188–191]	Chip formation largely depends on zinc content and phase composition [188–191]	Described general disadvantages of very long chips (seeFig. 16)
	High chip compression [188–191]	CuZn-Alloys with up to 37% Zinc consist purely of ductile α-CuZn phase [188–191]	Limited productivity in highly automated machining
	Very long chips [188–191]		
	More segmented chips (heterogeneous brass materials, high zinc contents up to $m_{Zn} = 42\%$) [188–191]	Materials consist of a mixture of α- and β-CuZn which increases hardness and tensile strength while reducing ductility[188–191]	Chip segmentation / breakability improves with increasing contents of β-CuZn and rising tensile strengths [189–192]
Aluminium Alloys	Long ribbon chips [168],[193]	Chip shape caused by material properties when cutting (non-) hardenable alloys in a soft state[168], [193]	Described general disadvantages of very long chips (seeFig. 16)
	Enhanced chip breakage in hardened wrought and casting alloys [168],[193]	Chip breakage favored by presence of hard and brittle inclusions in these alloys (silicon content up to 12%) [168],[193]	Optimization of chip breaking and machinability must synergistically consider the process parameters, tool and lubrication conditions[194], [195] (as with other materials)
Magnesium Alloys	Lamellar chip formation[168] Spiral chip segments[168]	Chip morphology should not represent a critical issue for the machinability of the material[168]	Chip form is affected by the variation of cutting conditions; chip ignition has to be verified and avoided[196]
Heat-treatable steels	Continuous or segmented chip formation[174]	Macroscopic shape and chip breaking mechanisms strongly depend on chip groove geometry, cross section of the (un) deformed chip and chip flow angle (AlSI1045)[174]	Selection of chip breaking alloying elements is usually limited by the intended use of the workpiece to be produced [168].
	Chip shape varies largely depending on process conditions and microstructure resulting from the heat treatment [168]	Chip shape depends more on microstructure (heat treatment) than on alloy content[168]	One possibility to improve machining is to carry out the roughing operation before the material is quenched and tempered[168].
Case hardening steels	Long chips when machined before heat treatment [168]	High proportion of ferrite before heat treatment[168]	Described general disadvantages of very long chips (seeFig. 16) Chip breaking improvable by adding lead or sulfur or adapted

(*continued on next page*)

Table 1 (*continued*)

Material	Frequent Type of Chip Formation and Chip Shape	Mechanisms/ Observation	Possibilities to Improve Machining Performance
			tool geometries / chip grooves.
	Long, tangled chips below critical feed [197] (20MnCrS5)	Chip breakability depends on heat treatment and resulting shape of pearlite[197]	Large nodular pearlite leads to improved chip breakability (higher degree of segmentation, MnS-inclusions) compared to partially spheroid or lamellar pearlite.[197]
	Chips are annealed and break easily (case-hardened state)[168]	High temperatures in the cutting zone [168]	Favorable chip form, but high-temperature increases tool wear
Austenitic stainless steels	Long ribbon and snarled ribbon chips when machined in quenched or solution-annealed condition[168]	High toughness in combination with a pronounced tendency to work hardening[168]	Chip formation and fracture have to be realized by adapted tool geometries[168]
		Chip shapes lead to additional load on too[168]	Improvements in chip formation by adapted alloy contents usually not possible due to given requirements for workpiece[168]
Hardened Steel (> 50 HRC)	Mostly segmented (saw tooth) chips are formed [198–201]	Material hardly deformable due to martensitic structure[198–200]	High dynamic stresses on cutting tool can induce surface crumbling and formation of cracks in cutting tool[198–201]
		Material separation begins with formation of cracks on the surface of the workpiece → segment pushed out between rake face and crack → next crack develops before material gap is closed → segments remain connected [198]	High levels of mechanical and thermal load on workpiece surface [198–201]
			Strain hardening → induces residual compressive stress, which grows further below surface with increasing flank wear on cutting edge [198–201]
Titanium alloys	Lamellar chips are typically expected when machining under conventional cutting conditions [168]	Alternation of compression and sliding phenomena in the shear zone during chip formation results in mechanical and thermal alternate load to the cutting tool[168]	Stress state can lead to tool fatigue and tool failure due to the formation of cracks and fractures of the cutting tool edges, coupled with evident negative effects in terms of part surface quality[168]. Extent of load is related mainly with the choice of process parameters and

Table 1 (*continued*)

Material	Frequent Type of Chip Formation and Chip Shape	Mechanisms/ Observation	Possibilities to Improve Machining Performance
			cutting conditions. Chip breakage by applying targeted high-pressure-cutting fluid supply[168] / use of liquid gases results in improved chip formation, machined surface quality and tool wear[202],[203]
Inconel 718	Lamellar / segmented chip formation [204–206]	Localization of shear, shear instability, periodic variation of the cutting force [204–206] (see Fig. 15b)	Restricted surface quality and workpiece accuracy[207]
			Increased (abrasive) tool wear, severe notch wear
			Adaption of cutting tool geometry to reduce notch wear
	Long chips. Mostly, ribbon, tubular or helical chips[206], [208],[209]	Work hardening of material → hard, sharp saw tooth-shaped chip[168], [210]	Disadvantages of very long chips + hard sharp saw tooth edges complicate swarf handling[210], [211]
			Excellent chip breakage by applying targeted high-pressure-cutting fluid supply[208], [209],[212]
Grey Cast Iron	Short spiral chips or chip segments [213–215]	Favorable chip form, formation type can be challenging	Short chips ensure unhindered evacuation of chips and enable high grades of process automation
	Mostly segmented or discontinuous chip formation [213],[215–217]	High dynamic loads on cutting edge [213],[216]	Tool wear, poor surface quality
GJL	Tends to form discontinuous chips[213],[217]	Chip separation is oriented towards lowest resistance in the material→ graphite lamellae [218]/ entire lamellae can slide off[215]	Material may be partially separated in the workpiece surface, which leads to surface damages and high surface roughness [215],[218]
		Material matrix and graphite particles are deformed in the cutting zone[219]	
GJV	Shorter chips occur when machining GJV than GJL[219]	Deformation and shear of the material is oriented towards the graphite inclusions[215], [219]	Surface damages and high surface roughness can be indicated by chip formation process
		Deformation of material is localized in the graphite inclusions[219]	

(*continued on next page*)

Table 1 (*continued*)

Material	Frequent Type of Chip Formation and Chip Shape	Mechanisms/ Observation	Possibilities to Improve Machining Performance
GJS	Mostly segmented chip formation / continuous chips possible with sharp cutting edges [168],[213],[217]	Graphite S damage the surface less than L or V when detached from workpiece surface [215]	Better surface finish is achieved when machining GJS than GJL and GJV[215]
Austempered Ductile Iron, ADI (S)	Short spiral chips [216]	Partially comparable to GJS due to graphite morphology	High rake angles at small chip thickness lead to nearly continuous chip formation [216]
	Distinct segmentation (tools with negative rake angles→ chips often consist of one segment)[216]	Ductile austenitic-ferritic structure of ADI reacts brittle at high strain rates [216] Austenitic matrix is transformed to martensitic structure as a result of deformation by cutting edge → disproportionate hardening of material.[216]	Pressure of material with austenitic-ferritic structure against rake face → severe crater wear[216] Segmented chip formation: cutting edge is exposed to high stress and is abruptly relieved when segment shears off[216] / force maxima lead to cutting edge chipping and tool failure[168], [216].
Austempered Gray Iron, AGI (L)	Segmented chip formation[219] Short chips (secondary chip breaking)[219]	Partially comparable to GJL due to graphite morphology	
Titanium Aluminides	Discontinuous and segmented chips [168]	Material has high brittleness and limited capacity to deform plastically [168]	Chip morphology and machining results can be improved by an adjustment of the cutting edge geometry and process parameters[220], [221].
	Angular, needle-shaped chip lamellae are often formed[222]	Micro-cracks and micro-fractures on surface of workpieces, characterized by poor surface quality, [125],[223].	

markets, a high degree of automatization is favored in machining. Therefore, chip evacuation is critical. Different materials are included in the group of Copper alloys, which are characterized by a copper content of at least 50%. Overall, the machinability is affected by their chemical composition, heat treatment, and primary shaping processes. Klocke (see [168], and references therein) has proposed the following categorization in three groups with respect to their machinability:

- Group 1: Alloys with the addition of elements as lead, sulfur, selenium and tellurium to improve chip fracture/breakage: this group is likely the most machinable.
- Group 2: Alloys with zinc, tin, nickel, aluminium and silicon, without chip-breaking additives (among others: copper/tin/zinc and copper/nickel/zinc alloys): the machinability might vary significantly as a function of the amounts of alloying elements. Usually, acceptable chip forms are obtained;
- Group 3: Pure copper and copper alloys with zinc (i.e., brass), tin, nickel and aluminium appear to be moderately to poorly machinable. In particular, brass and pure copper show a high chip compression, which affects the tribology at the interface between chip and tool rake face, resulting in high mechanical stresses on the cutting edge;

The content of lead in brass alloys will be drastically reduced in the near future due to changes in legislation, shifting the needs of these industries from group 1 to group 3 [224–227]. Therefore, intensive research is performed regarding the development of low-leaded materials with improved machinability, especially regarding chip formation [188]. The brass alloy CuZn21Si3P uses Silicon as a substitute for lead and has gained some relevance in industrial applications today. Alloyed in brass, Silicon forms the highly brittle intermetallic κ- and γ- phases which provides segmented chip formation in machining. Other materials utilize so-called micro-alloys with traces of Indium in heterogeneous brass alloys to provide improved chip breakage in machining [188], [190]. Bismuth has very similar properties regarding machinability as lead while being harmless to the human body. Its broad industrial utilization as a chip-breaking alloy is prevented by its high cost and the deterioration of CuZnBi-alloys under continuous load [188].

5.2.2. *Aluminium alloys*

The chip morphology and chip formation mechanisms are key parameters for the machinability assessment of aluminum alloys, particularly when large amounts of chips have to be removed at high MRRs. The chip form can be influenced by the alloy composition, heat treatment and process kinematics. Due to the described effects of very long chips on machinability in combination with the frequently very high material removal rates in aluminium machining, the process conditions should be optimized with regard to chip breakage.

The influence of cutting conditions on chip formation has been investigated in recent research studies. Orthogonal cutting tests performed on the 6061-T6 aluminum alloy under a wide range of cutting speed (100–1900 m/min) and feed (0.06–0.15 mm/rev) produced different kind of chips [228]. When increasing the cutting speed, the shear slip distance and shear angle increased, while chip thickness, friction angle, length of shear plane, tool-chip contact length and first deformation zone width decreased [229], [230]. The increase of tool-chip contact length was noticed when increasing cutting depth and feed rate in high-speed dry milling of A6061 [231]. With regard to the 7050-T7451 alloy, both cutting speed and feed rate are factors affecting the transition from continuous to segmented chip, which was observed for high cutting speed (2000–2500 m/min) in the feed rate of 0.05–0.20 mm/tooth [232]. Further, Guo et al. [233] investigated high-speed grinding of Al/SiCp metal matrix composites shows improved surface quality and reduced subsurface damage compared to low-speed grinding due to grain refinement mechanisms in the Al matrix and increased ductility of SiC particles, which reduces property discrepancies between the heterogeneous constituents.

Moreover, chip formation, breaking and removal appears to be a challenging issue when drilling multi-layered material structures (e.g., aluminium and titanium stacks), because of the different material properties [234].

5.2.3. *Steel materials*

Steel materials cover a wide range of material properties due to the variety of formable alloys, metallographic constituents and different applicable heat treatments. Table 1 shows an overview of the influences of chip formation and morphology on machinability for different steel materials. Due to the adjustable properties, it is often possible to achieve favorable chip formation through an adapted design of the material. When machining steel materials in the uninterrupted cut, the focus is more on the macroscopic chip shape than the chip formation mechanism when evaluating machinability. Steel components are often produced automatically and in large quantities. Therefore, reliable chip breaking and chip evacuation are a basic prerequisite for efficient machining [168].

Nevertheless, many research works have been carried out on the

influence of the chip formation mechanism on machinability. Hoppe [176] showed that the chip formation mechanism influences the resultant force when machining the heat-treatable steel ALSI1045. The force components changed with the cutting speed, which was caused by differences in chip formation, the temperature in the cutting zone and the material properties at high strain rates. An increased cutting speed transferred the type of chip formation from continuous to segmented chip formation and lead to a decreased resultant force. As the mechanisms that lead to reduction of the resultant force did not change when the type of chip formation changed, the chip formation mechanism was excluded as the cause for the force reduction at this point. With a further increase of the cutting speed to 3000 m/min, the resultant force raised up back to values which were measured at low cutting speeds. Mechanisms like adiabatic shearing or melting of areas in the chip or at its bottom, which cause instabilities, gained significance. The remaining material of the lamella has to carry the load. The material is deformed slightly but fast in this area, which leads to high strength as a result of its strain sensitivity. Therefore, the strain sensitivity was identified as a reason for the increased resultant force.

5.2.4. Titanium alloys

When machining titanium alloys, both the chip formation mechanism and the resulting chip shape are reasons for the poor machinability of the material. Due to the material properties of low thermal conductivity and high strength, a distinct lamellar chip formation occurs and long chips result in an uninterrupted cut (see Table 1). Chip shape and size are significantly affected by the choice of process parameters and, more in general, cutting conditions. In dry and cryogenic Ti-6Al-4 V turning, increasing depth of cut and decreasing feed rate reduced chip thickness, distance between serrations and tool-chip contact length, while increasing chip length and shear band angle. Moreover, the degree of chip segmentation and dominant deformation modes and amount are affected by the extent of tool wear, due to the change in tool geometry and the increase in cutting temperature. Dry turning of Ti-6Al-4 V with worn tools is characterized by severe friction between the rake face and chip, significant plastic deformation and shear on the machined surface in the chip [235]. When milling, a full characterization of the complex three-dimensional chip morphology, possibly including the analysis of microstructural and mechanical behavior of machined chips, can be performed through multi-view approaches [236]. Further, Pouliquen et al. [237] found that α phase fraction controls forces and chip morphology in machining titanium alloy Ti5553. Lower α fractions facilitate continuous chip flow while higher levels promote shear localization and serrated chips. Denkena et al. [238] showed oxygen reduction minimizes Ti-6Al-4 V chip segmentation by mitigating oxidation and enabling continuous chips. Li et al. [239] used simulation to elucidate segmentation dependence on parameters in Ti-6Al-4 V turning. Lv et al. [240] experimentally studied adiabatic shear in milling Ti40. Additively manufactured titanium alloys pose machining challenges with morphology variations relative to wrought alloys [241–244]. Feed rate plays an essential role governing chip shape in different processes. Fracture behavior and hardness primarily influence machinability of AM vs wrought Ti-alloys. Optimizing cutting conditions is key to improve surface integrity of AM Ti-alloys.

5.2.5. Nickel-based alloys

Due to their excellence corrosion resistance and high temperature strength, aero-engine components are often manufactured from nickel-based super alloys. A particularly common alloy is Inconel 718 (NiCr19NbMo). The characteristics of the mostly lamellar or segmented chip formation during machining the material are one main reason for its classification as difficult-to-cut, see Table 1. Therefore, the chip formation mechanisms and machinability of nickel-based alloys have been addressed in numerous research papers and reviews [64,207,208,210,245,246].

As shown in Fig. 17a, the segmentation intensifies with increasing cutting speed until individual chip segments result[204]. During the accumulation of the chip lamella a transverse material flow results, Fig. 17b [205]. The type of chip formation leads to a high alternating thermal and mechanical stress on the cutting tool. As a result, fatigue and crack development phenomena follow [247]. The combination of the material's tendency to work harden and the formation of lamellar chips leads to the formation of a sharp, hard sawtooth-shaped chip edge which causes abrasive wear on the cutting tool when the chip flows off [168,210]. These interactions lead to the formation of severe notch wear during turning of Inconel 718 with ceramic, CBN or solid carbide tools. Additionally, the chips flow laterally in emerging notches and intensify the wear development by mechanical snagging with the cutting tool material particles. Furthermore, the dynamic load on the cutting edge as a result of the lamellar chip formation contributes to the fact that milling of Inconel 718 is subject to strong restrictions with regard to the cutting parameters [168,207].

By changing the cutting conditions, the macroscopic chip shape differs significantly. With increasing cutting speed, chip compression decreases, which influences the resulting chip shape. Pawade and Joshi [206] showed a transition from long snarled to spiral chips by increasing the cutting speed from 125 m/min to 475 m/min during turning of Inconel 718. Similarly, strong changes in chip shape occurred with the variation of the feed rate, the depth of cut or cutting edge rounding. Thermal effects further affect the resulting chip form when the feed rate

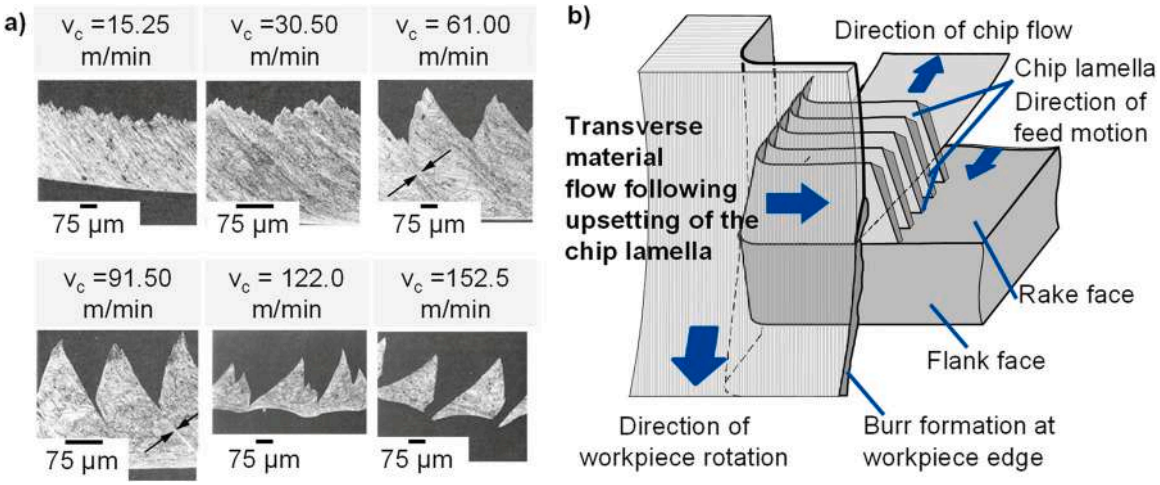

Fig. 17. Chip formation of Inconel 718 according to [204], [205].

is varied, as the feed rate determines how much heat can be dissipated by the chip into the environment. Process conditions, which resulted in spiral chips, lead to lower surface roughness than processes which emerged snarled ribbon chips.

5.2.6. Grey Cast Iron

Cast iron materials are iron-carbon alloys with a carbon content of more than 2.06%. They are divided into grey and white cast iron, related to the color of their fractured surfaces. The carbon in grey cast iron is present in the form of graphite. Referring to the shape of the graphite particles a subdivision into three groups is common: lamellar graphite (GJL), vermicular graphite (GJV) or spheroidal graphite (GJS). Cast iron with lamellar graphite is the most frequently produced group [168]. The basic structure of the materials is ferritic-pearlitic or purely pearlitic. By specific heat treatment, more ductile austenitic-ferritic microstructures with increased strength can be achieved [248]. Ausferritic cast iron with lamellar graphite (AGI) and with spheroidal graphite (ADI) belong to this group. Cast iron generally has good machinability. However, the characteristics of the chip formation process depend strongly on the graphite shape and the structure of the surrounding matrix [213], [215], [217], [219]. The shape of short chips, as is typical in cast machining, is basically favorable for machinability (see Fig. 15). However, the segmented or discontinuous chip formation mechanisms present certain challenges.

Graphite lamellae with a size in the range of the chip thickness are relevant for the discontinuous chip formation when machining GJL [213]. Micro cracking is induced near the graphite lamellae due to stress concentration. The chip separation is oriented towards the lowest resistance in the material, which is the graphite lamellae [218]. Entire lamellae can slide off [215]. As a result, the material may be partially separated in the workpiece surface, which leads to surface damages and high surface roughness [215], [218]. If irregular fracture occurs, the tool moves over a free space until the separation of the next chip fragment is induced [217]. By adjusting the cutting conditions, a transition of the chip formation from discontinuous to segmented chip formation can be achieved [213]. The chip formation characteristics for machining GJL, GJS, GJV, ADI and AGI (here labelled according to the normative references) are listed in Table 1.

Chip formation during the machining of cast materials is dominated by the shape of the graphite inclusions and affects the machinability of the materials. The significantly better surface quality that can be achieved when machining GJS than GJL, for example, is attributed to chip formation. To evaluate the machinability of grey cast iron and to determine the influence of the chip formation mechanism on the machinability, the matrix structure has to be taken into account.

5.2.7. Titanium aluminides

The issues related to the complex machinability of titanium alloys are exacerbated when it comes to titanium aluminides, which are heat resistant intermetallic alloys that have been identified as potential candidates to substitute nickel-based superalloys in some aerospace applications. The material properties lead to the formation of discontinuous and segmented chips [168]. Angular, needle-shaped chip lamellae are often formed [222] (see Table 1). Moreover, it has to be highlighted that, differences in machinability outcomes can be traced back to the different chemical composition (thus, to the different microstructures) of the titanium aluminides [249], [250], or to the manufacturing route for workpiece production (as for the latter, additive manufacturing has been exploited [251]).

Some of the effects of the lubrication/cooling conditions on chip morphology (and, thus, on machinability results) have been experimentally highlighted in turning tests performed on a 45–2-2 XD alloy under dry cutting, conventional flood cooling, high pressure lubricant supply, cryogenic cooling with liquid nitrogen and MQL. With respect to dry machining, a chip size reduction was noticed when applying MQL and conventional flood cooling. In comparison to wet cutting, the chips obtained with LN2 showed an increase in length and curvature radius. The increase in chip breaking due to the increase of the lubricant supply pressure (already discussed for Ti-6Al-4 V) was confirmed [203].

5.3. Analysis of chip formation mechanisms and open challenges

The experimental approaches described in the literature typically involve the chip collection, cold mounting in epoxy resin, polishing and etching to reveal the geometric features and microstructures. Chips are then examined by using optical microscopes and/or scanning electron microscopes (eventually by exploiting XPS or TKD analyses), depending on the level of detail of the assessment. Some research studies are specifically focused on the chip morphology and chip formation mechanisms are intended to propose multi-view approaches to characterize 2D and/or 3D chip morphology [236]. Some others aim to correlate chip morphology with one or more metrics pertaining to the machinability assessment (tool wear, cutting forces, surface roughness, et cetera), or to define the correlation between chip morphology and the variation of the cutting process parameters. In general, literature lacks holistic approaches including chip morphology within multi-objective analyses toward a full machinability characterization.

An empirical method used in industrial practice is the preparation of chip shape diagrams for selected combinations of materials and tools, as shown in Fig. 18. The diagrams show whether chip breaking is achieved depending on the feed rate and cutting speed [157], [252–255]. There are different methods to influence chip shape and fracture. Most of them are based on an increased deformation of the chip to induce chip breakage. This is achieved by the use of tools with chip breaking geometries, adapted tool feeds or targeted high-pressure cutting fluid supply as discussed in Section 7. The prediction of chip geometry parameters and chip breakage is complex and the conditions of the cutting process as well as the properties of the tool and the machined material must be taken into account [157], [172], [256]. Since chip control has a great influence on machinability, empirical and analytical models to predict chip formation and breakage are continuously developed [171], [257–261]. Modern approaches enable the measurement of the strain and strain rate fields directly in the shear zone using digital image correlation and high-resolution cameras and thus the analysis of chip formation with high spatial resolution [262], [263].

6. The relationship between surface integrity and machinability

6.1. Machinability and surface integrity

The machining process often result in the creation of new surfaces that manifest as a new surface state known as *surface integrity*. Surface integrity is defined as the condition of a freshly exposed surface/subsurface of a component after a manufacturing operation. Surface

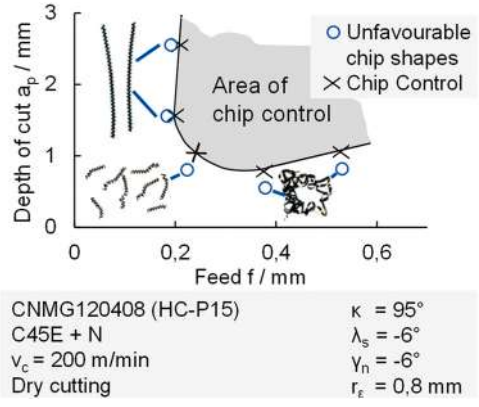

Fig. 18. Chip form diagram according to [174].

integrity can have many different attributes such as roughness, residual stress, severely plastically deformed layers, tribofilms, and textures/preferred orientations.

Machining is a primarily shearing process during which the finished surface/subsurface undergoes severe plastic deformation. This deformation is a thermo-mechanical behaviour. During the metal cutting process, the power consumed is converted into heat. Heat generation occurs at the shear plane and the chip-tool interface. Almost 90% of the heat is conducted away by the chip and coolant; the rest of it is conducted into the workpiece material. With gradual tool wear, a new surface is formed that results in additional friction. Thus, new surface results in additional friction. The tool wear not only increases the interface temperature but also affects the physical properties such as roughness and size tolerances and sometimes results in surface damage (metallurgical defects) in the materials. The strain-induced during the machining process manifests as dislocations near the surface resulting in nanoscale subgrains [264], [265]. The thickness of the severe plastic deformation zone could range from a few hundred nanometers to a few microns. The induced strain also gives rise to residual stresses. These are generally recognised as surface integrity, which can be used as a factor to evaluate the machinability of different materials, especially when it comes to difficult-to-cut materials, e.g., nickel/titanium-based superalloys. In addition, Axinte et al. [266] conducted a detailed literature review which analysed sub-surface plastic deformation post-machining using in-situ micro-pillar compression testing. Microscopic indentation and compression of superficial layers elucidated micro-scale material reactions such as plastic deformation and material removal mechanisms.

Lower tool life, plus higher cutting temperatures and forces are the indicators of poor machinability. Consequently, all these factors adversely affect surface integrity. Lower tool life results in higher temperatures that can cause surface damage, tensile residual stresses, and softening. Higher tool wear also results in higher roughness and geometric issues such as roundness error and size variation. Hard particles such as metal carbides and oxide inclusions reduce machinability but soft inclusions like sulfides are intentionally added to improve machinability. Poor machinability drastically increases machining costs by reducing tool life and generating surface damages metallurgical defects, tensile residual stresses, and geometric errors. This damage worsens with continued tool wear. Thus, the dynamic nature of the machining process creates ever-challenging aspects for surface integrity that have been a great topic of commercial and academic interest for the past century.

Since cutting temperature, cutting forces, and material microstructure underpin machinability as well as surface integrity, this section evaluates the influence of these fundamental factors on both characteristics. The data discussed in the first three sections cover three case studies performed at The Timken Company R&D laboratories supplemented by the latest studies available in the literature.

6.2. *Influence of machinability on surface integrity*

For the past few decades, researchers have been conducting detailed and systematic studies on machining and surface integrity. In 2013, Jawahir et al. [267] conducted a collaborative work group study on surface integrity. Most recently, in 2021, Liao et al. [268] published a comprehensive and systematic study that included a wide spectrum of advanced characterization techniques such as transmission electron microscopy (TEM), scanning electron microscopy (SEM), transmission Kikuchi diffraction (TKD), electron backscatter diffraction (EBSD), precision electron diffraction (PED), glancing angle X-ray diffraction (GAXRD), atom probe tomography, neutron diffraction, synchrotron diffraction, and so on. The study encompassed the fundamental mechanisms of different material removal techniques and their effect on surface integrity. As a follow-up, La Monaca et al. [269] published a review paper on the effect of surface integrity on the service life of a component. Both review papers covered the whole gamut of research that has been performed over recent years.

Among these, the qualified surface integrity factors for machinability evaluation included surface roughness, the thickness of the white layer, plastic deformation, and residual stress, (please refer to the example given in Fig. 19). The choice of a suitable value for the surface integrity criterion therefore depends not only on the materials properties but also on various cutting conditions such as tool wear, cutting speed, and coolant applications. Among the parameters, the cutting speed has a major influence on the material deformation at the machined surface (see Fig. 19a). As the cutting speed increases from 50 m/min to 140 m/min, the thickness of the deformation layer also increases, as evidenced by the kernel average misorientation (KAM) images in Fig. 9a [268], similarly Ren et al., [270] observed similar results. Even though the cutting conditions might be identical, the surface integrity of different materials is difficult to compare from case to case. Because of the large number of possibilities for selecting the boundary conditions for tool life studies designed to evaluate machinability, the comparability of different studies is limited. Furthermore, the surface integrity is also highly influenced by the type of machining process. For example, when machining Inconel 718 using different methods such as conventional milling, laser assisted milling, and water jet cutting, the surface roughness is observed to be the lowest for water jet cutting (see Fig. 19b). This is because water jet cutting utilizes a narrowly focused, precisely controlled high-pressure abrasive water stream to smoothly erode through materials without any mechanical contact, frictional heat, or material deformation that would roughen the cutting surfaces, which is typically observed in conventional milling or laser assisted milling [268]. In addition to surface roughness, the residual stress generation in the workpiece is also affected by changes in cutting tool properties. From Fig. 19c, the residual stress is highest at the surface of the metal and decreases with depth, because the surface of the metal is subjected to the greatest amount of plastic deformation and rapid cooling during machining. Moreover, the residual stress is also higher when machining with conventional cutting tools rather than with PCBN cutting tools under aggressive cutting conditions, which many industries need to meet their production rates. This is because conventional cutting tools generate more heat and cause more plastic deformation than PCBN cutting tools [271]. Within individual test series, however, surface integrity offers a sensitive and validly evaluable criterion for comparing the machinability of similar/or same types of materials (but of different composition/using different heat treatments).

One fundamental viewpoint, states that the interface temperature, mechanical load, and the material microstructure, that dominate a material's machinability, play an influential role in microstructural issues of its surface integrity. While the influence of cutting force and temperature has been extensively discussed in previous sections, in this section we will focus on the influence of the material microstructure and properties by taking examples from difficult-to-cut materials, e.g. hardened steels and superalloys.

In the case of hardened steel, microstructural features such as carbides, retained austenite, and martensite lath can influence surface integrity. Previous studies on machining focused on improvements in tool life or controlling the surface damage, and systematic studies on the influence of material microstructure on surface integrity are few and far between. Recent studies [272] have shown that subtle variations, such as carbide size and distribution, affect grindability which in turn has an impact on geometrical aspects such as roundness error. Similarly, Hoier et al. [273] found batch-to-batch variation in the grindability of medium carbon steel. The authors attributed higher wheel wear (lower machinability) to a higher fraction of hard inclusions. The higher wheel wear further affects surface integrity reflecting the variations in the residual stresses.

Hua et al. [274] conducted hard turning trials on 52100 hardened steel with different hardness levels (55HRc and 62HRc) using the same cutting parameters. The authors found a significant difference in the residual stress pattern. The sample with higher hardness showed a

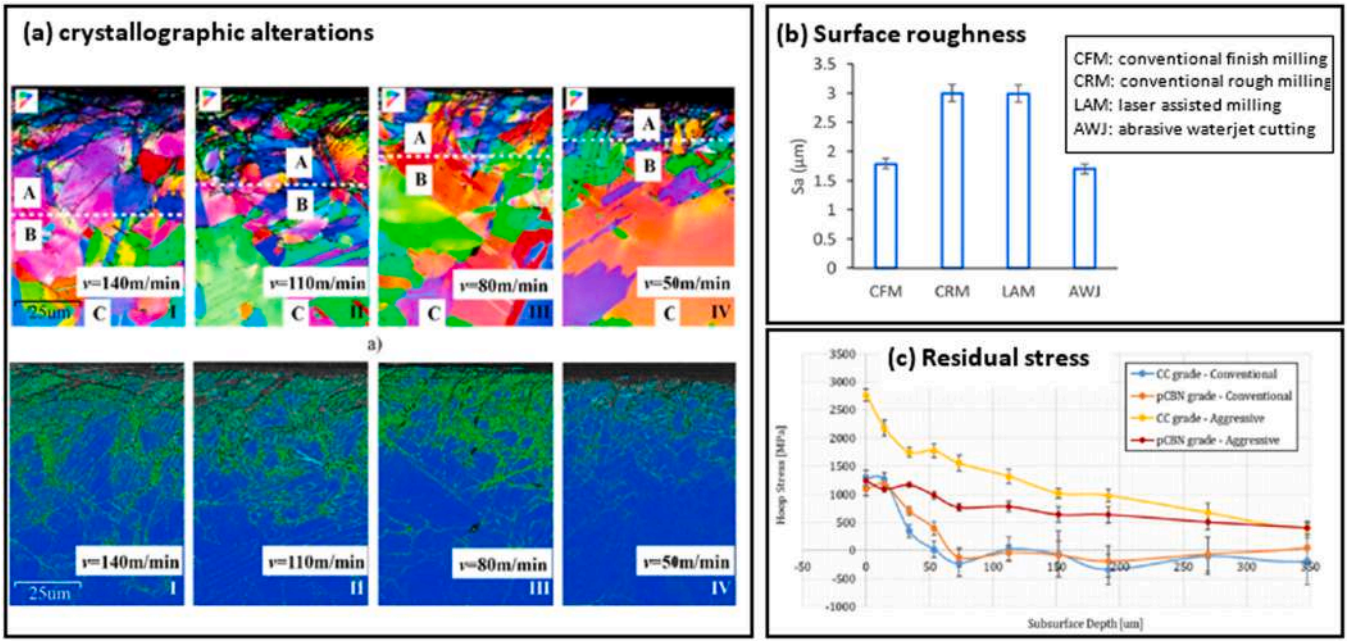

Fig. 19. Using surface integrity to evaluate the machinability: (a) microstructural crystallographic alterations for indicating machinability under different cutting speeds [268]; (b) surface roughness for indicating machinability under different cutting tools and parameters [268]; (c) Residual Stress profiles for different cutting scenario measured in the hoop direction [271].

higher magnitude of compressive stress. The authors attributed the increase in the compressive stress to the balancing act of higher tensile stresses behind the cutting tool. Although the authors did not comment on the machinability aspect, it is known that higher hardness results in lower machinability because the cutting tool creates abrasive wear. Another approach to improve surface integrity of the workpiece involves using a drag finishing method on the broaching tool edges. This enables superior control over key parameters including rounding radius, material removal rate, reproducibility, and surface finish.

The microstructure and properties of mechanically performant superalloys, (e.g., nickel-based alloys, which are developed for higher working temperatures) can lead to a significant decrease in their machinability and thereby to reduced lower surface integrity. The primary influence of Ni-based microstructures comes from their precipitations, (γ' phases), which can significantly affect their machinability when cutting with parameters that produce different cutting temperatures. This leads to strengthening/softening effects on the workpiece. It has been revealed that the increase of the γ' fraction significantly decreases grain plastic deformation under aggressive cutting parameters including higher cutting temperatures, due to the consequent reduced softening effect [275].

There is plenty of research on surface integrity after machining, but systematic studies investigating the effect of machinability (or material microstructure) on surface integrity are rare. Therefore, targeted experiments were designed at The Timken Company as well as from some recent works of literature to understand the effects of machinability on surface integrity for bearing steel grades. Those experiments are presented here in the form of three case studies.

6.2.1. Case Study I: Effect of retained austenite on machinability and surface integrity on 52100 steel

Hard turning trials were conducted on 52100 steel tubes of dimensions 90 mm (OD), 65 mm (ID), and 75 mm length. The percentage of retained austenite was varied by hardening at different austenitising temperatures. Although the final microstructures consisted of different vol% retained austenite (6.7%, 11.7%, and 30% RA) as shown in the inset Fig. 20 micrographs, hardness was maintained between 60 and 62HRc. The steel tubes were machined using identical cutting conditions

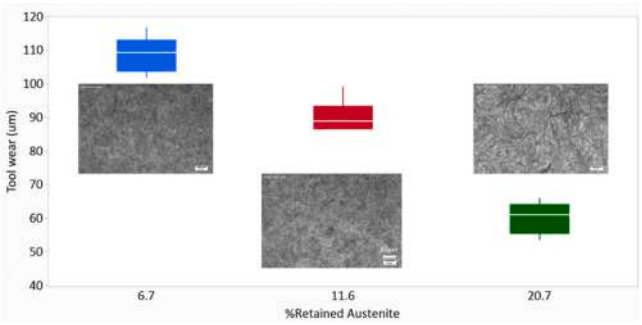

Fig. 20. Effect of %RA on tool wear on 52100 bearing steels (inset respective microstructures).

for 20 min. Five repetitions for each microstructure variation were conducted.

Tool wear, retained austenite, and roughness values were recorded. Results indicate that tool wear dramatically decreases with the increase in the retained austenite (Fig. 20). The decrease in the tool wear could be due to the dissolution and size reduction of e and q carbides at higher austenitization temperatures. The decrease in the tool wear also indicated an improvement in the surface roughness. In-situ neutron diffraction studies [276] on uniaxial tensile testing on through hardened bearing steels have shown that austenite has lower yield strength compared to martensite. Therefore, the lower strength of austenite also correlated with the improvement in the tool life. Residual stress investigations provide further insights into the influence of machinability on surface integrity.

As shown in Fig. 21, retained austenite strongly influences the residual stress pattern. The maximum compressive residual stress (CRS) decreases progressively with an increase in the %RA. The increase in the maximum CRS with increases in the retained austenite is most likely due to transformation-induced plasticity. The strain-induced martensitic transformation of austenite is a thermo-mechanical process. The transformation of austenite to martensite is expansive, which leads to compressive residual stresses.

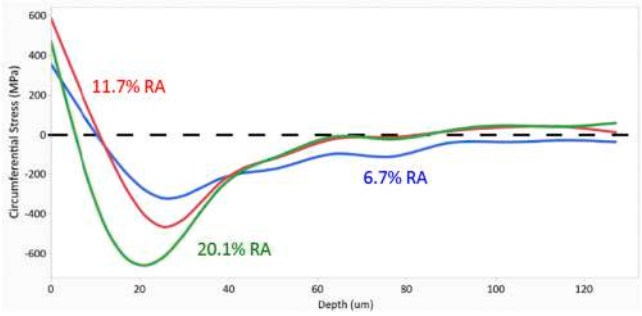

Fig. 21. Effect of %RA on residual stresses after hard machining of 52100 steel.

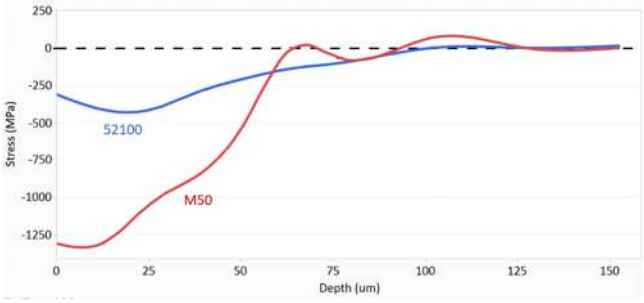

Fig. 23. Effect of material chemistry on residual stress.

Under loading conditions, this transformation occurs at the M_d temperature [277]. Similar to Hertzian stresses, the maximum shear stress from machining also occurs at the subsurface, which correlates with the maximum CRS at the subsurface. No such effect is observed at the surface. This could be because the surface tensile stresses are influenced by the high temperature during the cutting operation or the stresses from the heat treatment. From this study, it is evident that increases in the retained austenite improve machinability by decreasing tool wear and improving surface roughness and also maximum compressive residual stress.

6.2.2. *Case Study II: Effect of material chemistry (M50 vs. 52100) on machinability and surface integrity*

AISI 52100 is a commonly used bearing steel, while M50 is a specialty steel used in aerospace bearing applications. M50 steel has high wear resistance and high-temperature dimensional stability due to its high alloying content from Cr, Mo, and V additions. Bearing rings from both grades of steels were hardened, tempered, and machined using identical cutting parameters. Its high alloying content gives M50 steel composition of hard alloy carbides (Fig. 22) making it slightly harder (62HRc) than 52100 (60HRc). The abrasive action of the hard carbides results in high insert wear and reduced machinability. The residual stress profile on through hardened 52100 and M50 steels is shown in Fig. 23. As seen in the figure, both steel grades exhibited compressive residual stress at the surface until a depth of 100 μm.

Given the high ductility (due to its higher alloy content) and higher strength, it is not surprising to see that the M50 steel exhibited the highest surface compressive stress compared to the 52100 material. This is supported by the previous observation [274] that higher hardness materials show a higher magnitude of CRS. Thus, this example suggests that, under certain conditions, machinability and CRS could be in an inverse relationship with each other. The exact mechanism behind this phenomenon is unknown, so detailed TEM and XRD analyses need to be performed for a better understanding of grain size, aspect ratio, and dislocation pinning.

6.2.3. *Case Study III: Effect of RA on machinability and surface integrity in carburized steel*

The effect of material microstructure on machinability and surface integrity was further investigated by Bedekar et al. [278] The author varied the retained austenite in SAE 8620 carburized steel followed by hard machining using an identical set of parameters. The retained austenite in the case microstructure was maintained at 8% and 30% respectively. Advanced characterization techniques such as TEM (transmission electron microscopy), GAXRD (glancing angle X-ray diffraction), and nanoindentation were employed.

The authors observed that white layers developed at much earlier stages (100 mm flank wear) on samples with 8% RA, which was not the case for 30% RA. The delay in the formation of white layers in the 30% RA sample indicates that higher machinability microstructures generate lower cutting temperatures thereby extending the insert life. TEM investigations found that the subgrain size of the 30% RA samples was comparable to that of the 8%RA (Figs. 24 and 25) due to the identical machining parameters.

The residual stress patterns (Fig. 24) showed that the surface residual stress for the 30% RA sample was slightly tensile while the sample with 8% RA showed compressive residual stress. This agrees with the previous observations on 52100 bearing steel (Fig. 21 [274]). The total depth of compressive residual stress in 30% RA was shallower than the 8% RA which is also consistent with the previous observations (Fig. 21 and [274]). The magnitude of maximum CRS for both groups of samples was comparable. This might be due to the higher carbon in the solution on the carburized steel that stabilized the retained austenite and restricted the TRIP transformation.

The observations in this study are consistent with Case Study I showing that higher %RA enables better machinability, reduces the

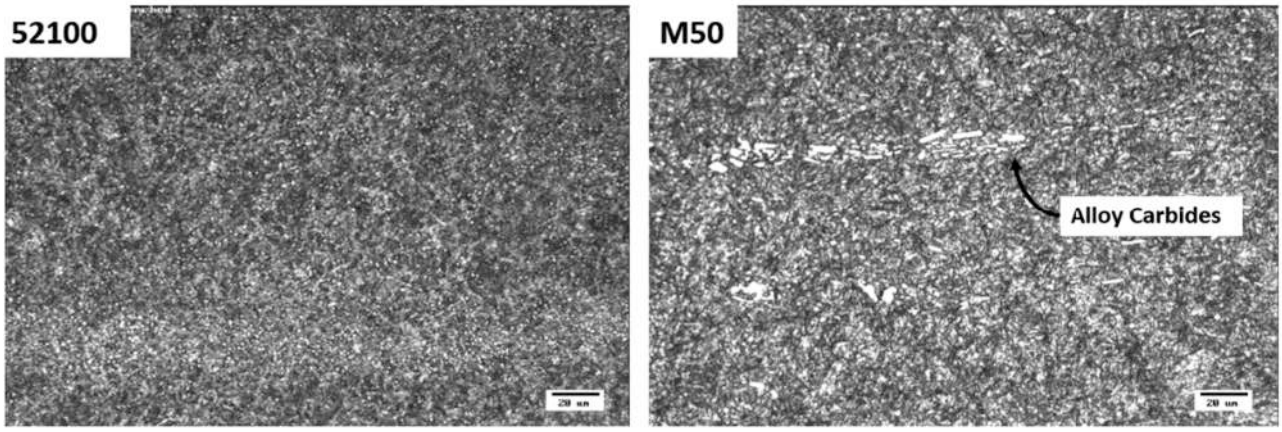

Fig. 22. Optical microstructures of hardened 52100 (left) and M50 steel (left).

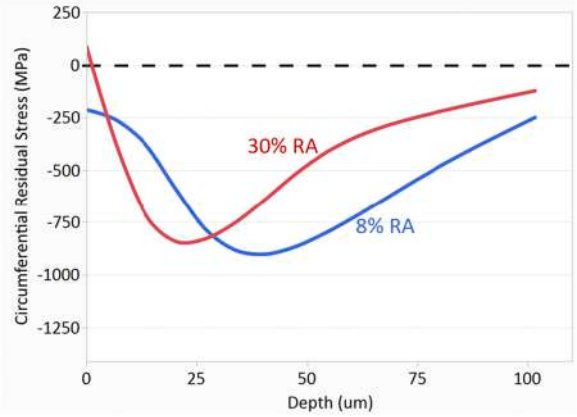

Fig. 24. Effect of %RA on residual stress of carburized AISI 8620 steel.

propensity for white layer development, and produces compressive residual stresses, thus demonstrating that microstructural constituents play a pivotal role in machinability, which ultimately influences surface integrity.

6.2.4. *Case Study IV: Influence of machinability on surface integrity in nickel-based superalloy*

Nickel-based superalloys, such as Inconel 718, Waspaloy and Udimet 720Li, and RR1000, are notoriously low-machinability materials, because of their low thermal conductivity, the tendency for strain hardening, and high strength at elevated temperatures. This leads to poor surface integrity from a variety of surface/subsurface damage such as material drag, cracking, and severe plastic deformation layers (SPD) when these materials are machined with inappropriate parameters or tool conditions. These anomalies can have a detrimental effect on the fatigue performance of safety-critical components during their operational life. Thus, industrial surface quality standards specify that severe plastic deformations and/or thermally abused layers on the part surfaces are not acceptable.

Due to the specific material properties of nickel-based superalloys, the cutting conditions (e.g. applied cutting tool material, wear condition, and cutting speeds that can yield different cutting temperatures and stress) can cause them to differ significantly in their machinability and eventually influence the surface integrity. According to Rachid [14], the high cutting temperature and stress from the tool wear and high cutting speed maps lead to recrystallised areas on the near surface of the machined layers, as shown in Fig. 26. In particular, the increase in subsurface deformation with tool wear and cutting speed is noticeable in the strain contouring maps. This low machinability leads to the high tensile residual stress in the near surface when the cutting tool is worn, especially for CBN cutting tools under high cutting speed, as a result of the substantial increase in cutting temperature and severe strain work hardening in the SPD layers [279].

Moreover, while a great variety of Ni-based superalloys are available, their machinability is are different and lead to various sensitivities to machining operations when SPD layers are generated. An in-depth metallurgical and mechanical analysis via abusive drilling operations [280] of the machinability and surface integrity of four different Ni-based superalloys, (Alloy 718, Waspaloy, Alloy 720Li, and RR1000) has been studied. It was found that alloy 720Li and RR 1000 are reported to have better mechanical performances at higher operating temperatures, they seem to be more sensitive to abusive drilling conditions, as evidenced by the thicker severe plastic deformation layers and higher tensile residual stresses observed in Fig. 27. It is concluded that while more mechanically performant alloys have been developed for higher temperatures, these combinations of properties are likely to lead to a decrease in their machinability. This eventually leads to a reduced tolerance to intense heat and mechanical loads that could develop when inadequate machining conditions are present and consequently yield poorer surface integrity [280].

7. Methods to enhance machinability

In principle, machinability has always played a role in the machining of any material. Therefore, many methods have been developed over the years to enable and continuously improve the machinability of new materials. One of the most obvious but nevertheless not always optimally used method with regard to machinability is represented by different cooling strategies. Further potential can be exploited by means of thermally assisted hybrid machining processes as well as optimised cutting tool design. In the following three subchapters, different concepts for improving machinability will be presented and evaluated.

7.1. *Coolant strategies*

Effective coolant delivery is critical when machining difficult-to-cut materials like nickel and titanium aerospace alloys to control temperature rise at the cutting zone, reduce tool wear, and sustain surface finish and integrity. Hence, a wide variety of cooling and lubrication strategies are used to improve the machinability [100]. In addition to classic

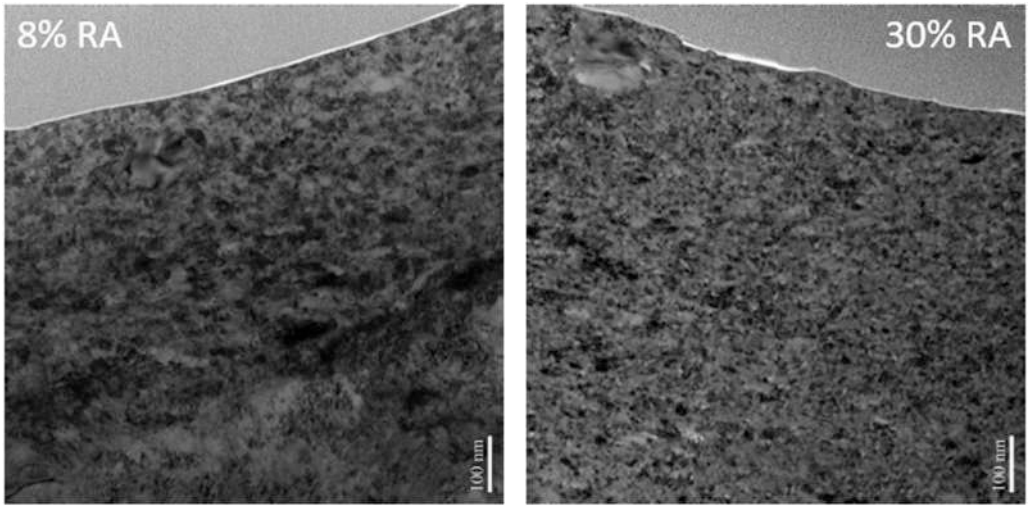

Fig. 25. TEM analysis of SPD layer of 8%RA and 30%RA carburized AISI 8620 steel.

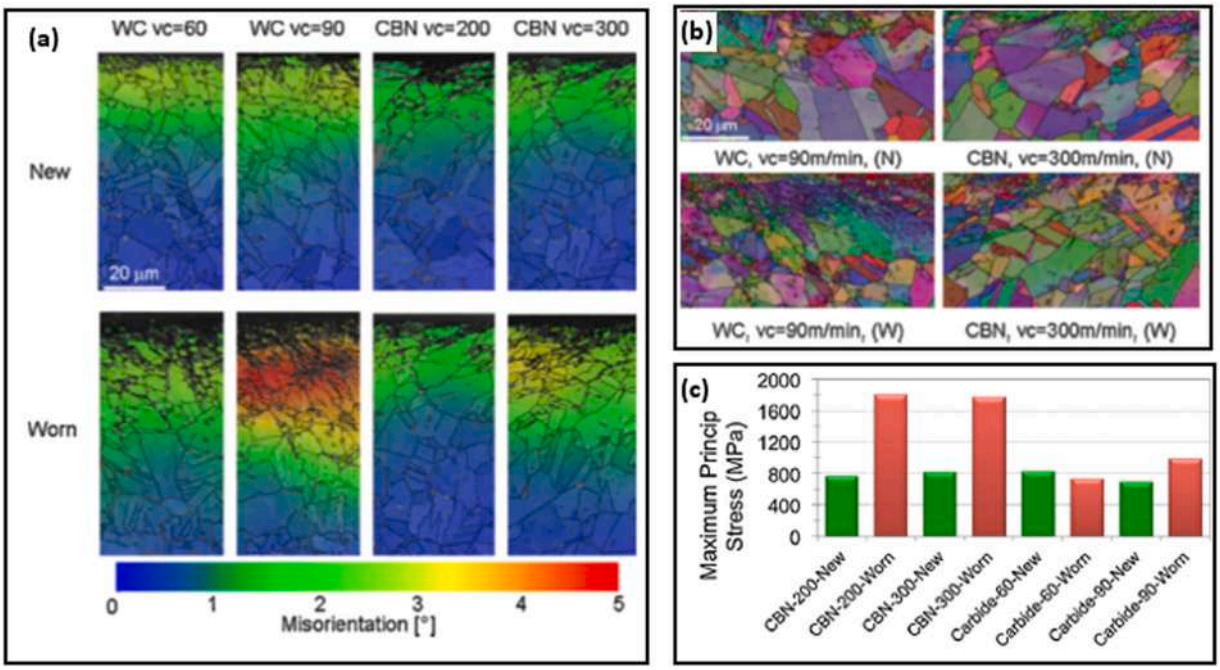

Fig. 26. Strain contouring maps obtained from EBSD measurements and surface residual stress show that the machinability of Nickel-based superalloy can be significantly influenced by the cutting conditions and yield poor surface integrity.

cooling-lubricant emulsions, there are synthetic cooling-lubricant solutions as well as the use of pure/natural oils. Furthermore, there are concepts in which fluids are largely dispensed with, such as high-pressure coolant, cryogenic cooling and MQL. The key techniques aim to provide cooling as well as lubrication effects to overcome the challenges posed by elevated temperatures and friction when machining nickel and titanium alloys. Integrating these diverse strategies facilitates uninterrupted and efficient machining of difficult-to-machine aerospace materials [281]. Hence, these approaches seek to fulfil the main objectives of a cooling strategy, which are "lubrication", "cooling" and "chip removal" [88]. Accordingly, the concepts can be classified as shown in Fig. 28, in which the different concepts are compared in terms of their performance with respect to the main objectives [88], [282]. To a large extent, the main tasks determine the machinability of a cutting process, which includes cutting forces, tool-wear and tool-life, surface roughness and surface integrity, chip formation and chip control, and part accuracy [283–285]. The better the influence of the cooling lubrication strategy on machinability is understood, the more specifically machinability can be improved for a specific task.

Water-miscible coolants are used at high process temperatures and cutting speeds with simultaneously low tool-pressures. Lubricating oils are mainly used at high contact pressures between rake face and chip surface, such as those encountered in different machining process. Both concepts are highly effective in terms of cooling, chip removal and lubrication, which is why they are standard in industry. As sustainable production is becoming increasingly important, the elimination of cooling fluids is desirable, resulting in insufficient cooling and lubricating, and thus in a deteriorated machinability (shortened tool life, due to wear mechanisms or breakage [286,287] and increase of process forces [288–290]). These effects can be attributed to the lack of lubrication of the cutting area [291]. At the same time, complex machining operations, such as gear skiving, can show an opposite trend in terms of wear behaviour when using compressed air instead of using pure oil as flood cooling [292]. The same behaviour can be observed in the comparison between dry machining and flood cooling in terms of surface roughness [286,293]. The results for A390 alloy, AISI 4340 as well as 6061 aluminium alloy show that the surface quality of the produced technical surface, by means of surface roughness, is of a higher quality when using cooling lubricants in the machining process. This contrasts with the studies on complementary machining, where the use of cooling lubricant results in a higher surface roughness compared to dry process operation [294].

In machining operations that are significantly characterized by high friction, MQL can improve machinability. MQL uses compressed air to introduce very small quantities of oil particles into the cutting area to maximize heat dissipation while providing requisite chip evacuation and lubrication. With MQL, the consumption of cooling fluid is reduced by an efficient application of oil mist via tool-internal channels or external nozzles. Though cooling effects are moderate, the oil prevents pressure welding of chips and reduces friction [281]. The oil mist flow rate usually is lower than 50 ml/h [88]. The effectiveness of MQL relies on the extent to which the oil reaches the cutting zone. This is not only influenced by number and position of nozzles [295,296], but also by the oil spray characteristic [297]. Among which, Lacalle et al. [298] investigation of the effect of spray cutting fluids in high speed milling, stated that the reduction of the quantity of cutting oil in the machining process, in relation to conventional emulsion coolants that leads to lower machining costs. Further, in milling, MQL can reach lower process forces and longer tool lives than dry machining [299]. For turning, lower process forces [286,300], longer tool lives [286,301] and lower surface roughness [301,302] were reported compared to dry cutting. Furthermore, for difficult-to-machine materials, MQL eliminated built-up edge related failures, thereby significantly improving surface finish and surface integrity [281]. Pereira et al. [303] evaluated alternative environmentally friendly oils including high oleic sunflower oil, sunflower oil, castor oil and ECO-350 recycled oil for MQL machining of Inconel 718, high oleic sunflower oil improved tool life by 15% compared to industrial canola oil, while achieving similar environmental impact. In addition to the environmental concern, it must be mentioned, that the process parameters of MQL, also in comparison to dry machining and flood cooling, have influence [295]. For drilling, similar process forces and tool lives were reported, compared to flood cooling [304] or even higher tool lives and a lower surface roughness [305]. Regarding machining temperatures flood cooling usually perform better than MQL, while MQL often reaches comparable machining forces and tool lives as well as lower roughness values.

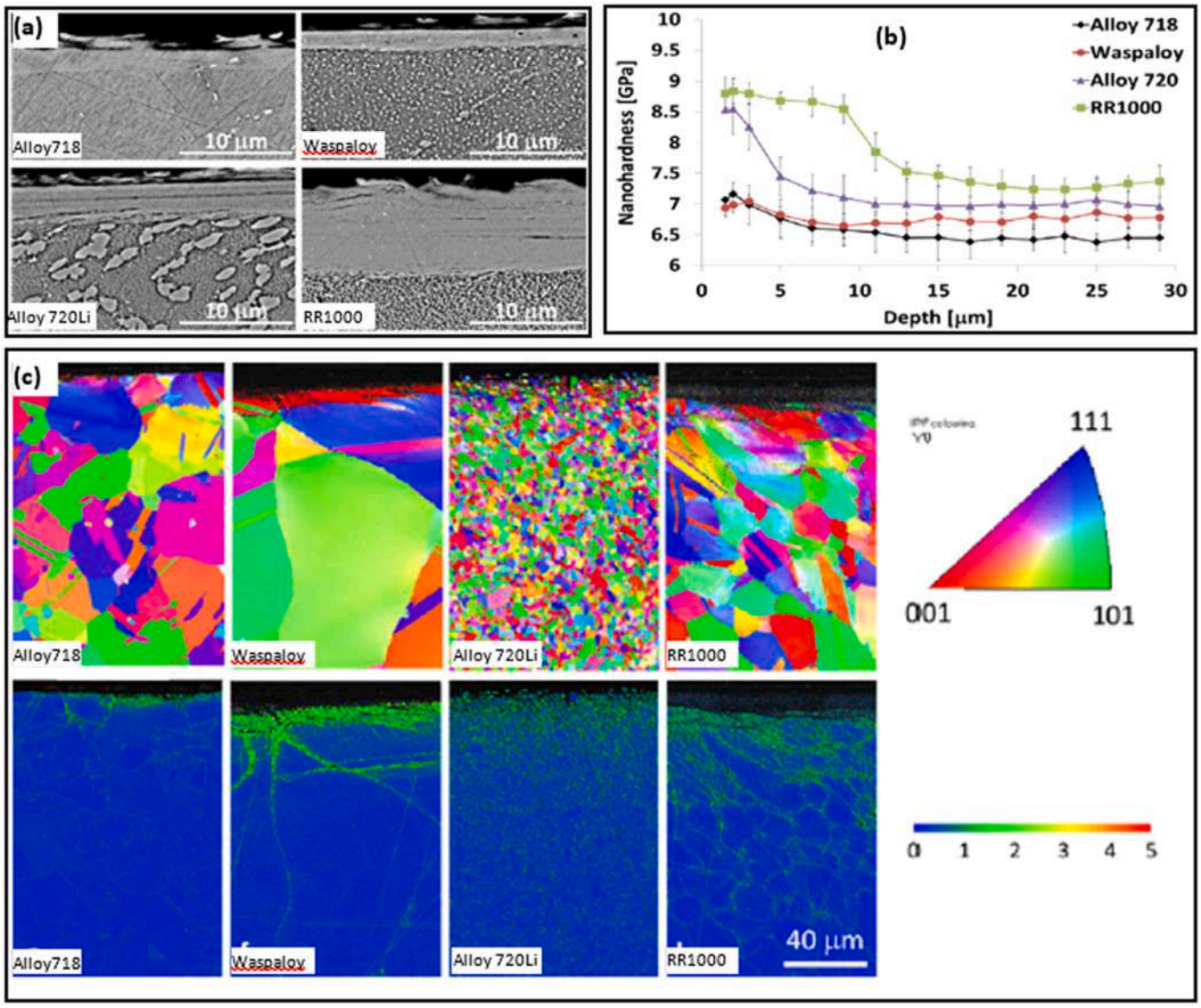

Fig. 27. SEM-SEI views, Nanohardness profiles, EBSD inverse pole figure, and strain contouring of deformed areas in the near machined surface of different alloys show that more mechanically performant alloys lead to low machinability [280].

For processes where primarily high temperatures occur, the use of cryogenic cooling can significantly improve machinability. Cryogenic cooling, usually employing liquid nitrogen, limits temperature rise by chilling the cutting zone. The cryogenic delivery reduced cutting temperatures by 300 °C during silicon nitride machining - well below the tool material's softening point, which enables improved tool life and surface quality [281]. Optimising the orientations of cryogenic nozzles might maximize heat extraction during the machining process. However it must be noticed that pure CO_2 lacks lubricating properties, which may lead to undesirable surface qualities for workpiece materials which lead to adhesion, e.g. Inconel 718 [306]. Studies on the combination of cryogenic cooling and MQL with external supply nozzles show that the additional use of oil leads to longer tool life for difficult to cut materials and to an improvement of the surface roughness [307,308]. The combination of nitrogen and MQL as a cooling strategy has high requirements for the process parameters and is therefore considered in more detail in the following section 7.2 "Hybrid machining". Due to its lower temperature, LN_2 has a higher cooling potential than CO_2 snow (−196 °C vs. −78.5 °C). LN_2 was successfully used to reduce tool wear compared to dry machining [309] and flood cooling. The lubrication effect of LN_2 is not proven clearly: Compared to dry conditions, the friction coefficient decreased in [310], didn't change in [311] and slightly increased in due to LN_2 application. Consequently, the reported tool wear reduction mainly relies on the lower process temperatures. A challenge in LN_2 cooling is, that the medium tends to evaporate within the supply lines [312,313], which drastically lowers the heat transfer and thus the cooling ability [282]. Counteractions are the insulation of tools and supply lines. As a reliable solution to this issue, the usage of a sub-cooler was proposed and successfully tested for orthogonal turning [314].

Another promising approach are so-called sub-zero metalworking fluids which are applied at liquid state, but at temperatures well below 0 °C. This novel cooling approach combines low supply temperatures with beneficial lubrication effects, offering a high potential for an effective cooling capacity [315,316]. The application of sub-zero metalworking fluids has so far been investigated for turning [317,318] and milling [319]. In comparison to conventional flood cooling and cryogenic cooling strategies, the application of sub-zero metalworking fluids resulted in less tool wear when turning 42CrMo4 [320] and Ti-6Al-4 V [315]. This reduction of tool wear is attributed to the high cooling capacities in superposition with beneficial lubrication effects which efficiently decreases the occurring thermal loads. A promoted

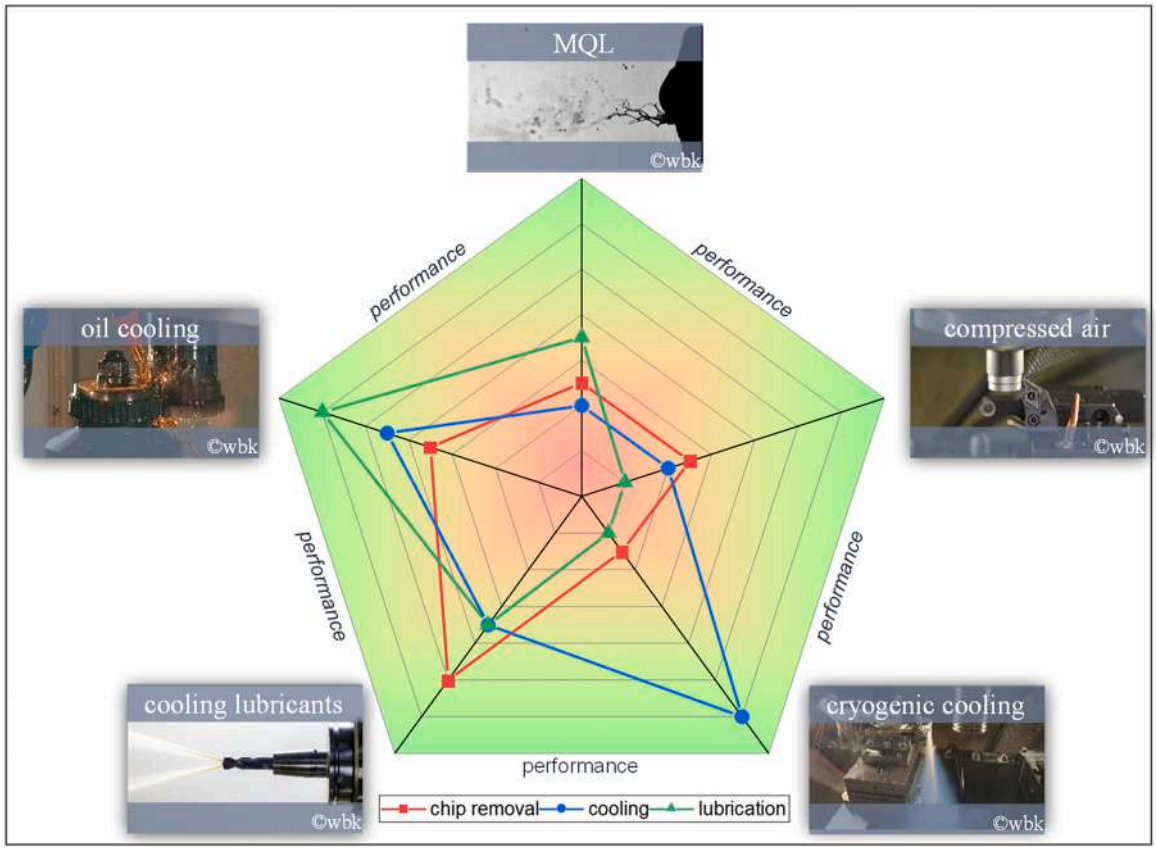

Fig. 28. Evaluation of the different cooling and lubrication strategies with regard to the main objectives chip removal, cooling, and lubrication [88], [282].

cooling capacity was also observed during hard turning of 100Cr6 [321, 322]. Better surface qualities were achieved due to beneficial lubrication effects of the liquid sub-zero metalworking fluid [323].

The high-pressure coolant systems directed at the tool-chip interface penetrate into the chip removal zone even during high-speed machining. In Inconel 718, the hydraulic wedge effect reduces frictional heat between the tool and workpiece, lowering thermal gradients, and enhances chip segmentation - transitions from long continuous to smaller C-type chips were observed with increasing pressure of the coolant system [281]. Regarding, the cutting type for carbide tools, such optimised high-pressure coolant delivery improved tool life. However, high-pressure impacts compromised ceramic tool integrity, which accelerates notching and fracture. Hence pressure limits should balance tool life and reliability based on tool material. While flood cooling media successfully removes chips from the tool and the workpiece, this remains a challenge for dry cutting, MQL and cryogenic cooling [324], which can lead to poorer machinability. When regarding finishing operations the part accuracy is of large importance. Flood cooling performs best because of its high thermal capacity and the high heat transfer between the part and the liquid oil or emulsion [325]. For dry and MQL cutting the accuracy is impaired due to the thermal extension of tool and workpiece.

To conclude, the previously presented coolant strategies in machining are to be classified in Table 2. These are to be compared with each other in relation to the main mechanisms. A solid circle represents the greatest potential to improve machinability for the respective main mechanism in comparison with the other concepts.

Table 2
Performance of cooling concepts in terms of machinability.

	cutting forces	tool-wear	surface roughness & integrity	chip formation and control	part accuracy
Flood cooling	●	◕	●	●	●
MQL	●	◕	●	◑	◕
Dry machining	◔	◔	◔	◔	◑
Cryogenic cooling	◑	●	◔	◑	◕
Sub-zero metal-working fluids	◕	●	◕	◕	No known investigations

7.2. Hybrid machining

The concept of hybrid machining has emerged as a strategy to improve the machinability through targeted introduction of energy sources and tools, such as lasers and ultrasonic vibrations. Commonly observed improvements realized in hybrid machining performance include reduced forces, improved chip form, and lower tool-wear [326,327]. For example, thermally assisted hybrid machining (e.g., via lasers or induction heating, or via high-speed dry cutting) may reduce cutting forces by promoting thermal softening of the workpiece material. A recent review on the topic of laser assisted machining of hard and brittle materials by You et al. [328] highlights the positive abilities of thermal softening to reduce cracks and other types of mechanical damage, while also discussing the need for careful pre-heating and control of laser power to avoid thermal damage. Generally speaking, thermal effects in machining typically result from increased cutting speeds or due to additional heat sources. Such effects will reduce process forces, yet result in thermal damage to the surface layer in the form of tensile residual stresses and undesirable/brittle phase transformations [329,330]. The process shows especially high potential in cutting ceramics and hardened steel [146,331]. Pujana et al. [332] studied ultrasonic vibration during Ti6Al4V drilling reduced feed forces and increased process temperatures compared to conventional drilling. Thus, by introducing heat in the cutting zone, the machinability of materials can be favoured.

All mechanical machining (cutting) is fundamentally a thermo-mechanical process and the material response of workpiece materials during cutting will be broadly governed by competition between thermal softening and strain/strain-rate hardening. In vibration-assisted machining, the tool/workpiece engagement is controlled and modulated to improve chip breaking and avoid undesirable tribological and chip formation regimes, such as built up edge and other material flow stagnation phenomena in the vicinity of the cutting edge. A recent review by Yang et al. [333] illustrates how tool life and machinability of materials with high strain hardening and low chip breakability can be greatly increased through ultrasonic vibration-assisted machining [334]. Consequently, vibration-assisted machining has seen numerous beneficial applications in optics and semiconductor applications, as well as in biomedical science and aerospace manufacturing. However, it should be noted that 'good vibrations' to improve machinability require careful study of the process physics and control over the amplitude and frequency of vibrations, as excessive vibrations may result in fatigue and damage to the workpiece material, as was observed in vibration-assisted grinding of ceramics [326,335].

7.3. Specific cutting tool design

Cutting tools are one of the key players determining machinability of engineering materials [336]. Commonly used cutting tool materials are high speed steel, tungsten carbide (WC), cermets, ceramics, polycrystalline cubic boron nitride (PCBN), polycrystalline diamond (PCD) [337]. Although cutting tool material, cutting edge shape and condition is of importance in terms of machining performance [81], cutting tool geometry also plays major role to enhance machining performance. Typical cutting tools are used in the machining industry for various operations including turning, milling, drilling, etc. Specific cutting tools with novel design are offer significant competition to generic cutting tool geometries for performing specific tasks and needs in machining process of advanced engineering materials such as composite, stainless steel, and aerospace alloys, etc. [64,338,339].

As discussed in previous sections, the advanced materials, including stainless steels, Ni- and Ti-based alloys that generally have low thermal conductivity, strain hardened response and low chip breakability, can have very low machinability [64]. These result in some well-acknowledged difficulties faced during chip removal process. Concerning cutting tools, although cutting edge shape and the cutting edge conditions are of great importance for improving machining performance [81], various macro level approaches have been utilized to resolve/reduce problems including developing new cutting tools or modifying the standard cutting tools depending on the requirement of process [83]. For instance, Oezkaya et al. [83] proposed flank face modification to enhance performance of cutting tools in drilling Inconel 718 alloy to increase tool life. Poulachon et al. [340] studied that controlling progressive flank wear of PCBN cutting tools is critical for ensuring part quality in hard turning of alloy steels. A generalized model built on key influences like cutting parameters, tool microstructure and work material hardness enables reliable prediction of tool wear rates for optimised performance. Besides, texturing the cutting tools is another common approach to enhance machinability of advanced engineering materials. Surface texture increases the area of heat dissipation in between the tool and cutting fluid or ambient air and thereby reduce the temperature of machining, adhesion, cutting forces, and friction at the contact interface [341]. This will contribute reducing or eliminating applied cutting fluid [341,342].

Many scientific works have been published in the literature to show the effectiveness of textured cutting tools on machinability of various materials [343] including steels [78], [344], Inconel alloys [345], Ti alloys [346] and carbon fiber reinforced plastics (CFRP) [347] during turning process [348], milling process [349], drilling process [350] and grinding processes [351]. The performance of textured cutting tools depends on some critical parameters such as groove dimensions including depth, width, diameter [344,352]. Besides, textured area, texture orientation, the surface of cutting tools texture generated, etc. [353]. Liao et al. [354] proposed novel concept on texturing tool through macro and micro channels on the rake face of cutting tools as depicted in Fig. 29. The contribution of this novel concept on machinability can be summarized as reduced friction coefficient, forces, shear energy, and chip breakability. Some researchers preferred to utilize micro holes instead of micro channels. For instance, Rao et al. [355] tested the performance of micro-hole patterns on the rake and flank face of PCD cutting tool. They reported that PCD tools with micro-hole patterns are capable of reducing cutting temperature, tool wear and surface roughness by approximately 30%, 50% and 40%, respectively. In addition to micro-channels, some industries are manufacturing spindles with integrated micro channels, where a high pressure of almost 200 bars can be utilized to pump the coolant while machining hard-to-cut materials.

8. Conclusion

This review paper is one of the results of CIRP's Collaborative Working Group on integrated machining performance for assessment of cutting tools (IMPACT). It provides an assessment of current state-of-the-art development in machinability evaluation and relevant knowledge for maximizing machining performance in the context of metal machining. While there is no complete and unanimously accepted definition of machinability concept existing, in this paper an in-depth analysis of tool performance, cutting force and temperature, chip form and breakability, surface integrity has been conducted to understand the current best-practices in machinability evaluation. It is expected that the fundamental knowledge obtained from the in-depth analysis of machinability evaluation should open new possibilities for the research community to develop better practice to improve machining performance.

The main conclusions of this review are as follows:

(1) The correlations of machinability with regard to the tool reveals that tool life as an indicator of machinability requires a holistic view of the machining process. This approach must include the influences of the workpiece properties, the tool properties as well as the process parameters in order to obtain a reliable assessment of the tool life. In the sense of comparability of the investigation results, the parameters for quantifying the tool life as well as the

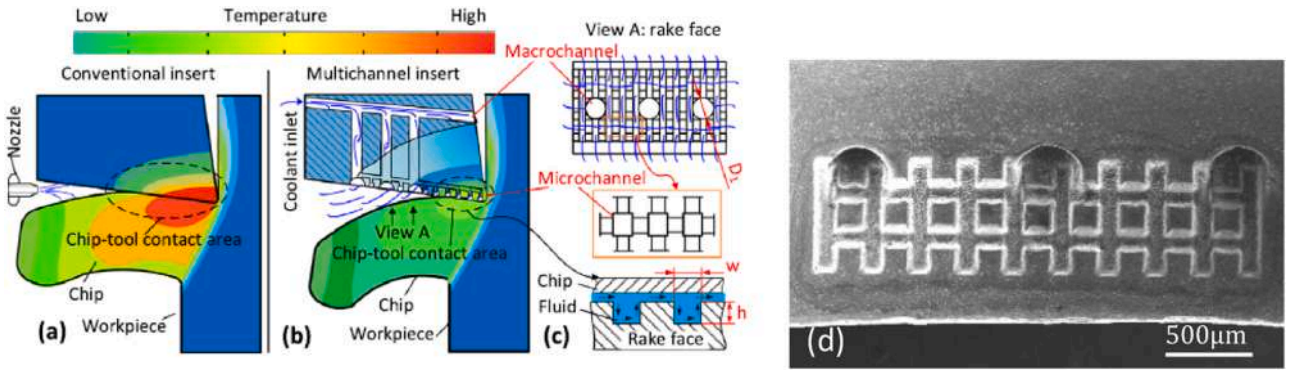

Fig. 29. (a) Conventional cutting tool's solution (b)-(d) the concept of proposed multichannel irrigation cutting insert [354].

tool life criteria must also be selected on the basis of scientific considerations.

(2) Cutting forces and process temperatures are mostly used in combination to evaluate the machinability. In general, the more difficult to machine of the material, the higher cutting force and temperature will be generated in machining process. However, as they are also significantly influenced by the complex interactions between the tool-workpieces, evaluating the materials machinability based on cutting force and temperatures has to be considered under particular circumstance.

(3) Every machining process is based on the separation of chips from the workpiece, and machinability is strictly related to the chip shape and chip formation mechanism. The lack of chip control generally implies negative effects on part quality and tool wear/tool failure. The complex correlation between tool, workpiece material, process parameters, chip morphology, breakability and machinability has been analyzed, together with the most common methods used in the industrial practice to manage and affect chip shape and fracture.

(4) Machinability can be effectively influenced by the metallurgical conditions (e.g., microstructure, chemistry, residual stress) of the materials and can significantly influence the surface integrity. Using limited variables such as material chemistry, retained austenite, and heat treatment technique, it was found that surface integrity aspects such as residual stresses, subgrain size, and retained austenite show trends in machinability. The data suggests that under laboratory conditions, it is possible to get cues about machinability from surface integrity.

(5) Apart from materials properties, machinability is mainly influenced by the cutting tool performance, cutting force and temperature, chip form and breakability as well as surface integrity. Hence, the machinability can be improved by the (i) optimised coolant strategies, e.g., MQL for high friction cutting and cryogenic cooling for high temperature cutting; (ii) hybrid machining, e.g., thermally assisted hybrid machining to soften the workpiece material reduce the cutting force; (iii) specific cutting design, e.g., texturing the cutting tools or other modifications of the tool flank/rake surface.

The major challenges in machinability for the future include the standardization of machinability evaluation and quantification methods of different materials for comprehensive industrial practice and application. On the other hand, gathering a good deal of industrial and laboratorial data to form a digitalized database for a wide range of engineering materials will also benefit the future globalized knowledge share for the community. Apart from that, how to optimize the machining performance of the total machining system based on these data is also one of the channelings that needs to be addressed. This will also be discussed in other topic groups (i.e., Topic B-E) of CIRP CWG IMPACT.

Declaration of Competing Interest

The authors declare that they have no known competing financial interests or personal relationships that could have appeared to influence the work reported in this paper.

Acknowledgement

The authors would like to thank Prof. Ibrahim S. Jawahir form University of Kentucky who initiated and led the CIRP collaborative working group (CWG) on integrated machining performance for assessment of cutting tools (IMPACT). We also thank Prof. Dragos Axinte and Dr. Omkar Mypati from University of Nottingham, Prof. Thomas Bergs and Dr. Markus Meurer from RWTH Aachen University, Prof. Dirk Biermann and Dr. Ivan Iovkov from TU Dortmund University, Prof. Berend Denkena, Mr. Lars Ellersiek, Jonas Matthies and Felix Zender from Leibniz Universität Hannover, Prof. Luca Settineri from Politecnico di Torino and Dr. Ulrika Brohede from Swerim AB, and Mr. Florian Sauer from Karlsruhe Institute of Technology. They have all made big effort and contribution to Topic A of CIRP CWG IMPACT as well as this paper. Zhirong Liao acknowledge the support of the United Kingdom Engineering and Physical Sciences Research Council (EPSRC) through grant number EP/V055011/1 for project SENSYCUT.

References

[1] ASM Handbook Volume 16: Machining. ASM International; 1989.
[2] Field M, Kahles JF, Cammett JT. A review of measuring methods for surface integrity. C I R P 1972;vol. 21(2):219–38.
[3] Liao Z, et al. Surface integrity in metal machining-Part I: Fundamentals of surface characteristics and formation mechanisms. Int J Mach Tools Manuf 2021:103687.
[4] la Monaca A, et al. Surface integrity in metal machining-Part II: Functional performance. Int J Mach Tools Manuf 2021:103718.
[5] F.W. Taylor, *On the art of cutting metals*, vol. 23. American society of mechanical engineers, 1906.
[6] Woldman NE, Gibbons RC. Machinability and machining of metals. McGraw-Hill; 1951.
[7] Poulachon G, Bandyopadhyay BP, Jawahir IS, Pheulpin S, Seguin E. The influence of the microstructure of hardened tool steel workpiece on the wear of PCBN cutting tools. Int J Mach Tools Manuf 2003;vol. 43(2):139–44. https://doi.org/10.1016/S0890-6955(02)00170-0.
[8] Liu H, et al. The state of the art for numerical simulations of the effect of the microstructure and its evolution in the metal-cutting processes. Int J Mach Tools Manuf 2022;vol. 177(January):103890. https://doi.org/10.1016/j.ijmachtools.2022.103890.
[9] Li B, Liu H, Zhang J, Xu B, Zhao W. Multi-mechanism-based twinning evolution in machined surface induced by thermal-mechanical loads with increasing cutting speeds. Int J Mach Tools Manuf 2023;vol. 192(September):104074. https://doi.org/10.1016/j.ijmachtools.2023.104074.
[10] Olofson CT, Gurklis JA, Boulger FW. Machining and grinding of ultrahigh-strength steels and stainless steel alloys. Battelle Memorial Insititute; 1967.
[11] Olofson CT, Gurklis JA, Boulger FW. Machining and Grinding of Nickel- and Cobalt-base Alloys. Battelle Memorial Inst Columbus Ohio; 1966.
[12] Mills B, Redford AH. Machinability of engineering materials. Mach Eng Mater 1983. https://doi.org/10.1007/978-94-009-6631-4.

[13] Fang XD, Jawahir IS. Predicting total machining performance in finish turning using integrated fuzzy-set models of the machinability parameters. Int J Prod Res 1994;vol. 32(4):833–49. https://doi.org/10.1080/00207549408956974.
[14] Enache S, Străjescu E, Opran C, Minciu C, Zamfirache M. Mathematical model for the establishment of the materials machinability. CIRP Ann Jan. 1995;vol. 44(1): 79–82. https://doi.org/10.1016/S0007-8506(07)62279-3.
[15] Schoop J, Poonawala HA, Adeniji D, Clark B. AI-enabled dynamic finish machining optimization for sustained surface integrity. Manuf Lett 2021;vol. 29: 42–6.
[16] Denkena B, Lucas A, Bassett E. Effects of the cutting edge microgeometry on tool wear and its thermo-mechanical load. CIRP Ann 2011;vol. 60(1):73–6.
[17] Damir A, Shi B, Attia MH. Flow characteristics of optimized hybrid cryogenic-minimum quantity lubrication cooling in machining of aerospace materials. CIRP Ann 2019;vol. 68(1):77–80.
[18] Mian NS, Fletcher S, Longstaff AP, Myers A. Efficient thermal error prediction in a machine tool using finite element analysis,. Meas Sci Technol 2011;vol. 22(8): 85107.
[19] Shoja S, Norgren S, Andrén HO, Bäcke O, Halvarsson M. On the influence of varying the crystallographic texture of alumina CVD coatings on cutting performance in steel turning. Int J Mach Tools Manuf 2022;vol. 176(March). https://doi.org/10.1016/j.ijmachtools.2022.103885.
[20] I. Iso, "ISO 3865:1993. Tool-life testing with single-point turning tools," ISO 38651993. Tool-life Test. with single-point Turn. tools, 1993.
[21] de Normalización OI. ISO 8688-1: 1989: Tool Life Testing in Milling-Part 1: Face Milling. International Organization for Standarization; 1989.
[22] Zum Gahr KH. 4. Tribological aspects of microsystems, vol. 6. Elsevier Masson SAS; 1998. https://doi.org/10.1016/S1386-2766(98)80005-4.
[23] Liu E, An W, Xu Z, Zhang H. Experimental study of cutting-parameter and tool life reliability optimization in inconel 625 machining based on wear map approach. J Manuf Process 2020;vol. 53(January 2019):34–42. https://doi.org/10.1016/j.jmapro.2020.02.006.
[24] Da Silva WM, Suarez MP, Machado AR, Costa HL. Effect of laser surface modification on the micro-abrasive wear resistance of coated cemented carbide tools. Wear 2013;vol. 302(1–2):1230–40. https://doi.org/10.1016/j.wear.2013.01.035.
[25] Tamil Alagan N, Hoier P, Zeman P, Klement U, Beno T, Wretland A. Effects of high-pressure cooling in the flank and rake faces of WC tool on the tool wear mechanism and process conditions in turning of alloy 718. Wear 2019;vol. 434–435(April):102922. https://doi.org/10.1016/j.wear.2019.05.037.
[26] Nordgren A, Samani BZ, MSaoubic R. Experimental study and modelling of plastic deformation of cemented carbide tools in turning. Procedia CIRP 2014;vol. 14: 599–604. https://doi.org/10.1016/j.procir.2014.03.021.
[27] Olovsjö S, Nyborg L. Influence of microstructure on wear behaviour of uncoated WC tools in turning of Alloy 718 and Waspaloy. Wear 2012;(vol. 282–283): 12–21. https://doi.org/10.1016/j.wear.2012.01.004.
[28] Grzesik W. Advanced machining processes of metallic materials. Elsevier; 2008.
[29] Iturbe A, Hormaetxe E, Garay A, Arrazola PJ. Surface integrity analysis when machining inconel 718 with conventional and cryogenic cooling. Procedia CIRP 2016;vol. 45(Table 1):67–70. https://doi.org/10.1016/j.procir.2016.02.095.
[30] Devillez A, Schneider F, Dominiak S, Dudzinski D, Larrouquere D. Cutting forces and wear in dry machining of Inconel 718 with coated carbide tools. Wear 2007; vol. 262(7–8):931–42. https://doi.org/10.1016/j.wear.2006.10.009.
[31] Pirtini M, Lazoglu I. Forces and hole quality in drilling. Int J Mach Tools Manuf 2005;vol. 45(11):1271–81. https://doi.org/10.1016/j.ijmachtools.2005.01.004.
[32] Hajdu D, Astarloa A, Kovacs I, Dombovari Z. The curved uncut chip thickness model: a general geometric model for mechanistic cutting force predictions. Int J Mach Tools Manuf 2023;vol. 188(December 2022):104019. https://doi.org/10.1016/j.ijmachtools.2023.104019.
[33] Shekhar S, Bediz B, Ozdoganlar OB. Tool-tip dynamics in micromachining with arbitrary tool geometries and the effect of spindle speed. Int J Mach Tools Manuf 2023;vol. 185(December 2022):103981. https://doi.org/10.1016/j.ijmachtools.2022.103981.
[34] Kumar A, Maurya A, Kandadi VM, Mahato A. Introduction of rolling motion at the tool-tip in metal cutting. Int J Mach Tools Manuf 2023;vol. 186(January):104001. https://doi.org/10.1016/j.ijmachtools.2023.104001.
[35] J.Paulo Davim, Machinability of Advanced Materials, vol. 9781848213; 2014. doi: 10.1002/9781118576854.
[36] Endler I, et al. "Novel aluminum-rich Ti1 - xAlxN coatings by LPCVD. Surf Coatings Technol 2008;vol. 203(5–7):530–3. https://doi.org/10.1016/j.surfcoat.2008.04.098.
[37] Bassett E, Köhler J, Denkena B. On the honed cutting edge and its side effects during orthogonal turning operations of AISI1045 with coated WC-Co inserts. CIRP J Manuf Sci Technol 2012;vol. 5(2):108–26. https://doi.org/10.1016/j.cirpj.2012.03.004.
[38] Bouzakis KD, et al. Effect of cutting edge preparation of coated tools on their performance in milling various materials. CIRP J Manuf Sci Technol 2014;vol. 7 (3):264–73. https://doi.org/10.1016/j.cirpj.2014.05.003.
[39] Brinksmeier E, Janssen R. Drilling of multi-layer composite materials consisting of carbon fiber reinforced plastics (CFRP), titanium and aluminum alloys. *CIRP Ann* - Manuf Technol 2002;vol. 51(1):87–90. https://doi.org/10.1016/S0007-8506(07)61472-3.
[40] Mills B, Redford AH. Machinability of engineering materials. London: Applied Science Publishers; 1983.
[41] Wang X, Huang C, Zou B, Liu H, Zhu H, Wang J. A new method to evaluate the machinability of difficult-to-cut materials. Int J Adv Manuf Technol Oct. 2014; vol. 75(1–4):91–6. https://doi.org/10.1007/s00170-014-6126-7.
[42] Li X, Liu X, Yue C, Liang SY, Wang L. Systematic review on tool breakage monitoring techniques in machining operations. Int J Mach Tools Manuf 2022; vol. 176(November 2021):103882. https://doi.org/10.1016/j.ijmachtools.2022.103882.
[43] MacHai C, Biermann D. Machining of β-titanium-alloy Ti-^{10}V–^{2}Fe-3Al under cryogenic conditions: cooling with carbon dioxide snow. J Mater Process Technol 2011;vol. 211(6):1175–83. https://doi.org/10.1016/j.jmatprotec.2011.01.022.
[44] Uhlmann E, Zanatta AM, Mahr F, Gomes JO. Influence of inclusion contents on the micro-machinability of three plastic mold steels. Int J Adv Manuf Technol Oct. 2013;vol. 68(9–12):2451–60. https://doi.org/10.1007/s00170-013-4835-y.
[45] Dadgari A, Huo D, Swailes D. Investigation on tool wear and tool life prediction in micro-milling of Ti-6Al-4V. Nami Jishu yu Jingmi Gongcheng/*Nanotechnology Precis Eng* 2018;vol. 1(4):218–25. https://doi.org/10.1016/j.npe.2018.12.005.
[46] Aamir M, Tolouei-Rad M, Giasin K, Vafadar A. Machinability of Al2024, Al6061, and Al5083 alloys using multi-hole simultaneous drilling approach. J Mater Res Technol 2020;vol. 9(5):10991–1002. https://doi.org/10.1016/j.jmrt.2020.07.078.
[47] Abouridouane M, Klocke F, Döbbeler B. Characterisation and modelling of the machinability of ferritic-pearlitic steels in drilling operations. Procedia CIRP 2017;vol. 58:79–84. https://doi.org/10.1016/j.procir.2017.03.197.
[48] Songmene V, Zaghbani I, Kientzy G. Machining and machinability of tool steels: effects of lubrication and machining conditions on tool wear and tool life data. Procedia CIRP 2018;vol. 77(September):505–8. https://doi.org/10.1016/j.procir.2018.08.252.
[49] Lalbondre R, Krishna P, Mohankumar GC. An experimental investigation on machinability studies of steels by face turning. Procedia Mater Sci 2014;vol. 6: 1386–95. https://doi.org/10.1016/j.mspro.2014.07.118.
[50] Geng H, Wu X, Wang H, Min Y. Effects of copper content on the machinability and corrosion resistance of martensitic stainless steel. J Mater Sci Jan. 2008;vol. 43 (1):83–7. https://doi.org/10.1007/s10853-007-2084-x.
[51] Hoseiny H, et al. The effect of the martensitic packet size on the machinability of modified AISI P20 prehardened mold steel. J Mater Sci 2012;vol. 47(8):3613–20. https://doi.org/10.1007/s10853-011-6208-y.
[52] Pérez-Salinas CF, del Olmo A, López de Lacalle LN. Estimation of drag finishing abrasive effect for cutting edge preparation in broaching tool. Materials (Basel) 2022;vol. 15(15). https://doi.org/10.3390/ma15155135.
[53] Nayyar V, Kaminski J, Kinnander A, Nyborg L. An experimental investigation of machinability of graphitic cast iron grades; Flake, compacted and spheroidal graphite iron in continuous machining operations. Procedia CIRP 2012;vol. 1(1): 488–93. https://doi.org/10.1016/j.procir.2012.04.087.
[54] Sun FJ, Qu SG, Li G, Pan YX, Li XQ. Comparison of the machinability of titanium alloy forging and powder metallurgy materials. Int J Adv Manuf Technol 2016; vol. 85(5–8):1529–38. https://doi.org/10.1007/s00170-015-8045-7.
[55] Armendia M, Garay A, Iriarte LM, Arrazola PJ. Comparison of the machinabilities of Ti6Al4V and TIMETAL® 54M using uncoated WC-Co tools. J Mater Process Technol Jan. 2010;vol. 210(2):197–203. https://doi.org/10.1016/j.jmatprotec.2009.08.026.
[56] Priarone PC, Robiglio M, Settineri L. On the concurrent optimization of environmental and economic targets for machining. J Clean Prod 2018;vol. 190: 630–44. https://doi.org/10.1016/j.jclepro.2018.04.163.
[57] Carvalho MRDD, Antonialli AÍS, Diniz AE. A machinability evaluation based on the thermal and mechanical properties of two engine valve steels. Int J Adv Manuf Technol 2020;vol. 110(11–12):3209–19. https://doi.org/10.1007/s00170-020-06108-w.
[58] Klocke F, Döbbeler B, Lakner T. Influence of cooling nozzle orientation on the machinability of TiAl6V4 and 42CrMo4+QT in rough milling. Procedia CIRP 2018;vol. 77(Hpc):66–9. https://doi.org/10.1016/j.procir.2018.08.217.
[59] Nath C, Brooks Z, Kurfess TR. On machinability study and process optimization in face milling of some alloys with indexable copy face mill inserts. Procedia Manuf 2015;vol. 1:487–500. https://doi.org/10.1016/j.promfg.2015.09.008.
[60] Teti R. Machining of composite materials. CIRP Ann 2002;vol. 51(2):611–34.
[61] Ånmark N, et al. The effect of inclusion composition on tool wear in hard part turning using PCBN cutting tools. Wear 2015;(vol. 334–335):13–22. https://doi.org/10.1016/j.wear.2015.04.008.
[62] Hegde A, Sharma S, Gowri Shankar MC. Machinability and related properties of austempered ductile iron: a review. J Mech Eng Sci 2018;vol. 12(4):4180–90. https://doi.org/10.15282/jmes.12.4.2018.14.0360.
[63] Daber S, Prasad Rao P. Formation of strain-induced martensite in austempered ductile iron. J Mater Sci 2008;vol. 43(1):357–67. https://doi.org/10.1007/s10853-007-2258-6.
[64] M'Saoubi R, et al. High performance cutting of advanced aerospace alloys and composite materials Jan. 2015;vol. 64(2):557–80.
[65] Wang J, Zhang G, Chen N, Zhou M, Chen Y. A review of tool wear mechanism and suppression method in diamond turning of ferrous materials. Int J Adv Manuf Technol 2021;vol. 113(11–12):3027–55. https://doi.org/10.1007/s00170-021-06700-8.
[66] Paul E, Evans CJ, Mangamelli A, McGlauflin ML, Polvani RS. Chemical aspects of tool wear in single point diamond turning. Precis Eng 1996;vol. 18(1):4–19.
[67] Zong WJ, Sun T, Li D, Cheng K. Design criterion for crystal orientation of diamond cutting tool. Diam Relat Mater 2009;vol. 18(4):642–50. https://doi.org/10.1016/j.diamond.2008.11.003.
[68] Huang W, Yan J. Mechanisms of tool-workpiece interaction in ultraprecision diamond turning of single-crystal SiC for curved microstructures. Int J Mach Tools Manuf 2023;vol. 191(July):104063. https://doi.org/10.1016/j.ijmachtools.2023.104063.

[69] Weinert K, König W. A consideration of tool wear mechanism when machining metal matrix composites (MMC). *CIRP Ann* - Manuf Technol 1993;vol. 42(1): 95–8. https://doi.org/10.1016/S0007-8506(07)62400-7.
[70] Kannan S, Kishawy HA, Balazinski M. Flank wear progression during machining metal matrix composites. *J Manuf Sci Eng* Trans ASME 2006;vol. 128(3):787–91. https://doi.org/10.1115/1.2164508.
[71] Xavior MA, Kumar JPA. Machinability of hybrid metal matrix composite - a review. Procedia Eng 2017;vol. 174:1110–8. https://doi.org/10.1016/j.proeng.2017.01.264.
[72] Velavan K, Palanikumar K, Natarajan E, Lim WH. Implications on the influence of mica on the mechanical properties of cast hybrid (Al+10%B4C+Mica) metal matrix composite. J Mater Res Technol 2021;vol. 10:99–109. https://doi.org/10.1016/j.jmrt.2020.12.004.
[73] Yang X, Zhang B, Bai Q, Zheng M, Tang J. Grain size influence on chip formation in high-speed machining of pure iron. Int J Adv Manuf Technol 2020;vol. 108 (5–6):1357–66. https://doi.org/10.1007/s00170-020-05512-6.
[74] Byrne G, Dornfeld D, Denkena B. Advancing cutting technology. *CIRP Ann* - Manuf Technol 2003;vol. 52(2):483–507. https://doi.org/10.1016/S0007-8506(07)60200-5.
[75] Biermann D, Steiner M, Krebs E. Investigation of different hard coatings for micromilling of austenitic stainless steel. Procedia CIRP 2013;vol. 7:246–51. https://doi.org/10.1016/j.procir.2013.05.042.
[76] Bouzakis KD, Michailidis N, Skordaris G, Bouzakis E, Biermann D, M'Saoubi R. Cutting with coated tools: coating technologies, characterization methods and performance optimization. *CIRP Ann* - Manuf Technol 2012;vol. 61(2):703–23. https://doi.org/10.1016/j.cirp.2012.05.006.
[77] Bouzakis KD, et al. The effect of substrate pretreatments and HPPMS-deposited adhesive interlayers' materials on the cutting performance of coated cemented carbide inserts. *CIRP Ann* - Manuf Technol 2010;vol. 59(1):73–6. https://doi.org/10.1016/j.cirp.2010.03.065.
[78] Enomoto T, Sugihara T, Yukinaga S, Hirose K, Satake U. Highly wear-resistant cutting tools with textured surfaces in steel cutting. *CIRP Ann* - Manuf Technol 2012;vol. 61(1):571–4. https://doi.org/10.1016/j.cirp.2012.03.123.
[79] Klocke F, Schroeder T, Bouzakis E, Klein A. Manipulation of coating and subsurface properties in reconditioning of WC-Co carbide cutting tools. Surf Coatings Technol 2007;vol. 202(4–7):1194–8. https://doi.org/10.1016/j.surfcoat.2007.06.023.
[80] Bathe T, Biermann D. Developments in pre- and post-treatment of thin films and their influences on surface topography and coating adhesion strength of cutting tools. Prod Eng 2019;vol. 13(6):751–9. https://doi.org/10.1007/s11740-019-00921-3.
[81] Denkena B, Biermann D. Cutting edge geometries. *CIRP Ann* - Manuf Technol 2014;vol. 63(2):631–53. https://doi.org/10.1016/j.cirp.2014.05.009.
[82] Tiffe M, Aßmuth R, Saelzer J, Biermann D. Investigation on cutting edge preparation and FEM assisted optimization of the cutting edge micro shape for machining of nickel-base alloy. Prod Eng 2019;vol. 13(3–4):459–67. https://doi.org/10.1007/s11740-019-00900-8.
[83] Oezkaya E, Bücker M, Strodick S, Biermann D. A thermomechanical analysis leading to a novel flank face design providing longer tool lives for tools used in the drilling of Inconel 718. Int J Adv Manuf Technol 2019;vol. 102(9–12): 2977–92. https://doi.org/10.1007/s00170-019-03417-7.
[84] Guo K, Zhang Y, Sun J. Towards stable milling: principle and application of active contact robotic milling. Int J Mach Tools Manuf 2022;vol. 182(August):103952. https://doi.org/10.1016/j.ijmachtools.2022.103952.
[85] Iakovakis E, Avcu E, Roy MJ, Gee M, Matthews A. Dry sliding wear behaviour of additive manufactured CrC-rich WC-Co cemented carbides. Wear 2021;vol. 486–487(September):204127. https://doi.org/10.1016/j.wear.2021.204127.
[86] Balázs BZ, Geier N, Takács M, Davim JP. A review on micro-milling: recent advances and future trends. Int J Adv Manuf Technol 2021;vol. 112(3–4):655–84. https://doi.org/10.1007/s00170-020-06445-w.
[87] Younas M, Jaffery SHI, Khan A, Khan M. Development and analysis of tool wear and energy consumption maps for turning of titanium alloy (Ti6Al4V). J Manuf Process 2021;vol. 62:613–22. https://doi.org/10.1016/j.jmapro.2020.12.060.
[88] Weinert K, Inasaki I, Sutherland JW, Wakabayashi T. Dry machining and minimum quantity lubrication. *CIRP Ann* - Manuf Technol 2004;vol. 53(2): 511–37. https://doi.org/10.1016/S0007-8506(07)60027-4.
[89] Jemielniak K. Review of new developments in machining of aerospace materials. J Mach Eng 2021;vol. 21(1):22–55. https://doi.org/10.36897/jme/132905.
[90] Wolf T, Iovkov I, Biermann D. Influence of a discontinuous process strategy on microstructure and microhardness in drilling inconel 718. J Manuf Mater Process 2021;vol. 5(2). https://doi.org/10.3390/jmmp5020043.
[91] Kumar MN, Kanmani Subbu S, Vamsi Krishna P, Venugopal A. Vibration assisted conventional and advanced machining: a review. Procedia Eng 2014;vol. 97: 1577–86. https://doi.org/10.1016/j.proeng.2014.12.441.
[92] Pecat O, Brinksmeier E. Tool wear analyses in low frequency vibration assisted drilling of CFRP/Ti6Al4V stack material. Procedia CIRP 2014;vol. 14:142–7. https://doi.org/10.1016/j.procir.2014.03.050.
[93] Pereira O, Rodríguez A, Fernández-Abia AI, Barreiro J, López de Lacalle LN. Cryogenic and minimum quantity lubrication for an eco-efficiency turning of AISI 304. J Clean Prod 2016;vol. 139:440–9. https://doi.org/10.1016/j.jclepro.2016.08.030.
[94] Pereira O, et al. The use of hybrid CO_2+MQL in machining operations. Procedia Eng 2015;vol. 132:492–9. https://doi.org/10.1016/j.proeng.2015.12.524.
[95] Pereira O, Rodríguez A, Barreiro J, Fernández-Abia AI, de Lacalle LNL. Nozzle design for combined use of MQL and cryogenic gas in machining. Int J Precis Eng Manuf - Greening Technol 2017;vol. 4(1):87–95. https://doi.org/10.1007/s40684-017-0012-3.
[96] Pereira O, Celaya A, Urbikaín G, Rodríguez A, Fernández-Valdivielso A, Noberto López de Lacalle L. CO_2 cryogenic milling of Inconel 718: cutting forces and tool wear. J Mater Res Technol 2020;vol. 9(4):8459–68. https://doi.org/10.1016/j.jmrt.2020.05.118.
[97] Platt T, Meijer A, Biermann D. Conduction-based thermally assisted micromilling process for cutting difficult-to-machine materials. J Manuf Mater Process 2020; vol. 4(2). https://doi.org/10.3390/jmmp4020034.
[98] Agrawal C, Khanna N, Pruncu CI, Singla AK, Gupta MK. Tool wear progression and its effects on energy consumption and surface roughness in cryogenic assisted turning of Ti-6Al-4V. Int J Adv Manuf Technol 2020;vol. 111(5–6):1319–31. https://doi.org/10.1007/s00170-020-06140-w.
[99] Wong SV, Hamouda AMS. The development of an online knowledge-based expert system for machinability data selection. Knowledge-Based Syst 2003;vol. 16(4): 215–29. https://doi.org/10.1016/S0950-7051(02)00083-7.
[100] Abbá E, Speidel A, Liao Z, Axinte D, Novovic D. A bar of cutting fluid: Deep Eutectic Fluids with a novel flavour. Mater Today Adv 2022;vol. 16. https://doi.org/10.1016/j.mtadv.2022.100291.
[101] Zhang P, Gao D, Hong D, Lu Y, Wang Z, Liao Z. Intelligent tool wear monitoring based on multi-channel hybrid information and deep transfer learning. J Manuf Syst 2023;vol. 69(September 2022):31–47. https://doi.org/10.1016/j.jmsy.2023.06.004.
[102] Taniguchi N. On the evaluation of machinability, grindability and other workabilities based on specific cost of production. Ann CIRP SVIV 1971:471–6.
[103] Arriol AI, Whitentone I, Heigel J, Arrazola PJ. Relationship between machinability index and in-process parameters during orthogonal cutting of steels. *CIRP Ann* Manuf Technol 2011;vol. 60(1):93–6.
[104] Arrazola P-J, Garay A, María Iriarte L, Armendia M, Marya S, Le Maître F. Machinability of titanium alloys (Ti6Al4V and Ti555.3). J Mater Process Technol 2009;vol. 209(5):2223–30. https://doi.org/10.1016/j.jmatprotec.2008.06.020ï.
[105] Gonçalves RA, Da Silva MB. Influence of copper content on 6351 aluminum alloy machinability. Procedia Manuf Jan. 2015;vol. 1:683–95. https://doi.org/10.1016/J.PROMFG.2015.09.014.
[106] Songmene V, Balazinski M. Machinability of graphitic metal matrix composites as a function of reinforcing particles. CIRP Ann Jan. 1999;vol. 48(1):77–80. https://doi.org/10.1016/S0007-8506(07)63135-7.
[107] Denkena B, Krödel A, Pape O. Increasing productivity in heavy machining using a simulation based optimization method for porcupine milling cutters with a modified geometry. Procedia Manuf 2019;vol. 40:14–21. https://doi.org/10.1016/J.PROMFG.2020.02.004.
[108] Bergmann B, Grove T. Basic principles for the design of cutting edge roundings. CIRP Ann Jan. 2018;vol. 67(1):73–8. https://doi.org/10.1016/J.CIRP.2018.04.019.
[109] Klocke DF, Klöpper C, Lung D, Essig C. Fundamental wear mechanisms when machining austempered ductile iron (ADI). CIRP Ann Jan. 2007;vol. 56(1):73–6. https://doi.org/10.1016/J.CIRP.2007.05.020.
[110] Kienzle O, Victor H. Einfluss der Wäbehandlung von Stählen auf die Hauptschnittkraft beim Drehen. Stahlern und Eisen 1954;vol. 74(9):530–9.
[111] Moriwaki T. Machinability of copper in ultra-precision micro diamond cutting. CIRP Ann Jan. 1989;vol. 38(1):115–8. https://doi.org/10.1016/S0007-8506(07)62664-X.
[112] Ottersbach M, Zhao W. Experimental investigations on the machinability of tungsten carbides in orthogonal cutting with diamond-coated tools. Procedia CIRP Jan. 2016;vol. 46:416–9. https://doi.org/10.1016/J.PROCIR.2016.04.008.
[113] Usui E, Takeyama H. A photoelastic analysis of machining stresses. J Eng Ind Nov. 1960;vol. 82(4):303–7. https://doi.org/10.1115/1.3664233.
[114] Amini E. Photoelastic analysis of stresses and forces in steady cutting. J Strain Anal Jun. 1968;vol. 3(3):206–13. https://doi.org/10.1243/03093247V033206.
[115] Childs THC, Mahdi MI, Barrow G. On the stress distribution between the chip and tool during metal turning. CIRP Ann Jan. 1989;vol. 38(1):55–8. https://doi.org/10.1016/S0007-8506(07)62651-1.
[116] Kato S, Yamaguchi K, Yamada M. Stress distribution at the interface between tool and chip in machining. J Eng Ind May 1972;vol. 94(2):683–9. https://doi.org/10.1115/1.3428229.
[117] DeChiffre L. Lubrication in cutting—critical review and experiments with restricted contact tools. ASLE Trans Jan. 1981;vol. 24(3):340–4. https://doi.org/10.1080/05698198108983030.
[118] Usui E, Kikuchi K, Hoshi K. The theory of plasticity applied to machining with cut-away tools. J Eng Ind May 1964;vol. 86(2):95–104. https://doi.org/10.1115/1.3670497.
[119] Sutter G, List G. Very high speed cutting of Ti–6Al–4V titanium alloy – change in morphology and mechanism of chip formation. Int J Mach Tools Manuf Mar. 2013;vol. 66:37–43. https://doi.org/10.1016/J.IJMACHTOOLS.2012.11.004.
[120] Kose E, Kurt A, Seker U. The effects of the feed rate on the cutting tool stresses in machining of Inconel 718. J Mater Process Technol Jan. 2008;vol. 196(1–3): 165–73. https://doi.org/10.1016/J.JMATPROTEC.2007.05.019.
[121] R.B. Amor, "Thermomechanische Wirkmechanismen und Spanbildung bei der Hochgeschwindigkeitszerspanung.," Leibniz Universität Hannover, 2003.
[122] Gao W, et al. Machine tool calibration: measurement, modeling, and compensation of machine tool errors. Int J Mach Tools Manuf 2023;vol. 187 (March). https://doi.org/10.1016/j.ijmachtools.2023.104017.
[123] B. Denkena, E.P. Stephan, M. Maischak, D. Heinisch, and M. Andres, "Numerical Computation Methods for Modeling the Phenomenon of Tool Extraction," pp. 285–308, 2013, doi: 10.1007/978–3-642–32448-2_13.

[124] Nakayama K, Shaw MC, Brewer RC. Relationship between cutting forces, temperaturs, built-up edge and surface finish. Ann CIRP 1966;no. 14:221–3.
[125] Aspinwall DK, Dewes RC, Mantle AL. The machining of γ-TiAI intermetallic alloys. CIRP Ann Jan. 2005;vol. 54(1):99–104. https://doi.org/10.1016/S0007-8506(07)60059-6.
[126] Schmidt A. Heat in metal cutting. ASM International,; 1949.
[127] Shaw MC. Energy conversion in cutting and grinding. CIRP Ann Jan. 1996;vol. 45 (1):101–4. https://doi.org/10.1016/S0007-8506(07)63025-X.
[128] Bedekar V, Shivpuri R, Chaudhari R, Hyde RS. Nanostructural evolution of hard turning layers in response to insert geometry, cutting parameters and material microstructure. CIRP Ann Jan. 2013;vol. 62(1):63–6. https://doi.org/10.1016/J.CIRP.2013.03.090.
[129] Davies MA, Ueda T, M'Saoubi R, Mullany B, Cooke AL. On the measurement of temperature in material removal processes. CIRP Ann Jan. 2007;vol. 56(2): 581–604. https://doi.org/10.1016/J.CIRP.2007.10.009.
[130] Arrazola PJ, Özel T, Umbrello D, Davies M, Jawahir IS. Recent advances in modelling of metal machining processes. *CIRP Ann* - Manuf Technol 2013;vol. 62 (2):695–718. https://doi.org/10.1016/J.CIRP.2013.05.006.
[131] Trigger KJ. Progress report No. 2 on chip–tool interface temperatures. " *Trans ASME* 1949;vol. 71:163–74.
[132] Sölter J, Gulpak M. Heat partitioning in dry milling of steel. *CIRP Ann* - Manuf Technol 2012;vol. 61(1):87–90. https://doi.org/10.1016/J.CIRP.2012.03.046.
[133] Moufki A, Molinari A, Dudzinski D. Modelling of orthogonal cutting with a temperature dependent friction law. J Mech Phys Solids 1998;vol. 46(10): 2103–38.
[134] Merchant ME. Basic mechanics of the metal-cutting process. J Appl Mech Sep. 1944;vol. 11(3):168–75. https://doi.org/10.1115/1.4009380.
[135] Kumar LD, Ajay V. Modelling of temperature profile in metal cutting process. Int J Innov *Res Dev* 2012;vol. 8:216–27.
[136] Komanduri R. Some clarifications on the mechanics of chip formation when machining titanium alloys. Wear Feb. 1982;vol. 76(1):15–34. https://doi.org/10.1016/0043-1648(82)90113-2.
[137] Vieregge G. Die Energieverteilung und die Temperatur bei der Zerspanung. Werkstatt und Betrieb 1996;vol. 86(11):101–4.
[138] Abrão AM, Aspinwall DK, Ng EG. Temperature evaluation when machining hardened hot work die steel using PCBN tooling. Ind Diam Rev 1996;vol. 59(569): 40–4.
[139] Loeen E, Shaw M. On the analysis of cutting tool temperature. ASME Trans J Eng Ind 1954;vol. 76(1):217–31.
[140] Klocke F, König W. Fertigungsverfahren 1: Drehen, Fräsen, Bohren. 8th ed..,. Springer-Verlag; 2008. https://doi.org/10.1007/978-3-540-35834-3.
[141] Armendia M, Garay A, Villar A, Davies MA, Arrazola PJ. High bandwidth temperature measurement in interrupted cutting of difficult to machine materials. CIRP Ann Jan. 2010;vol. 59(1):97–100. https://doi.org/10.1016/J.CIRP.2010.03.059.
[142] Toenshoff HK, Amor B, Andrea PR. Chip formation in high speed cutting (HSC) SMEtechnical paper. in International Machining an Grinding Conference 1999.
[143] Ueda T, Al Huda M, Yamada K, Nakayama K, Kudo H. Temperature Measurement of CBN Tool in Turning of High Hardness Steel. CIRP Ann Jan. 1999;vol. 48(1): 63–6. https://doi.org/10.1016/S0007-8506(07)63132-1.
[144] Tanaka R, Morishita H, Lin YC, Hosokawa A, Ueda T, Furumoto T. Cutting Tool Edge Temperature in Finish Hard Turning of Case Hardened Steel. Key Eng Mater Feb. 2009;vol. 407–408:538–41.
[145] Kikuchi M. The use of cutting temperature to evaluate the machinability of titanium alloys. Acta Biomaterialia Feb. 2009;vol. 5(2):770–5. https://doi.org/10.1016/J.ACTBIO.2008.08.016.
[146] Kikuchi M, Okuno O. Machinability evaluation of titanium alloys (Part 2)-Analyses of cutting force and spindle motor current. Dent Mater 2004;vol. 23(4): 621–7. https://doi.org/10.4012/DMJ.23.621.
[147] Eric MN. "Materials machinability in relation to the cutting temperature. Tribol Ind 2002;vol. 24(3–4).
[148] Nedic BP, Eric MD. Cutting temperature measurement and material machinability. Therm Sci 2014;vol. 18:S259–68. https://doi.org/10.2298/TSCI120719003N.
[149] Mia M, Dhar NR. Response surface and neural network based predictive models of cutting temperature in hard turning. J Adv Res Nov. 2016;vol. 7(6):1035–44. https://doi.org/10.1016/J.JARE.2016.05.004.
[150] Sandstrom DR, Hodowany JN. Modeling The physics of metal cutting in high-speed machining. Mach Sci technolongy 1998;vol. 2(2):343–53. https://doi.org/10.1080/10940349808945675.
[151] Saelzer J, Berger S, Iovkov I, Zabel A, Biermann D. In-situ measurement of rake face temperatures in orthogonal cutting. CIRP Ann Jan. 2020;vol. 69(1):61–4. https://doi.org/10.1016/J.CIRP.2020.04.021.
[152] Tönshoff HK, et al. Spanbildung und Temperaturen beim Spanen mit hohen Schnittgeschwindigkeiten. Wiley-VCH Verlag,; 2005. https://doi.org/10.1002/3527605142.ch1.
[153] Neugebauer R, et al. Velocity effects in metal forming and machining processes. CIRP Ann Jan. 2011;vol. 60(2):627–50. https://doi.org/10.1016/J.CIRP.2011.05.001.
[154] Schulz H, Moriwaki T. High-speed Machining. CIRP Ann Jan. 1992;vol. 41(2): 637–43. https://doi.org/10.1016/S0007-8506(07)63250-8.
[155] Kronsberg M. Machining science and application: theory and practice for operation and development of machining processes. Oxford: Pergamon Press,; 1966.
[156] Odelros S, Kaplan B, Kritikos M, Johansson M, Norgren S. Experimental and theoretical study of the microscopic crater wear mechanism in titanium machining. Wear Apr. 2017;vol. 376–377:115–24. https://doi.org/10.1016/J.WEAR.2017.01.104.
[157] Shaw MC, Cookson JO. Metal cutting principles. Second edi..,. Oxford University Press,; 2005. https://doi.org/10.1016/0301-679x(85)90013-1.
[158] Boothroyd G. "Fundermentals of metal machining and machine tools. McGraw-Hill. in International Student Edition. 3rd ed..,. McGraw-Hill: CRC Press,; 1981. p. 92–106.
[159] Oxley PLB. Mechanics of machining: an analytical approach to assessing machinability:, published by Ellis Horwood, Chichester, 1989, 242 pp. Wear 1989:74–96. https://doi.org/10.1016/0043-1648(91)90332-O.
[160] S. Altmüller, "Simultanes funfachsige Frasen von Freiformflachen aus Titan.," Rheinisch-Westfalische Technische Hochschule Aachen (RWTH), 2000.
[161] Jacobus K, DeVor RE, Kapoor SG. Machining-Induced Residual Stress: Experimentation and Modeling. J Manuf Sci Eng Feb. 2000;vol. 122(1):20–31. https://doi.org/10.1115/1.538906.
[162] Cui ZP, Zhang HJ, Zong WJ, Li G, Du K. Origin of the lateral return error in a five-axis ultraprecision machine tool and its influence on ball-end milling surface roughness. Int J Mach Tools Manuf 2022;vol. 178(June). https://doi.org/10.1016/j.ijmachtools.2022.103907.
[163] Umbrello D. Influence of material microstructure changes on surface integrity in hard machining of AISI 52100 steel. Int J Adv Manuf Technol Oct. 2011;vol. 54: 887–98. https://doi.org/10.1007/s00170-010-3003-x.
[164] Zan S, Liao Z, Robles-Linares JA, Garcia Luna G, Axinte D. Machining of long ceramic fibre reinforced metal matrix composites – How could temperature influence the cutting mechanisms? Int J Mach Tools Manuf 2023;vol. 185 (January):103994. https://doi.org/10.1016/j.ijmachtools.2023.103994.
[165] Benedicto E, Carou D, Rubio EM. Technical, Economic and Environmental Review of the Lubrication/Cooling Systems Used in Machining Processes. Procedia Eng Jan. 2017;vol. 184:99–116.
[166] Nakayama K, Ogawa M. Basic Rules on the Form of Chip in Metal Cutting. in Gen Assem of CIRP, 28th, Manuf Technol 1978;vol. 27(1):17–21.
[167] Altintas Y, Ber A. Manufacturing Automation: Metal Cutting Mechanics, Machine Tool Vibrations, and CNC Design. Applied Mechanics Re 2001;vol. 54(5). https://doi.org/10.1115/1.1399383.
[168] Klocke F. Manufacturing Processes 1: Cutting 2011.
[169] Merchant ME. Mechanics of the metal cutting process. I. Orthogonal cutting and a type 2 chip. J Appl Phys 1945;vol. 16(5). https://doi.org/10.1063/1.1707586.
[170] Jawahir IS. Chip-forms, Chip Breakability and Chip Control. Springer,; 2014. p. 178–94. https://doi.org/10.1007/978-3-662-53120-4_6394.
[171] S. 1986- Buchkremer and IIF - Institut für Industriekommunikation und Fachmedien GmbH Apprimus Verlag, "Predictive tool and process design for efficient chip control in metal cutting".
[172] Astakhov VP, Shvets SV, Osman MOM. Chip structure classification based on mechanics of its formation. J Mater Process Technol 1997;vol. 71(2). https://doi.org/10.1016/S0924-0136(97)00081-2.
[173] Jawahir IS, van Luttervelt CA. Recent Developments in Chip Control Research and Applications. *CIRP Ann* - Manuf Technol 1993;vol. 42(2). https://doi.org/10.1016/S0007-8506(07)62531-1.
[174] C. A. 1978- Essig, "Vorhersage von Spanbruch bei der Zerspanung mit geometrisch bestimmter Schneide mit Hilfe schädigungsmechanischer Ansätze".
[175] Clos R, Lorenz H, Schreppel U, Veit P. Verformungslokalisierung und Spanbildung in Inconel 718. in *Hochgeschwindigkeitsspanen metallischer Werkstoffe* 2005. https://doi.org/10.1002/3527605142.ch19.
[176] der V, Hoppe aus Gladbeck S, Dr-Ing Dr-Ing Eh mult U-PH, Tönshoff K, Hoppe S. Experimental and numerical analysis of chip formation in metal cutting. Dissertation Thesis. Laboratory for Machine Tools and Production Engineering (WZL) of RWTH Aachen University,; 2003.
[177] Molinari A. Shear Band Analysis. Solid State Phenom Jan. 1988;vol. 3–4:447–67. https://doi.org/10.4028/WWW.SCIENTIFIC.NET/SSP.3-4.447.
[178] Meyers MA. Dynamic Behavior of Materials. Dyn Behav Mater Sep. 1994. https://doi.org/10.1002/9780470172278.
[179] Wright TW. The physics and mathematics of adiabatic shear bands. Cambridge Univ. Press,; 2002.
[180] Li L, Chen H, Liao Z, Yang Y, Axinte D. Investigation of the grain deformation to orthogonal cutting process of the textured Alloy 718 fabricated by laser powder bed fusion. Int J Mach Tools Manuf 2023;vol. 190(January):104050. https://doi.org/10.1016/j.ijmachtools.2023.104050.
[181] G. Vieregge, "Zerspanung Der Eisenwerkstoffe, 2 nd ed.," *Stahleisen M.B. H., Düsseldorf*, 1970.
[182] Lazoglu I, Altintas Y. Prediction of tool and chip temperature in continuous and interrupted machining. Int J Mach Tools Manuf 2002;vol. 42(9):1011–22. https://doi.org/10.1016/S0890-6955(02)00039-1.
[183] Tschätsch H. Applied Machining Technology. Appl Mach Technol 2009. https://doi.org/10.1007/978-3-642-01007-1.
[184] Yeo SH, Ong SH. Assessment of the thermal effects on chip surfaces. J Mater Process Technol 2000;vol. 98(3):317–21. https://doi.org/10.1016/S0924-0136(99)00264-2.
[185] Cui X, Zhao B, Jiao F, Zheng J. Chip formation and its effects on cutting force, tool temperature, tool stress, and cutting edge wear in high- and ultra-high-speed milling. Int J Adv Manuf Technol 2016;vol. 83(1–4):55–65. https://doi.org/10.1007/s00170-015-7539-7.
[186] Korkut I, Boy M, Karacan I, Seker U. Investigation of chip-back temperature during machining depending on cutting parameters. Mater Des 2007;vol. 28(8): 2329–35. https://doi.org/10.1016/j.matdes.2006.07.009.

[187] Tekiner Z, Yeşilyurt S. Investigation of the cutting parameters depending on process sound during turning of AISI 304 austenitic stainless steel. Mater Des 2004;vol. 25(6):507–13. https://doi.org/10.1016/j.matdes.2003.12.011.
[188] Nobel C. "Drehbearbeitung bleiarmer Kupfer-Zink-Legierungen. Lab. Mach. Tools Prod. Eng. RWTH Aachen *Univ.*. 2016.
[189] Hofmann U, Nobel C, Baier S, Buchkremer S, Döbbeler B, Klocke F. Über den Einfluss von Werkstoffkennwerten auf das Spanbruchverhalten von bleiarmem Messing. Materwiss Werksttech Jun. 2018;vol. 49(6):753–68. https://doi.org/10.1002/MAWE.201600772.
[190] Baier S, Schraknepper D. Entwicklung angepasster Werkzeuge und Prozesse zur Steigerung der Produktivität und Prozesssicherheit beim Fräsen innovativer bleifreier Kupferwerkstoffe: Schlussbericht zu IGF-Vorhaben Nr. 20029 N. RWTH Aachen University, Aachen 2021.
[191] Nobel C, Klocke F, Lung D, Wolf S. Machinability Enhancement of Lead-free Brass Alloys. Procedia CIRP Jan. 2014;vol. 14:95–100. https://doi.org/10.1016/J.PROCIR.2014.03.018.
[192] Baier S, Kokozinski L, Schraknepper D, Bergs T. Tool geometry analysis for plunge milling of lead-free CuZn-alloys. *ESAFORM 2021* Int Conf Mater Forming, Liège, Belgium 2021. https://doi.org/10.25518/ESAFORM21.3793.
[193] Roy P, Sarangi SK, Ghosh A, Chattopadhyay AK. Machinability study of pure aluminium and Al–12% Si alloys against uncoated and coated carbide inserts. Int J Refract Met Hard Mater May 2009;vol. 27(3):535–44. https://doi.org/10.1016/j.ijrmhm.2008.04.008.
[194] Eapen J, Murugappan S, Arul S. A Study on Chip Morphology of Aluminum Alloy 6063 during Turning under Pre Cooled Cryogenic and Dry Environments. Mater Today Proc Jan. 2017;vol. 4(8):7686–93. https://doi.org/10.1016/j.matpr.2017.07.103.
[195] Cagan SC, Venkatesh B, Buldum BB. Investigation of surface roughness and chip morphology of aluminum alloy in dry and minimum quantity lubrication machining. Mater Today Proc Jan. 2020;vol. 27:1122–6. https://doi.org/10.1016/j.matpr.2020.01.547.
[196] Shi K, Zhang D, Ren J, Yao C, Huang X. Effect of cutting parameters on machinability characteristics in milling of magnesium alloy with carbide tool. 168781401662839 Adv Mech Eng 2016;vol. 8(1). https://doi.org/10.1177/1687814016628392.
[197] Surreddi KB, Björkeborn K, Klement U. Effect of heat treatment on chip formation in a case hardening steel. J Mater Chem Eng 2013;vol. 1(1):1–7.
[198] König W, Berktold A, Koch KF. Turning versus Grinding - A Comparison of Surface Integrity Aspects and Attainable Accuracies. *CIRP Ann* - Manuf Technol 1993;vol. 42(1):39–43. https://doi.org/10.1016/S0007-8506(07)62387-7.
[199] Toenshoff HK, Arendt C, Amor RBen, Tonshoff HK, Arendt C, Amor RBen. Cutting of Hardened Steel. CIRP Ann Jan. 2000;vol. 49(2):547–66. https://doi.org/10.1016/S0007-8506(07)63455-6.
[200] Barry J, Byrne G. The Mechanisms of Chip Formation in Machining Hardened Steels. J Manuf Sci Eng Aug. 2002;vol. 124(3):528–35. https://doi.org/10.1115/1.1455643.
[201] Berktold A., "Drehräumen gehärteter Stahlwerkstoffe," *Laboratory for Machine Tools and Production Engineering (WZL) of RWTH Aachen University*, 1992.
[202] Bermingham MJ, Palanisamy S, Kent D, Dargusch MS. A comparison of cryogenic and high pressure emulsion cooling technologies on tool life and chip morphology in Ti–6Al–4V cutting. J Mater Process Technol Apr. 2012;vol. 212(4):752–65. https://doi.org/10.1016/j.jmatprotec.2011.10.027.
[203] Klocke F, Settineri L, Lung D, Claudio Priarone P, Arft M. "High performance cutting of gamma titanium aluminides: Influence of lubricoolant strategy on tool wear and surface integrity,". Wear Apr. 2013;vol. 302:1136–44.
[204] Komanduri R, Schroeder TA, Komandur R, Schroeder TA. On Shear Instability in Machining a Nickel-Iron Base Superalloy. J Eng Ind May 1986;vol. 108(2):93–100. https://doi.org/10.1115/1.3187056.
[205] Gerschwiler K. Untersuchungen zum Verschleißverhalten von Cermets beim Drehen und Fräsen - RWTH Publications. Laboratory for Machine Tools and Production Engineering (WZL) of RWTH Aachen University 1998.
[206] Pawade RS, Joshi SS. Mechanism of chip formation in high-speed turning of inconel 718. Mach Sci Technol Jan. 2011;vol. 15(1):132–52. https://doi.org/10.1080/10910344.2011.557974.
[207] Liu C, Wan M, Zhang W, Yang Y. Chip Formation Mechanism of Inconel 718: A Review of Models and Approaches. Dec. 01. Chinese Journal of Mechanical Engineering (English Edition), vol. 34. Springer,; 2021. https://doi.org/10.1186/s10033-021-00552-9.
[208] Ezugwu EO, Bonney J. Finish Machining of Nickel-Base Inconel 718 Alloy with Coated Carbide Tool under Conventional and High-Pressure Coolant Supplies. Tribol Trans Jan. 2004;vol. 48(1):76–81. https://doi.org/10.1080/05698190590899958.
[209] Klocke F, Krämer A, Sangermann H, Lung D. Thermo-Mechanical Tool Load during High Performance Cutting of Hard-to-Cut Materials. Procedia CIRP Jan. 2012;vol. 1(1):295–300. https://doi.org/10.1016/j.procir.2012.04.053.
[210] Choudhury IA, El-Baradie MA. Machinability of nickel-base super alloys: a general review, vol. 77. Elsevier,; 1998. p. 278–84. https://doi.org/10.1016/S0924-0136(97)00429-9.
[211] Poulachon G, Moisan AL. Hard Turning: Chip Formation Mechanisms and Metallurgical Aspects. ASME Int Mech Eng Congr Expo Proc 1999;vol. 1999-U (August):219–27. https://doi.org/10.1115/IMECE1999-0677.
[212] Splettstoesser A, Schraknepper D, Bergs T. Influence of the frequency of pulsating high-pressure cutting fluid jets on the resulting chip length and surface finish. Int J Adv Manuf Technol Dec. 2021;vol. 117(7–8):2185–96. https://doi.org/10.1007/s00170-021-07177-1.
[213] Klose H-J. Einfluss der Werkstoffmorphologie auf die Zerspanbarkeit niedriglegierter Gusseisen. VDI-Verl 1993.
[214] Edward EM, Trent M, Wright PK. Metal cutting. 4th ed.,. *Bost*: Butterworth-Heinemann,; 2000. p. 446.
[215] Podolsky C. Zerspanung von Gusseisen mit Vermiculargraphit. PZH Produktionstechn Zent Garbsen 2008.
[216] Prof H, et al. Vorwort und Danksagung Die vorliegende Arbeit entstand während meiner Tätigkeit als wissenschaftlicher Mitarbeiter am Laboratorium für Werkzeugmaschinen und Betriebslehre (WZL) der Rheinisch-Technischen Hochschule Aachen. Lab Mach Tools Prod Eng RWTH Aachen *Univ* 2007.
[217] Marwanga RO, Voigt RC. "Influence of graphite morphology, matrix structure on gray iron machining,". Mod Cast 2000;vol. 90:53–7.
[218] G. Warnecke, "Zerspanen von Gußeisen GG 20, Schnittvorgang im Feingefüge, Variation der Schnittgeschwindigkeit – Institute of Production Engineering and Machine Tools – Leibniz University Hannover," *Enc. Cin. Göttingen*, 1972.
[219] Lung S. Erklärungsmodell für die spanende Bearbeitung von ausferritischen Gusseisen mit Lamellengraphit: Technologie der Fertigungsverfahren: Amazon.co.uk: Lung, Sven: 9783863597801: Books. Laboratory for Machine Tools and Production Engineering (WZL) of RWTH Aachen University, Apprimus Verlag, Aachen 2019.
[220] Klocke F, Lung D, Arft M, Priarone PC, Settineri L. On high-speed turning of a third-generation gamma titanium aluminide. Int J Adv Manuf Technol Apr. 2013;vol. 65(1–4):155–63. https://doi.org/10.1007/s00170-012-4157-5.
[221] Uhlmann E, Herter S, Gerstenberger R, Roeder M. Quasi-static chip formation of intermetallic titanium aluminides. Prod Eng 2009;vol. 3(3):261–70. https://doi.org/10.1007/s11740-009-0166-0.
[222] Pérez RGVV. Wear mechanisms of WC inserts in face milling of gamma titanium aluminides. Wear Jul. 2005;vol. 259(7–12):1160–7. https://doi.org/10.1016/j.wear.2005.02.062.
[223] Castellanos SD, et al. Machinability of titanium aluminides: A review. Proc Inst Mech Eng Part L J Mater Des Appl Nov. 2018;vol. 233(3):426–51. https://doi.org/10.1177/1464420718809386.
[224] "Candidate List of substances of very high concern for Authorisation (published in accordance with Article 59(10) of the REACH Regulation) ⟨https://echa.europa.eu/de/candidate-list-table⟩," 2020.
[225] Commission Delegated Directive (EU) 2018/741 of 1 March 2018 amending, for the purposes of adapting to scientific and technical progress, Annex III to Directive 2011/65/EU of the European Parliament and of the Council as regards an exemption for lead as a. 2018.
[226] "Directive 2000/53/EC of the European Parliament and of the Council of 18 September 2000 on end-of life vehicles," 2000.
[227] "DIRECTIVE 2002/95/EC OF THE EUROPEAN PARLIAMENT AND OF THE COUNCIL of 27 January 2003 on the restriction of the use of certain hazardous substances in electrical and electronic equipment," 2003.
[228] Issahaq MN, et al. Dual-scale folding in cutting of commercially pure aluminum alloys. Int J Mach Tools Manuf 2022;vol. 181(August 2022):103932. https://doi.org/10.1016/j.ijmachtools.2022.103932.
[229] Xu D, Feng P, Li W, Ma Y, Liu B. Research on chip formation parameters of aluminum alloy 6061-T6 based on high-speed orthogonal cutting model. Int J Adv Manuf Technol Mar. 2014;vol. 72(5–8):955–62. https://doi.org/10.1007/s00170-014-5700-3.
[230] Tang Z, et al. A new characterisation method for stress, hardness, microstructure, and slip lines using the stored energy field in the cutting deformation zones of workpiece. Int J Mach Tools Manuf 2022;vol. 178(May):103891. https://doi.org/10.1016/j.ijmachtools.2022.103891.
[231] T.H. Pham, D.T. Nguyen, T.L. Banh, and V.C. Tong, "Experimental study on the chip morphology, tool–chip contact length, workpiece vibration, and surface roughness during high-speed face milling of A6061 aluminum alloy:," ⟨https://doi.org/10.1177/0954405419863221⟩, vol. 234, no. 3, pp. 610–620, Jul. 2019, doi: 10.1177/0954405419863221.
[232] Wang B, Liu Z. Serrated chip formation mechanism based on mixed mode of ductile fracture and adiabatic shear. Proc Inst Mech Eng Part B J Eng Manuf Aug. 2014;vol. 228(2):181–90. https://doi.org/10.1177/0954405413497941.
[233] Guo S, Lu S, Zhang B, Cheung CF. Surface integrity and material removal mechanisms in high-speed grinding of Al/SiCp metal matrix composites. Int J Mach Tools Manuf 2022;vol. 178(June):103906. https://doi.org/10.1016/j.ijmachtools.2022.103906.
[234] Liu K, Li J, Sun J, Zhu Z, Meng H. Investigation on chip morphology and properties in drilling aluminum and titanium stack with double cone drill. Int J Adv Manuf Technol Aug. 2018;vol. 94(5–8):1947–56. https://doi.org/10.1007/s00170-017-0988-4.
[235] Dargusch MS, Sun S, Kim JW, Li T, Trimby P, Cairney J. Effect of tool wear evolution on chip formation during dry machining of Ti-6Al-4V alloy. Int J Mach Tools Manuf Mar. 2018;vol. 126:13–7. https://doi.org/10.1016/j.ijmachtools.2017.12.003.
[236] Sun J, Guo YB. A new multi-view approach to characterize 3D chip morphology and properties in end milling titanium Ti–6Al–4V. Int J Mach Tools Manuf Oct. 2008;vol. 48(12–13):1486–94. https://doi.org/10.1016/j.ijmachtools.2008.04.002.
[237] Pouliquen A, et al. Influence of the microstructure of a Ti5553 titanium alloy on chip morphology and cutting forces during orthogonal cutting. J Mater Process Technol 2023;vol. 319(July):118054. https://doi.org/10.1016/j.jmatprotec.2023.118054.
[238] Denkena B, Bergmann B, Schaper F. Investigation of chip formation of Ti–6Al–4V in oxygen-free atmosphere. Int J Adv Manuf Technol 2023;vol. 124(10):3601–13. https://doi.org/10.1007/s00170-022-10655-9.

[239] Li A, Zang J, Zhao J. Effect of cutting parameters and tool rake angle on the chip formation and adiabatic shear characteristics in machining Ti-6Al-4V titanium alloy. Int J Adv Manuf Technol 2020;vol. 107(7–8):3077–91. https://doi.org/10.1007/s00170-020-05145-9.
[240] Lv D, Wang B, Hou J, Wang H, Bian R. Characteristics of chip formation and its effects on cutting force and tool wear/damage in milling Ti-25 V-15Cr (Ti40) beta titanium alloy. Int J Adv Manuf Technol 2023;vol. 124(7–8):2279–88. https://doi.org/10.1007/s00170-022-10637-x.
[241] Liu D, Ni C, Wang Y, Zhu L. Review of serrated chip characteristics and formation mechanism from conventional to additively manufactured titanium alloys. J Alloys Compd 2024;vol. 970(October 2023):172573. https://doi.org/10.1016/j.jallcom.2023.172573.
[242] Zhu Z, et al. Evolution of 3D chip morphology and phase transformation in dry drilling Ti6Al4V alloys. J Manuf Process 2018;vol. 34(July):531–9. https://doi.org/10.1016/j.jmapro.2018.07.001.
[243] Ming W, Dang J, An Q, Chen M. Chip formation and hole quality in dry drilling additive manufactured Ti6Al4V. Mater Manuf Process 2020;vol. 35(1):43–51. https://doi.org/10.1080/10426914.2019.1692353.
[244] Kishawy HA, Nguyen N, Hosseini A, Elbestawi M. Machining characteristics of additively manufactured titanium, cutting mechanics and chip morphology. CIRP Ann 2023;vol. 72(1):49–52. https://doi.org/10.1016/j.cirp.2023.04.056.
[245] Ezugwu EO, Wang ZM, Machado AR. The machinability of nickel-based alloys: a review. J Mater Process Technol Feb. 1999;vol. 86(1–3):1–16. https://doi.org/10.1016/S0924-0136(98)00314-8.
[246] Zannoun H, Schoop J. Analysis of burr formation in finish machining of nickel-based superalloy with worn tools using micro-scale in-situ techniques. Int J Mach Tools Manuf 2023;vol. 189(October 2022):104030. https://doi.org/10.1016/j.ijmachtools.2023.104030.
[247] Liao Z, et al. Influence of surface integrity induced by multiple machining processes upon the fatigue performance of a nickel based superalloy. J Mater Process Technol 2021;vol. 298:117313. https://doi.org/10.1016/j.jmatprotec.2021.117313.
[248] Herfurth K. "Gusseisen mit Kugelgraphit – Einfluss der metallischen Grundmasse. Konstr + Giess 2007;vol. 34(2).
[249] Settineri L, Priarone PC, Arft M, Lung D, Stoyanov T. An evaluative approach to correlate machinability, microstructures, and material properties of gamma titanium aluminides. CIRP Ann Jan. 2014;vol. 63(1):57–60. https://doi.org/10.1016/j.cirp.2014.03.068.
[250] Zhang Y, et al. Microstructural modulation of TiAl alloys for controlling ultra-precision machinability. Int J Mach Tools Manuf 2022;vol. 174(November 2021):103851. https://doi.org/10.1016/j.ijmachtools.2022.103851.
[251] Tebaldo V, Faga MG. Influence of the heat treatment on the microstructure and machinability of titanium aluminides produced by electron beam melting. J Mater Process Technol Jun. 2017;vol. 244:289–303. https://doi.org/10.1016/j.jmatprotec.2017.01.037.
[252] Nakayama K. A Study on Chip-breaker. Bull JSME 1962;vol. 5(17):142–50. https://doi.org/10.1299/JSME1958.5.142.
[253] Nakayama K, Arai M. Comprehensive Chip Form Classification Based on the Cutting Mechanism. CIRP Ann Jan. 1992;vol. 41(1):71–4. https://doi.org/10.1016/S0007-8506(07)61155-X.
[254] D.I.N. Deutsches Institut für Normung e. V., "Klassifizierung und Bezeichnung von ungefähren Spankontrollbereichen für Wendeschneidplatten mit Spanformern," 2009.
[255] D. I. N. D. I. für Normung e. V. and DIN Deutsches Institut für Normung e. V. Klassifizierung und Bezeichnung von ungefähren Spankontrollbereichen für Wendeschneidplatten mit Spanformern, no. 10910. Beuth Verlag GmbH,; 2009.
[256] Jawahir IS, Balaji AK. Predictive modeling and optimization of turning operations with complex grooved cutting tools for curled chip formation and chip breaking. Mach Sci Technol 2000;vol. 4(3):399–443. https://doi.org/10.1080/10940340008945717.
[257] Spaans C. The Fundamentals of Three Dimensional Chip Curl, Chip Breaking and Chip Control: Dissertation Thesis. TU Delft 1971. https://doi.org/10.1007/BF01186875.
[258] Fang XD, Jawahir IS. An Analytical Model for Cyclic Chip Formation in 2-D Machining with Chip Breaking. CIRP Ann Jan. 1996;vol. 45(1):53–8. https://doi.org/10.1016/S0007-8506(07)63016-9.
[259] Klocke F, Lung D, Essig C. Chip Breakage Prediction by a Web-based Expert System. Burrs - Anal Control Removal 2010:107–13. https://doi.org/10.1007/978-3-642-00568-8_12.
[260] Peng B, Bergs T, Klocke F, Döbbeler B. An advanced FE-modeling approach to improve the prediction in machining difficult-to-cut material. Int J Adv Manuf Technol Apr. 2019;vol. 103(5–8):2183–96. https://doi.org/10.1007/s00170-019-03456-0.
[261] Liu H, Peng B, Meurer M, Schraknepper D, Bergs T. Three-dimensional multi-physical modelling of the influence of the cutting fluid on the chip formation process. Procedia CIRP Jan. 2021;vol. 102:216–21. https://doi.org/10.1016/j.procir.2021.09.037.
[262] Bergs T, Abouridouane M, Meurer M, Peng B. Digital image correlation analysis and modelling of the strain rate in metal cutting. CIRP Ann Jan. 2021;vol. 70(1):45–8. https://doi.org/10.1016/j.cirp.2021.04.055.
[263] Meurer M, Augspurger T, Tekkaya B, Schraknepper D, Lima AP, Bergs T. Development of a Methodology for Strain Field Analysis during Orthogonal Cutting. Procedia CIRP 2020;vol. 87:444–9. https://doi.org/10.1016/j.procir.2020.03.004.
[264] Bedekar V, Chaudhari RG, Shivpuri R. Nanostructural evolution of hard turning white layer during machining of through hardened 52100 steel. in *Transactions of the North American Manufacturing Research Institution of SME* 2013;vol. 41.
[265] Ramesh A, Melkote SN, Allard LF, Riester L, Watkins TR. Analysis of white layers formed in hard turning of AISI 52100 steel. Mater Sci Eng A 2005;vol. 390(1–2). https://doi.org/10.1016/j.msea.2004.08.052.
[266] Axinte D, Huang H, Yan J, Liao Z. What micro-mechanical testing can reveal about machining processes. Int J Mach Tools Manuf 2022;vol. 183(August):103964. https://doi.org/10.1016/j.ijmachtools.2022.103964.
[267] Jawahir IS, et al. Surface integrity in material removal processes: Recent advances. *CIRP Ann* - Manuf Technol 2011;vol. 60(2). https://doi.org/10.1016/j.cirp.2011.05.002.
[268] Liao Z, et al. Surface integrity in metal machining - Part I: Fundamentals of surface characteristics and formation mechanisms. Int J Mach Tools Manuf 2021;vol. 162(December 2020):103687. https://doi.org/10.1016/j.ijmachtools.2020.103687.
[269] la Monaca A, et al. Surface integrity in metal machining - Part II: Functional performance. International Journal of Machine Tools and Manufacture 2021;vol. 164. https://doi.org/10.1016/j.ijmachtools.2021.103718.
[270] Ren Z, et al. Understanding local cutting features affecting surface integrity of gear flank in gear skiving. Int J Mach Tools Manuf 2022;vol. 172(July 2021). https://doi.org/10.1016/j.ijmachtools.2021.103818.
[271] la Monaca A, Axinte DA, Liao Z, M'Saoubi R, Hardy MC. "Towards understanding the thermal history of microstructural surface deformation when cutting a next generation powder metallurgy nickel-base superalloy,". Int. J. Mach. Tools Manuf, vol. 168; Sep. 2021, 103765.
[272] Sridharan U, Peurifoy J, Bedekar V. Influence of material microstructure on grindability of bearing steel. CIRP Ann 2021;vol. 70(1). https://doi.org/10.1016/j.cirp.2021.04.009.
[273] Hoier P, et al. Influence of batch-to-batch material variations on grindability of a medium-carbon steel. J Manuf Process 2022;vol. 73. https://doi.org/10.1016/j.jmapro.2021.11.012.
[274] Hua J, et al. Effect of feed rate, workpiece hardness and cutting edge on subsurface residual stress in the hard turning of bearing steel using chamfer + hone cutting edge geometry. Mater Sci Eng A 2005;vol. 394(1–2). https://doi.org/10.1016/j.msea.2004.11.011.
[275] Liao Z, Axinte D, Mieszala M, M'Saoubi R, Michler J, Hardy M. On the influence of gamma prime upon machining of advanced nickel based superalloy. CIRP Ann Jan. 2018;vol. 67(1):109–12.
[276] Bedekar V, et al. Effect of nickel on the kinematic stability of retained austenite in carburized bearing steels - In-situ neutron diffraction and crystal plasticity modeling of uniaxial tension tests in AISI 8620, 4320 and 3310 steels. Int J Plast 2020;vol. 131. https://doi.org/10.1016/j.ijplas.2020.102748.
[277] W.A. Backofen,. Addison-Wesley Publishing Company, 1972.
[278] Bedekar V. Nanostructural evolution of hard turning layers in carburized steel. Columbus: The Ohio State University; 2013.
[279] M'Saoubi R, et al. Over multiple length scales. *CIRP Ann* - Manuf Technol 2012;vol. 61(1). https://doi.org/10.1016/j.cirp.2012.03.058.
[280] M'Saoubi R, Axinte D, Herbert C, Hardy M, Salmon P. Surface integrity of nickel-based alloys subjected to severe plastic deformation by abusive drilling. *CIRP Ann* - Manuf Technol 2014;vol. 63(1). https://doi.org/10.1016/j.cirp.2014.03.067.
[281] Ezugwu EO. Key improvements in the machining of difficult-to-cut aerospace superalloys. Int J Mach Tools Manuf 2005;vol. 45(12–13):1353–67. https://doi.org/10.1016/j.ijmachtools.2005.02.003.
[282] Jawahir IS, et al. Cryogenic manufacturing processes. CIRP Ann 2016;vol. 65(2):713–36. https://doi.org/10.1016/j.cirp.2016.06.007.
[283] Ghosh Chetan, S, Venkateswara Rao P. Application of sustainable techniques in metal cutting for enhanced machinability: a review. J Clean Prod 2015;vol. 100:17–34. https://doi.org/10.1016/j.jclepro.2015.03.039.
[284] Jawahir IS, Schoop J, Kaynak Y, Balaji AK, Ghosh R, Lu T. Progress Toward Modeling and Optimization of Sustainable Machining Processes. J Manuf Sci Eng Sep. 2020;vol. 142(11). https://doi.org/10.1115/1.4047926.
[285] Palaniappan K, Sundararaman M, Murthy H, Jeyaraam R, Rao BC. Influence of workpiece texture and strain hardening on chip formation during machining of Ti–6Al–4V alloy. Int J Mach Tools Manuf 2022;vol. 173(June 2021):103849. https://doi.org/10.1016/j.ijmachtools.2021.103849.
[286] Varadarajan AS, Philip PK, Ramamoorthy B. Investigations on hard turning with minimal cutting fluid application (HTMF) and its comparison with dry and wet turning. Int J Mach Tools Manuf 2002;vol. 42(2):193–200. https://doi.org/10.1016/S0890-6955(01)00119-5.
[287] Priarone PC, Robiglio M, Settineri L, Tebaldo V. Milling and Turning of Titanium Aluminides by Using Minimum Quantity Lubrication. Procedia CIRP 2014;vol. 24:62–7. https://doi.org/10.1016/j.procir.2014.07.147.
[288] Williams JA, Tabor D. The role of lubricants in machining. Wear 1977;vol. 43(3):275–92. https://doi.org/10.1016/0043-1648(77)90125-9.
[289] Çakır O, Kıyak M, Altan E. Comparison of gases applications to wet and dry cuttings in turning. J Mater Process Technol 2004;vol. 153–154:35–41. https://doi.org/10.1016/j.jmatprotec.2004.04.190.
[290] Itoigawa F, Childs THC, Nakamura T, Belluco W. Effects and mechanisms in minimal quantity lubrication machining of an aluminum alloy. Wear 2006;vol. 260(3):339–44. https://doi.org/10.1016/j.wear.2005.03.035.
[291] Melkote SN, et al. Advances in material and friction data for modelling of metal machining. CIRP Ann 2017;vol. 66(2):731–54. https://doi.org/10.1016/j.cirp.2017.05.002.

[292] Arndt T, Klose J, Gerstenmeyer M, Schulze V. Tool wear development in gear skiving process of quenched and tempered internal gears. Forsch im Ingenieurwes 2021. https://doi.org/10.1007/s10010-021-00544-0.
[293] Sreejith PS. Machining of 6061 aluminium alloy with MQL, dry and flooded lubricant conditions. Mater Lett 2008;vol. 62(2):276–8. https://doi.org/10.1016/j.matlet.2007.05.019.
[294] Schwalm J, Gerstenmeyer M, Zanger F, Schulze V. Complementary machining: effect of tool types on tool wear and surface integrity of AISI 4140. Procedia CIRP 2020;vol. 87:89–94. https://doi.org/10.1016/j.procir.2020.02.035.
[295] Attanasio A, Gelfi M, Giardini C, Remino C. Minimal quantity lubrication in turning: effect on tool wear. Wear 2006;vol. 260(3):333–8. https://doi.org/10.1016/j.wear.2005.04.024.
[296] Hadad M, Sadeghi B. Minimum quantity lubrication-MQL turning of AISI 4140 steel alloy. J Clean Prod 2013;vol. 54:332–43. https://doi.org/10.1016/j.jclepro.2013.05.011.
[297] Iskandar Y, Tendolkar A, Attia MH, Hendrick P, Damir A, Diakodimitris C. Flow visualization and characterization for optimized MQL machining of composites. CIRP Ann 2014;vol. 63(1):77–80. https://doi.org/10.1016/j.cirp.2014.03.078.
[298] López De Lacalle LN, Angulo C, Lamikiz A, Sánchez JA. Experimental and numerical investigation of the effect of spray cutting fluids in high speed milling. J Mater Process Technol 2006;vol. 172(1):11–5. https://doi.org/10.1016/j.jmatprotec.2005.08.014.
[299] Zhang S, Li JF, Wang YW. Tool life and cutting forces in end milling Inconel 718 under dry and minimum quantity cooling lubrication cutting conditions. J Clean Prod 2012;vol. 32:81–7. https://doi.org/10.1016/j.jclepro.2012.03.014.
[300] Ekinovic S, Prcanovic H, Begovic E. Investigation of Influence of MQL Machining Parameters on Cutting Forces During MQL Turning of Carbon Steel St52-3. Procedia Eng 2015;vol. 132:608–14. https://doi.org/10.1016/j.proeng.2015.12.538.
[301] Dhar NR, Kamruzzaman M, Ahmed M. Effect of minimum quantity lubrication (MQL) on tool wear and surface roughness in turning AISI-4340 steel. J Mater Process Technol 2006;vol. 172(2):299–304. https://doi.org/10.1016/j.jmatprotec.2005.09.022.
[302] Sohrabpoor H, Khanghah SP, Teimouri R. Investigation of lubricant condition and machining parameters while turning of AISI 4340. Int J Adv Manuf Technol 2015;vol. 76(9):2099–116. https://doi.org/10.1007/s00170-014-6395-1.
[303] Pereira O, Martín-Alfonso JE, Rodríguez A, Calleja A, Fernández-Valdivielso A, López de Lacalle LN. Sustainability analysis of lubricant oils for minimum quantity lubrication based on their tribo-rheological performance. J Clean Prod 2017;vol. 164:1419–29. https://doi.org/10.1016/j.jclepro.2017.07.078.
[304] Braga DU, Diniz AE, Miranda GWA, Coppini NL. Using a minimum quantity of lubricant (MQL) and a diamond coated tool in the drilling of aluminum–silicon alloys. J Mater Process Technol 2002;vol. 122(1):127–38. https://doi.org/10.1016/S0924-0136(01)01249-3.
[305] Zeilmann RP, Nicola GL, Vacaro T, Teixeira CR, Heiler R. Implications of the reduction of cutting fluid in drilling AISI P20 steel with carbide tools. Int J Adv Manuf Technol 2012;vol. 58(5):431–41. https://doi.org/10.1007/s00170-011-3401-8.
[306] Busch K, Hochmuth C, Pause B, Stoll A, Wertheim R. Investigation of Cooling and Lubrication Strategies for Machining High-temperature Alloys. Procedia CIRP 2016;vol. 41:835–40. https://doi.org/10.1016/j.procir.2015.10.005.
[307] Shokrani A, Dhokia V, Newman ST. Hybrid Cooling and Lubricating Technology for CNC Milling of Inconel 718 Nickel Alloy. Procedia Manuf 2017;vol. 11:625–32. https://doi.org/10.1016/j.promfg.2017.07.160.
[308] Pusavec F, Hamdi H, Kopac J, Jawahir IS. Surface integrity in cryogenic machining of nickel based alloy—Inconel 718. J Mater Process Technol 2011;vol. 211(4):773–83. https://doi.org/10.1016/j.jmatprotec.2010.12.013.
[309] Bordin A, Bruschi S, Ghiotti A, Bariani PF. Analysis of tool wear in cryogenic machining of additive manufactured Ti6Al4V alloy. Wear 2015;vol. 328–329:89–99. https://doi.org/10.1016/j.wear.2015.01.030.
[310] Hong SY. LUBRICATION MECHANISMS OF LN2 IN ECOLOGICAL CRYOGENIC MACHINING. Mach Sci Technol Jun. 2006;vol. 10(1):133–55. https://doi.org/10.1080/10910340500534324.
[311] Courbon C, Pusavec F, Dumont F, Rech J, Kopac J. Tribological behaviour of Ti6Al4V and Inconel718 under dry and cryogenic conditions—Application to the context of machining with carbide tools. Tribol Int 2013;vol. 66:72–82. https://doi.org/10.1016/j.triboint.2013.04.010.
[312] Dix M, Wertheim R, Schmidt G, Hochmuth C. Modeling of drilling assisted by cryogenic cooling for higher efficiency. CIRP Ann 2014;vol. 63(1):73–6. https://doi.org/10.1016/j.cirp.2014.03.080.
[313] Pusavec F, et al. Analysis of the influence of nitrogen phase and surface heat transfer coefficient on cryogenic machining performance. J Mater Process Technol 2016;vol. 233:19–28. https://doi.org/10.1016/j.jmatprotec.2016.02.003.
[314] Stampfer B, Golda P, Schießl R, Maas U, Schulze V. Cryogenic orthogonal turning of Ti-6Al-4V. Int J Adv Manuf Technol 2020;vol. 111(1):359–69. https://doi.org/10.1007/s00170-020-06105-z.
[315] Kirsch B, Basten S, Hasse H, Aurich JC. Sub-zero cooling: a novel strategy for high performance cutting. CIRP Ann Jan. 2018;vol. 67(1):95–8. https://doi.org/10.1016/J.CIRP.2018.04.060.
[316] Basten S, Kirsch B, Hasse H, Aurich JC. Formulation of sub-zero metalworking fluids for cutting processes: influence of additives. CIRP J Manuf Sci Technol Nov. 2020;vol. 31:25–33. https://doi.org/10.1016/J.CIRPJ.2020.09.006.
[317] Basten S, Kirsch B, Gutzeit K, Hasse H, Aurich JC. Influence of the Supplying Technique of a Sub-Zero Metalworking Fluid on the Performance of Face Turning of Ti-6Al-4V Titanium Alloy. SSRN Electron J Nov. 2020. https://doi.org/10.2139/SSRN.3724124.
[318] Basten S, Kirsch B, Hasse H, Aurich JC. Sub-zero metalworking fluids for high performance cutting of difficult to cut materials. Procedia CIRP Jan. 2021;vol. 101:342–5. https://doi.org/10.1016/J.PROCIR.2020.11.016.
[319] Gutzeit K, et al. "Optimization of the cooling strategy during cryogenic milling of Ti-6Al-4 V when applying a sub-zero metalworking fluid,". Prod Eng Dec. 2022;vol. 1:1–10. https://doi.org/10.1007/S11740-022-01178-Z/FIGURES/10.
[320] Basten S, Kirsch B, Hasse H, Aurich JC. Turning of AISI 4140 (42CrMo4): a novel sub-zero cooling approach. Adv Prod Res 2019:313–23. https://doi.org/10.1007/978-3-030-03451-1_31.
[321] Basten S, et al. Influence of different cooling strategies during hard turning of AISI 52100 - part I: thermo-mechanical load, tool wear, surface topography and manufacturing accuracy. Procedia CIRP Jan. 2020;vol. 87:77–82. https://doi.org/10.1016/J.PROCIR.2020.02.085.
[322] Ankener W, et al. Influence of different cooling strategies during hard turning of AISI 52100 – part II: characterization of the surface and near surface microstructure morphology. Procedia CIRP Jan. 2020;vol. 87:119–24. https://doi.org/10.1016/J.PROCIR.2020.02.094.
[323] Gutzeit K, Bulun G, Stelzer G, Kirsch B, Seewig J, Aurich JC. Investigation of the surface integrity when cryogenic milling of Ti-6Al-4V using a sub-zero metalworking fluid. Procedia CIRP Jan. 2022;vol. 108(C):25–30. https://doi.org/10.1016/J.PROCIR.2022.03.010.
[324] Tai BL, Stephenson DA, Furness RJ, Shih AJ. Minimum quantity lubrication (MQL) in automotive powertrain machining. Procedia CIRP 2014;vol. 14:523–8. https://doi.org/10.1016/j.procir.2014.03.044.
[325] Bryan J. International status of thermal error research (1990). CIRP Ann 1990;vol. 39(2):645–56. https://doi.org/10.1016/S0007-8506(07)63001-7.
[326] B.L. M. Vanparys, W. Liu, "Influence of Machining Parameters and Tool Wear on the Material Removal Mechanisms in the Ultrasonic Assisted Grinding of Al2O3," in 3rd CIRP International Conference High Performance Cutting; 2008.
[327] He Y, Xiao G, Zhu S, Liu G, Liu Z, Deng Z. Surface formation in laser-assisted grinding high-strength alloys. Int J Mach Tools Manuf 2023;vol. 186(February). https://doi.org/10.1016/j.ijmachtools.2023.104002.
[328] You K, Yan G, Luo X, Gilchrist MD, Fang F. Advances in laser assisted machining of hard and brittle materials. J Manuf Process 2020;vol. 58(August):677–92. https://doi.org/10.1016/j.jmapro.2020.08.034.
[329] Karpuschewski B, et al. Comparison of process signatures for thermally dominated processes. CIRP J Manuf Sci Technol 2021;vol. 35:217–35. https://doi.org/10.1016/j.cirpj.2021.06.013.
[330] Mypati O, Panzer J, Robles-Linares JA, Zan S, Liao Z, Axinte D. Modelling and experimental study of laser-assisted milling of fibre reinforced SiC/Ti-6Al-4V metal matrix composite. Mater Des 2024;vol. 237(December 2023):112552. https://doi.org/10.1016/j.matdes.2023.112552.
[331] Uehara K, Takeshita H. Cutting ceramics with a technique of hot machining. CIRP Ann Jan. 1986;vol. 35(1):55–8. https://doi.org/10.1016/S0007-8506(07)61837-X.
[332] Pujana J, Rivero A, Celaya A, López de Lacalle LN. Analysis of ultrasonic-assisted drilling of Ti6Al4V. Int J Mach Tools Manuf 2009;vol. 49(6):500–8. https://doi.org/10.1016/j.ijmachtools.2008.12.014.
[333] Yang Z, Zhu L, Zhang G, Ni C, Lin B. Review of ultrasonic vibration-assisted machining in advanced materials. Int J Mach Tools Manuf 2020;vol. 156:103594.
[334] Liang X, Zhang C, Cheung CF, Wang C, Li K, Bulla B. Micro/nano incremental material removal mechanisms in high-frequency ultrasonic vibration-assisted cutting of 316L stainless steel. Int J Mach Tools Manuf 2023;vol. 191(April):104064. https://doi.org/10.1016/j.ijmachtools.2023.104064.
[335] Lauwers TJ and JL, Bleicher B, F, Ten Haaf P, Vanparys M, Bernreiter J. Investigation of the process-material interaction in ultrasonic assisted grinding of ZrO2 based ceramic materials. in 4th CIRP Int Conf High Performance Cutting 2010.
[336] Ezugwu EO, Wang ZM. Titanium alloys and their machinability a review. J Mater Process Technol 1997;vol. 68:262–74.
[337] Stephenson DA, Agapiou JS. Metal cutting theory and practice. CRC Press; 2018. https://doi.org/10.1201/9781315373119.
[338] Witty M, Bergs T, Schäfer A, Cabral G. Cutting tool geometry for plunge milling–process optimization for a stainless steel. Procedia CIRP 2012;vol. 1:506–11. https://doi.org/10.1016/j.procir.2012.04.090.
[339] Oezkaya E, Michel S, Biermann D. Experimental studies and FEM simulation of helical-shaped deep hole twist drills. Prod Eng 2018;vol. 12(1):11–23. https://doi.org/10.1007/s11740-017-0779-7.
[340] Poulachon G, Moisan A, Jawahir IS. Tool-wear mechanisms in hard turning with polycrystalline cubic boron nitride tools. Wear 2001;vol. 250–251(1–12):576–86. https://doi.org/10.1016/S0043-1648(01)00609-3.
[341] Sharma V, Pandey PM. Recent advances in turning with textured cutting tools: a review. J Clean Prod 2016;vol. 137:701–15. https://doi.org/10.1016/j.jclepro.2016.07.138.
[342] Ribeiro FSF, Lopes JC, Bianchi EC, de Angelo Sanchez LE. Applications of texturization techniques on cutting tools surfaces—a survey. Int J Adv Manuf Technol 2020;vol. 109(3):1117–35. https://doi.org/10.1007/s00170-020-05669-0.
[343] Arslan A, et al. Surface texture manufacturing techniques and tribological effect of surface texturing on cutting tool performance: a review. Crit Rev Solid State Mater Sci Nov. 2016;vol. 41(6):447–81. https://doi.org/10.1080/10408436.2016.1186597.
[344] Kümmel J, et al. Study on micro texturing of uncoated cemented carbide cutting tools for wear improvement and built-up edge stabilisation. J Mater Process

Technol 2015;vol. 215:62–70. https://doi.org/10.1016/j.jmatprotec.2014.07.032.
[345] Tamil Alagan N, Zeman P, Hoier P, Beno T, Klement U. Investigation of micro-textured cutting tools used for face turning of alloy 718 with high-pressure cooling. J Manuf Process 2019;vol. 37:606–16. https://doi.org/10.1016/j.jmapro.2018.12.023.
[346] Ze W, Jianxin D, Yang C, Youqiang X, Jun Z. Performance of the self-lubricating textured tools in dry cutting of Ti-6Al-4V. Int J Adv Manuf Technol 2012;vol. 62 (9):943–51. https://doi.org/10.1007/s00170-011-3853-x.
[347] Chen Y, Guo X, Zhang K, Guo D, Zhou C, Gai L. Study on the surface quality of CFRP machined by micro-textured milling tools. J Manuf Process 2019;vol. 37:114–23. https://doi.org/10.1016/j.jmapro.2018.11.021.
[348] Koshy P, Tovey J. Performance of electrical discharge textured cutting tools. CIRP Ann 2011;vol. 60(1):153–6. https://doi.org/10.1016/j.cirp.2011.03.104.
[349] Li Q, Yang S, Zhang Y, Zhou Y, Cui J. Evaluation of the machinability of titanium alloy using a micro-textured ball end milling cutter. Int J Adv Manuf Technol 2018;vol. 98(5):2083–92. https://doi.org/10.1007/s00170-018-2319-9.
[350] Ling TD, et al. Surface texturing of drill bits for adhesion reduction and tool life enhancement. Tribol Lett 2013;vol. 52(1):113–22. https://doi.org/10.1007/s11249-013-0198-7.
[351] Li HN, Axinte D. Textured grinding wheels: a review. Int J Mach Tools Manuf 2016;vol. 109:8–35. https://doi.org/10.1016/j.ijmachtools.2016.07.001.
[352] Ranjan P, Hiremath SS. Role of textured tool in improving machining performance: a review. J Manuf Process 2019;vol. 43:47–73. https://doi.org/10.1016/j.jmapro.2019.04.011.
[353] Özel T, Biermann D, Enomoto T, Mativenga P. Structured and textured cutting tool surfaces for machining applications. CIRP Ann 2021;vol. 70(2):495–518. https://doi.org/10.1016/j.cirp.2021.05.006.
[354] Liao Z, Xu D, Axinte D, M'Saoubi R, Thelin J, Wretland A. Novel cutting inserts with multi-channel irrigation at the chip-tool interface: modelling, design and experiments. CIRP Ann 2020.
[355] Rao CM, Rao SS, Herbert MA. Development of novel cutting tool with a micro-hole pattern on PCD insert in machining of titanium alloy. J Manuf Process 2018;vol. 36:93–103. https://doi.org/10.1016/j.jmapro.2018.09.028.